JOURNAL OF THE AMERICAN

# ROCKET

SOCIETY

*A journal devoted to rocket technology and the jet propulsion sciences*

VOLUME 22 SEPTEMBER-OCTOBER 1952 NUMBER 5

JOURNAL OF THE AMERICAN

# ROCKET

SOCIETY

**PUBLICATION OFFICE:**
*20th and Northampton Sts., Easton, Pa.*

**EXECUTIVE OFFICES:**
*Engineering Societies Building*
*29 West 39th Street, New York 18, N. Y.*




### Scope of the Journal

The Journal of the American Rocket Society is devoted to the advancement of the field of jet propulsion through the publication of original papers disclosing new knowledge and new developments. The term "jet propulsion" as used herein is understood to embrace all engines that develop thrust by rearward discharge of a jet through a nozzle or duct, and thus includes systems utilizing atmospheric air and underwater systems, as well as rocket engines. The Journal is open to contributions, either fundamental or applied, dealing with specialized aspects of jet and rocket propulsion, such as fuels and propellants, combustion, heat transfer, high temperature materials, mechanical design analyses, flight mechanics of jet-propelled vehicles, astronautics, and so forth. The Journal endeavors, also, to keep its subscribers informed of the affairs of the Society and of outstanding events in the rocket and jet propulsion field.

### Submission of Manuscripts

Manuscripts should be submitted in duplicate to the Editor-in-Chief, Martin Summerfield, Department of Aeronautical Engineering, Princeton University, Princeton, N. J. See instructions on the inside back cover.

### Security Clearance

Manuscripts must be accompanied by written assurance as to security clearance in the event the subject matter of the manuscript is considered to lie in a classified area. Alternatively, written assurance that clearance is unnecessary should be submitted. Full responsibility for obtaining authoritative clearance rests with the author.

### Advertisements

Information on advertising rates is obtainable from the Secretary of the Society.

### Limitation of Responsibility

Statements and opinions expressed in the Journal are to be understood as the individual expressions of the authors and do not necessarily reflect the views of the Editors or the Society.

### Copyright



### Subscription Rates

| | |
|---|---|
| One year (six bimonthly issues) | $7.50 |
| Foreign countries, including Canada | add .50 |
| Single copies | 1.25 |
| Back numbers | 1.50 |

Subscriptions and orders for single copies should be addressed to the Secretary of the Society.

### Change of Address

Notices of change of address should be sent to the Secretary of the Society at least 30 days prior to the date of publication.

### Explanation of Numbering of Issues

The September 1951 issue was the first of a new series of expanded scope and contents. This series is numbered on an annual volume basis, beginning each year with the January issue as Number 1. Correspondingly, the September issue was Number 5, and since 1951 was the 21st year of publication the new series started with Volume 21 Number 5. This replaced Number 86 of the previous series.


Published Bimonthly by the American Rocket Society, Inc.

Journal of the American Rocket Society, published bimonthly by the American Rocket Society at 20th and Northampton Streets, Easton, Pa., U.S.A. The Editorial Office is located at the Engineering Societies Building, 29 West 39th Street, New York 18, N. Y. Price $1.25 per copy, $7.50 per year. Entered as second-class matter at the Post Office at Easton, Pa., under the Act of March 3, 1879.

# LIQUID OXYGEN

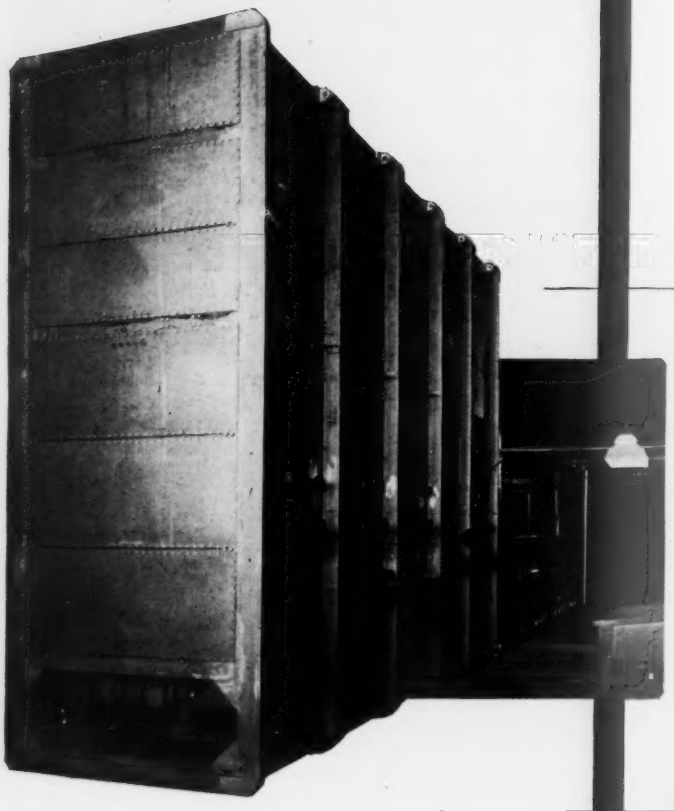

High performance, low cost, and relative ease of storage and handling make liquid oxygen not only the best oxidizer available but guarantee it a prominent place among high performance oxidizers in the future.

Liquid oxygen has certain advantages when comparing oxidizers:

1. **A potential supply unlimited**
2. **Production possible at source**
3. **Inexpensive**
4. **Non-toxic, non-corrosive, smoke-free combustion products**
5. **Easily ignited and smooth burning**
6. **Few limitations on component materials of construction**
7. **Not affected appreciably by ambient temperatures**

Arthur D. Little recently designed and constructed an air-transportable plant for the separation of oxygen from air. This plant was designed to produce 10 tons of liquid oxygen per day.

Experience in the technology of producing, handling and storing liquefied gases aided the Mechanical Division of Arthur D. Little in the design of this plant where minimum weight, small size and purity of product were the prime objectives. The Mechanical Division has further used its experience with liquid gases to design and produce the ADL Helium Refrigerator which is for the storage of liquid gases to reduce evaporation loss to zero.

Although liquid oxygen is produced in wartime chiefly for use as a propellant it may also be used for welding operations and breathing aids when converted to gas by the ADL Liquid-Oxygen Pump.

ADL
*Mechanical Division*

**ARTHUR D. LITTLE, Inc.**
*Mechanical Division*
30 MEMORIAL DRIVE • CAMBRIDGE, MASS.

Send for catalog R-4, describing these and other products and services of the Mechanical Division.

# *Designed for dependability*

## ...tested (and re-tested) for precision

KOLLSMAN devises, develops and manufactures high-precision

**Aircraft Instruments and Controls**
**Miniature AC Motors for Indicating and Remote Control Applications • Optical Parts and Optical Devices • Radio Communications and Navigation Equipment**

While our manufacturing divisions are engaged largely in defense production, the Kollsman Instrument Corporation welcomes the opportunity to apply its research experience to the solution of problems in instrumentation and control.

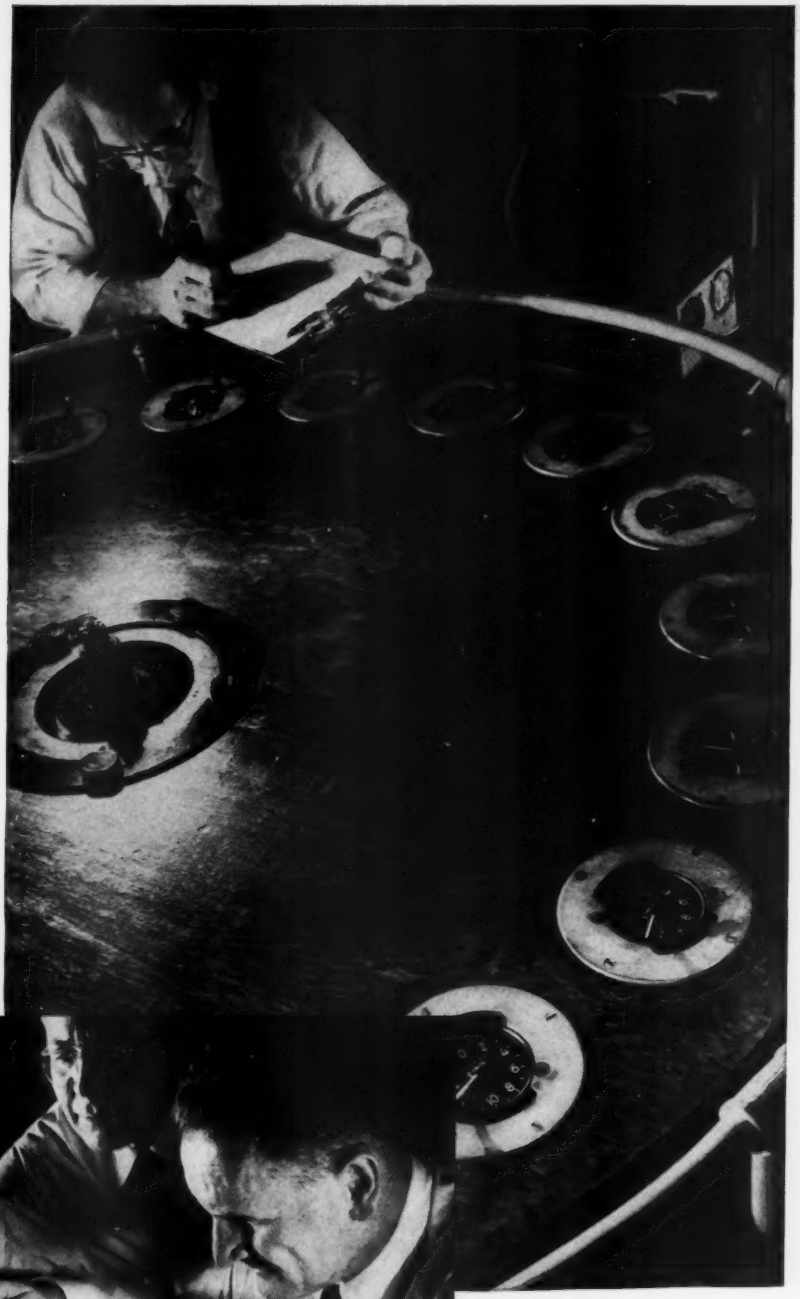

KOLLSMAN INSTRUMENT CORPORATION
ELMHURST, NEW YORK — GLENDALE, CALIFORNIA
SUBSIDIARY OF
*Standard* COIL PRODUCTS CO. INC.

SEPTEMBER-OCTOBER 1952
VOLUME 22 NUMBER 5

JOURNAL OF THE AMERICAN ROCKET SOCIETY

Editor-in-Chief
MARTIN SUMMERFIELD

# Isothermal Combustion Under Flow Conditions

KARL SCHELLER[1] and JAMES A. BIERLEIN[1]

Wright Air Development Center, Dayton, Ohio

**An analysis has been made of rocket engines which convert heat into mechanical energy by means of an isothermal expansion. The basic characteristics of such engines have been derived and compared with conventional rocket engines utilizing adiabatic expansions to obtain thrust. It has been found that, in general, an isothermal expansion is a less desirable work cycle than an adiabatic expansion for the conversion of heat into mechanical energy in jet propulsion devices.**

## Nomenclature

$A$ = area of duct
$\beta$ = ratio of limiting isothermal expansion temperature to the limiting adiabatic chamber temperature
$c_p$ = specific heat at constant pressure
$\epsilon$ = area ratio of nozzle
$H$ = enthalpy per unit mass
$\Delta H$ = heat release associated with the addition of a unit mass of material to the gas stream
$I$ = specific impulse
$I_{max}$ = maximum specific impulse attainable from a given propellant combination
$(I_t/I_s)_\sigma$ = ratio of the isothermal to the adiabatic specific impulse for the condition of excess heat available
$\sigma$ = ratio of the limiting adiabatic temperature to the stagnation temperature of the isothermal flow
$k$ = specific heat ratio
$M$ = Mach number at any station
$M_t$ = Mach number at the nozzle throat in an isothermal expansion
$M_1$ = a particular Mach number defined in the text
$p$ = static pressure
$Q$ = heat release per unit mass
$r$ = mixture ratio, defined in text
$\rho$ = mass density
$R$ = ideal gas constant for unit mass of fluid
$T$ = absolute static temperature
$T_0$ = isentropic stagnation temperature
$T_a$ = adiabatic static flame temperature based upon reactants at a fixed reference temperature.
$T_t$ = isothermal static expansion temperature
$v$ = velocity of gas
$w$ = mass rate of flow of gas

*Superscript*

$^*$ = the value of a quantity at the nozzle throat

*Subscripts*

$t$ = the value of the quantity for isothermal expansion
$s$ = the value of the quantity for isentropic expansion
1 = the value of a quantity at unity Mach number
$c$ = the value of a quantity in the combustion chamber
$e$ = the value of a quantity at the nozzle exit

IT HAS recently been suggested by Zwicky (1)[2] that a rocket engine operating on an isothermal expansion might offer attractive advantages. This kind of thermodynamic process is clearly desirable from the standpoint of minimizing the temperature which materials of construction must withstand. However, it is necessary also to consider the characteristics of such a process with respect to propellant economy and to the geometry of the associated engine. Seifert and Altman (2) have analyzed one special case of the general isothermal expansion problem and compared certain of its features with those of a conventional isentropic expansion. The purpose of this paper is to develop the characteristics of isothermal rockets in a more general way; it is also intended to compare the isothermal and adiabatic cycles on a more direct and meaningful basis than has heretofore been done.

An isothermal expansion in a jet engine may be conceived to occur in one of two ways which, for the sake of convenience, we shall refer to as Case 1 and Case 2 in subsequent discussion.

In Case 1, all of the working fluid in the engine is introduced into the combustion chamber, and the rate of injection, timing of the propellant flows, and geometry of the chamber and nozzle are such that partial combustion occurs in the chamber and raises the gas to a predetermined temperature level just before it enters the nozzle. The remainder of the combustion process is completed in the nozzle as the gas expands to its final pressure. The expansion in the nozzle is imagined to be so scheduled that in any section of the

Presented at the Annual Convention of the AMERICAN ROCKET SOCIETY, Atlantic City, N. J., November 30, 1951.

[1] Research Engineer, Flight Research Laboratory.

[2] Numbers in parentheses refer to the References on page 287.

nozzle the release of heat by combustion is just sufficient to balance the drop in temperature due to expansion, thus maintaining the gas at a constant static temperature. In terms of a gas-dynamic analogy, Case 1 corresponds to the continuous addition of heat to a gas flowing in a variable area duct. If all of the heat to the working fluid is supplied externally through heat exchangers, as for example in a jet engine activated by a nuclear reactor, the gas-dynamic analogy corresponds exactly to the physical model of the engine.

In Case 2, only a portion of the working fluid is introduced into the combustion chamber; the remainder is injected into the expanding gas in the nozzle at just such a rate that its combustion maintains the gas at a constant temperature. In this instance, the total mass of working fluid in the nozzle cannot be assumed constant without the introduction of a serious error. Hence, the gas-dynamic equivalent for the Case 2 rocket engine must be taken to correspond to the continuous addition of heat and mass to a gas flowing in a variable area duct.

### Development of Flow Equations

The problems of predicting the combined effect of a number of simultaneous influences (such as area change, heat addition, and mass addition) on the properties of a moving gas stream are very complex and will therefore be approached from the one-dimensional point of view. This treatment is justified by the satisfactory results achieved by the application of one-dimensional gas-dynamics to the problem of flow in conventional adiabatic nozzles, and should serve to supply a valid comparison between the isothermal and isentropic expansion cycles. In addition to the assumption of one-dimensional flow, it will also be assumed for this analysis that: (*a*) There are no discontinuities in the flow, and changes in stream properties are continuous. (*b*) The gas obeys the ideal gas law; also, the specific heat and molecular weight are the same for products and reactants and remain constant during the flow. (*c*) Fluid friction is negligible. (This assumption is more optimistic in the present problem than it is for the case of an adiabatic expansion. Considerable fluid turbulence is created by the process of heat and/or mass addition and this energy dissipation would be expected to be more significant than that due to wall friction alone.)

Consider a section of infinitesimal length of a nozzle in which the processes with which we are concerned are occurring. The mass injected at this section of the nozzle is assumed to enter as a gas with a negligible velocity component parallel to the moving gas stream. The external heat addition arises from the chemical reaction of the entering gases and is proportional to the amount of these gases. The conditions characterizing the flow through this section are as follows:

(*a*) Continuity

$$\frac{dw}{w} = \frac{d\rho}{\rho} + \frac{dA}{A} + \frac{dv}{v} \quad \ldots\ldots [1]$$

(*b*) Conservation of Momentum

$$\frac{dp}{p} + \frac{kM^2}{2}\frac{dv^2}{v^2} + kM^2\frac{dw}{w} = 0 \quad \ldots\ldots [2]$$

(*c*) Conservation of Energy

$$dQ = dH = c_p dT + {}^1/_2\, dv^2 \quad \ldots\ldots [3]$$

In these equations, $dH$ denotes the net enthalpy change associated with combustion. The Mach number is related to the other variables by the equation:

$$\frac{dM^2}{M^2} = \frac{dv^2}{v^2} - \frac{dT}{T} \quad \ldots\ldots [4]$$

It will be convenient, for our purposes, to make use of the isentropic stagnation temperature, which is defined as follows:

$$T_0 = T + \frac{v^2}{2c_p} = T\left[1 + \frac{k-1}{2}M^2\right] \quad \ldots\ldots [5]$$

The energy equation, in terms of this quantity, becomes

$$dQ = dH = c_p dT_0 \quad \ldots\ldots [6]$$

The above equations can be cast directly into usable form by application of the method of influence coefficients developed by Shapiro and Hawthorne (3). The working equations for the flow then become:

For Case 1 (heat addition only)

$$\frac{dM^2}{M^2} = -2\frac{\left[1 + \frac{k-1}{2}M^2\right]}{1 - M^2}\frac{dA}{A} + \frac{[1 + kM^2]\left[1 + \frac{k-1}{2}M^2\right]}{1 - M^2}\frac{dT_0}{T_0} \quad \ldots\ldots [7]$$

$$\frac{dT}{T} = 0 = \frac{[k-1]M^2}{1 - M^2}\frac{dA}{A} + \frac{[1 - kM^2]\left[1 + \frac{k-1}{2}M^2\right]}{1 - M^2}\frac{dT_0}{T_0} \quad \ldots\ldots [8]$$

$$\frac{dp}{p} = \frac{kM^2}{1 - M^2}\frac{dA}{A} - \frac{kM^2\left[1 + \frac{k-1}{2}M^2\right]}{1 - M^2}\frac{dT_0}{T_0} \quad \ldots\ldots [9]$$

For Case 2 (heat addition + mass addition)

$$\frac{dM^2}{M^2} = -2\frac{\left[1 + \frac{k-1}{2}M^2\right]}{1 - M^2}\frac{dA}{A} + \frac{[1 + kM^2]\left[1 + \frac{k-1}{2}M^2\right]}{1 - M^2}\frac{dT_0}{T_0} + 2\frac{[1 + kM^2]\left[1 + \frac{k-1}{2}M^2\right]}{1 - M^2}\frac{dw}{w} \quad \ldots\ldots [10]$$

$$\frac{dT}{T} = 0 = \frac{[k-1]M^2}{1 - M^2}\frac{dA}{A} + \frac{[1 - kM^2]\left[1 + \frac{k-1}{2}M^2\right]}{1 - M^2}\frac{dT_0}{T_0} - \frac{[k-1]\,[1 + kM^2]M^2}{1 - M^2}\frac{dw}{w} \quad \ldots\ldots [11]$$

$$\frac{dp}{p} = \frac{kM^2}{1 - M^2}\frac{dA}{A} - \frac{kM^2\left[1 + \frac{k-1}{2}M^2\right]}{1 - M^2}\frac{dT_0}{T_0} - \frac{2kM^2\left[1 + \frac{k-1}{2}M^2\right]}{1 - M^2}\frac{dw}{w} \quad \ldots\ldots [12]$$

Equations [7]–[12] completely define the characteristics of the flow for both Case 1 and Case 2. However, in order to obtain unique solutions for Case 2, the mode of mass addition must be specified in terms of the other variables in the flow.

For this purpose, consider the following model. All

of one component (either the oxidizer or the fuel) is introduced into the combustion chamber at the isothermal expansion temperature $T_t$. The deficient component is added along the duct, as a gas at temperature $T_t$, at the proper rate to maintain an isothermal expansion. The addition of mass is terminated when the stoichiometric mixture ratio is attained for the propellant combination under consideration. Since the propellants are assumed to have been preheated, the heat of combustion of the propellant combination is corrected by subtracting the sensible heat and latent heat of vaporization of the propellants. Then $\Delta H$, the effective heat of combustion so obtained, will be the energy release associated with the reaction of a unit mass of the added component with the gas stream. A simplified combustion reaction is assumed for which the heat of reaction is strictly proportional to the quantity of the second component introduced. Considering the energy flux into and out of an element of volume, it follows that

$$[\Delta H - C_p(T_0 - T_t)]dw = wc_p dT_0 \quad [13]$$

where $T_0$ is the total temperature of the stream entering the volume element. Furthermore, it follows that

$$\frac{dw}{w} = \frac{dT_0}{\Delta H/C_p - [T_0 - T_t]} \quad [14]$$

from the definition of $\Delta H$, it is evident that

$$\Delta H/C_p = T_s - T_t \quad [15]$$

where $T_s$ is the adiabatic flame temperature for a stoichiometric mixture. Hence

$$\frac{dw}{w} = \frac{dT_0}{T_s - T_0} \quad [16]$$

It will be convenient at this point to introduce another parameter, $M_f$, defined as follows:

$$T_s = T_t\left[1 + \frac{k-1}{2} M_f^2\right] \quad [17]$$

$M_f$ would be the Mach number of the flow in the duct if the isothermal expansion were carried out to the point where the total temperature of the stream is equal to the adiabatic flame temperature. In terms of this parameter

$$\frac{dw}{w} = \frac{dM^2}{M_f^2 - M^2} \quad [18]$$

where $M$ is the Mach number of the flow when the total temperature is $T_0$. It is now possible to solve the flow equations for both cases to arrive at integral relations between the significant variables.

For Case 1, operating upon Equations [7], [8], and [9] we find that

$$A/A_1 = \frac{1}{M}\exp\left[\frac{k}{2}(M^2 - 1)\right] \quad [19]$$

$$T_0/T_{01} = \frac{2 + (k-1)M^2}{k+1} \quad [20]$$

$$p/p_1 = \exp\left[-\frac{k}{2}(M^2 - 1)\right] \quad [21]$$

The subscript 1 appearing in the above equations denotes the value of the quantity so designated at the station for which the Mach number is unity.

Similarly for Case 2, the following relations can be derived:

$$A/A_1 = \frac{1}{M}\left[\frac{M_f^2 - 1}{M_f^2 - M^2}\right]^{kM_f^2+1} \exp\left[-\frac{k}{2}(M^2 - 1)\right] \quad [22]$$

$$T_0/T_{01} = \frac{2 + (k-1)M^2}{k+1} \quad [23]$$

$$p/p_1 = \left[\frac{M_f^2 - M^2}{M_f^2 - 1}\right]^{kM_f^2} \exp\left[\frac{k}{2}(M^2 - 1)\right] \quad [24]$$

where, as before, the subscript denotes the value of the quantity appearing in each of the equations at a Mach number of unity.

Since the Mach number at the throat need not necessarily be unity for an isothermal expansion, it will be instructive to determine the conditions at the throat for both cases of isothermal expansion. For Case 1, the value of the Mach number that yields a minimum value for the duct area is found from Equation [19] to be

$$M_t = k^{-1/2} \quad [25]$$

Similarly, from Equation [22] the value of the Mach number at the throat, $M_t$, is given by

$$M_t^2 = \frac{-(kM_f^2 + 3) + \sqrt{(kM_f^2 + 3)^2 + 4kM_f^2}}{2k} \quad [26]$$

We are now in a position to express the flow relations in terms of the familiar rocket design parameters $\epsilon$ and $p_c/p_e$. Cast in these terms they become:

For Case 1

$$M^2 = \frac{2}{k}\ln\,[p_c/p_e] \quad [27]$$

$$\epsilon = \frac{p_c}{p_e}\{2e\,\ln\,[p_c/p_e]\}^{-1/2} \quad [28]$$

$$T_s = T_t\left\{1 + \frac{k-1}{k}\ln\,[p_c/p_e]\right\} \quad [29]$$

For Case 2

$$p_c/p_e = \left[1 - \left(\frac{M}{M_f}\right)^2\right]^{-kM_f^2} \exp\left[-\frac{k}{2}M^2\right] \quad [30]$$

$$\epsilon = \frac{M_t}{M}\left[\frac{M_f^2 - M_t^2}{M_f^2 - M^2}\right]^{+kM_f^2} \exp\left[\frac{k}{2}(M_t^2 - M^2)\right] \quad [31]$$

In the temperature expression above for Case 1, $T_s$ is the isentropic stagnation temperature of the flow at the nozzle exit and is identical with the adiabatic flame temperature. $T_t$ has been defined previously as the isothermal expansion temperature. For Case 2, the ratio $T_t/T_s$ is independent of the pressure ratio and may be assigned upon the basis of other considerations. Its value will determine the Mach number attainable for a given pressure ratio and the geometric expansion ratio necessary to achieve this pressure ratio. It will be seen, upon inspection of the flow relations for Case 2, that for any temperature ratio selected, the free stream Mach number approaches the value $M_f$ as the pressure ratio $p_c/p_e$ and the expansion ratio approach infinity. In other words, these relations state that for the case of an isothermal expansion involving heat and mass addition, the total temperature of the stream can attain the adiabatic flame temperature only at the expense of an infinite expansion and pressure ratio.

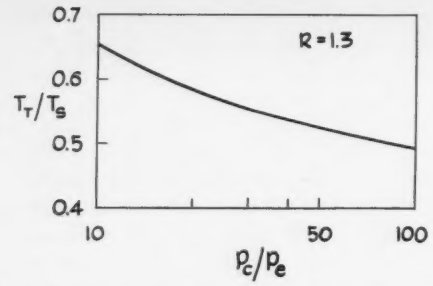


FIG. 1 RATIO OF ISOTHERMAL EXPANSION TEMPERATURE TO ADIABATIC FLAME TEMPERATURE AGAINST PRESSURE RATIO FOR CORRECT EXPANSION.

The principal attraction of an isothermal rocket lies in the possibility of operating it at temperatures lower than those prevailing in conventional rockets. In Fig. 1, the ratio of the isothermal expansion temperature to the adiabatic flame temperature is plotted as a function of the pressure ratio for conditions of correct expansion for the isothermal Case 1 (heat addition alone). Values for this plot were calculated from Equation [29]. It is interesting to note that in the range of pressure ratios normally used in rockets (20–50), the static temperature of the isothermal expansion is only about 60 per cent of the adiabatic flame temperature. It is well to observe also that the effect of pressure ratio diminishes with increasing pressure ratio, and that further substantial reductions in temperature can be achieved only at the expense of a vastly increased pressure ratio. Since for Case 2 the temperature ratio is independent of the pressure ratio, the comparison of the characteristics of the two types of isothermal expansions will be made at values of $T_t/T_s$ equal to 0.6 and 0.1 for the Case 2 expansion. The former value of $T_t/T_s$ will yield a comparison of the two processes at approximately the same expansion temperature; the latter value will serve to demonstrate the effect of temperature ratio on an isothermal expansion with mass addition.

The geometries of isothermal nozzles are compared with those of isentropic nozzles in Fig. 2, which depicts the relations between area expansion ratio and pressure ratio. Isentropic expansion and both types of isothermal expansion are shown, at a specific heat ratio of 1.3. The exit mass flows for the adiabatic expansion and the Case 1 isothermal expansion are equal. The exit mass flow for the Case 2 isothermal expansion is a function of the pressure ratio and is smaller than the exit mass flow for isentropic expansion at any finite pressure ratio under the conditions of the present analysis, which postulates equal mass flows at the time that all available chemical energy in the propellant has been released to the gas stream. The curves indicate that over the entire range of pressure ratios investigated, the isentropic nozzle requires a considerably smaller area ratio to expand to a given pressure ratio than either of the isothermal nozzles. The area ratio for the Case 2 isothermal expansion (with mass addition) is greater than that for the Case 1 process, increasing as the temperature ratio $T_t/T_s$ is increased.

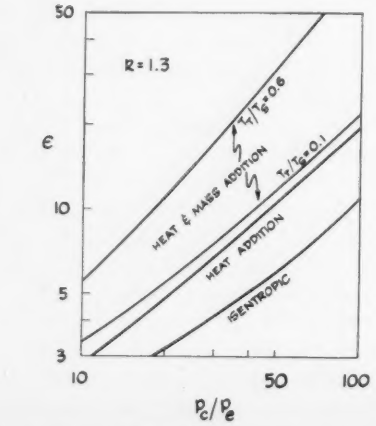


FIG. 2 AREA EXPANSION RATIO AGAINST PRESSURE RATIO.

To define completely the geometry of the nozzle, it is necessary to know, in addition to its expansion ratio, the throat area required for the passage of a given mass flow at any operating pressure ratio. We shall now derive expressions relating the throat area of an adiabatic nozzle to the throat areas of the two types of isothermal nozzles for the same total mass flow at the completion of chemical reaction.

Consider first the case of heat addition only. The mass of gas passing the throat is the same for both the adiabatic and isothermal flows; hence

$$v_t^* \rho_t^* A_t^* = v_s^* \rho_s^* A_s^* \quad [32]$$

where the subscripts $t$ refer to the isothermal expansion, the subscripts $s$ refer to the adiabatic expansion, and the asterisk denotes the values of the quantities at the throat of each nozzle. After insertion of the proper values for the density and velocity of the gas stream at the throat for both expansions in Equation [32], the following expression is obtained after some algebraic manipulation:

$$A_t^*/A_s^* = \sqrt{ke}\left[\frac{2}{k+1}\right]^{\frac{k+1}{2(k-1)}}\left[1 + \frac{k-1}{k}\ln(p_c/p_e)\right]^{1/2} \quad [33]$$

For the Case 2 isothermal process, with mass addition, the total mass flow through the throat is not equal to the common value prevailing for the Case 1 and isentropic expansions. Recasting Equation [18] gives

$$\frac{dw}{w} = \frac{2M dM}{M_f^2 - M^2} \quad [34]$$

from which it follows that

$$\frac{w^*}{w_c} = \frac{M_f^2}{M_f^2 - M_t^2} \quad [35]$$

where $w_c$ is the mass flow of propellant entering the nozzle from the combustion chamber, $w^*$ is the mass flow of propellant at the throat, $M_t$ is the Mach number of the flow at the throat, and $M_f$ is the parameter defined previously. If $r$ is the weight ratio of the deficient component to the other component in a stoichiometric mixture, the ratio of the mass flows at the throat will be given by:

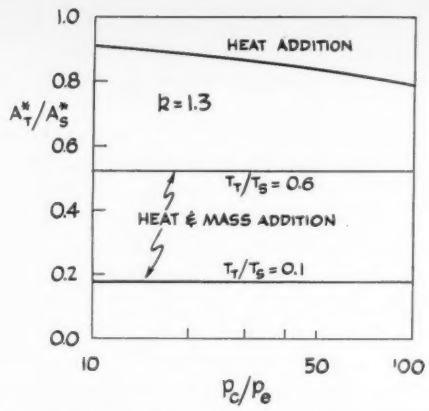


FIG. 3 RATIO OF THROAT AREA FOR ISOTHERMAL EXPANSION TO THROAT AREA FOR ADIABATIC EXPANSION AGAINST PRESSURE RATIO.

$$\frac{w^*}{w} = \frac{M_f^2}{(1+r)(M_f^2 - M_t^2)} \quad \ldots\ldots [36]$$

where $w$ is the mass rate of flow through the isentropic nozzle. Treating this case in a manner similar to that used in the previous instance, the result is

$$\frac{A_t^*}{A_s^*} = \frac{1}{M_t}\left[\frac{T_t}{T_s}\right]^{1/2}\left[\frac{2}{k+1}\right]^{\frac{k+1}{2(k-1)}} \left[\frac{M_f^2\left(1 - \frac{M_t^2}{M_f^2}\right)^{-kM_f^2}}{(1+r)(M_f^2 - M_t^2)}\right]\exp\left[-\frac{k}{2}M_t^2\right] \quad \ldots [37]$$

The throat area ratios for both types of isothermal expansion are shown in Fig. 3. For the case of heat addition alone, the throat area is approximately 10 per cent less than that for the adiabatic expansion over the entire pressure range plotted and decreases gradually with increasing pressure ratio. For the case of both heat and mass addition, the throat area ratio is independent of the pressure ratio and is a function of the temperature ratio $T_t/T_s$ alone. The curves in Fig. 3 have been calculated for a mixture ratio $r$ equal to unity. The throat area for the case of heat and mass addition is considerably smaller than it is for an adiabatic expansion and decreases with decreasing temperature ratio.

In order to achieve a balanced evaluation of the characteristics of an isothermal expansion, the possible penalty in performance incurred as a result of the lowered operating temperature must be investigated. This is best shown by the relation between the specific impulse of an isentropic and an isothermal expansion as a function of the operating pressure ratio. The velocity of the gas stream at the nozzle exit may be determined from the following equation for an isothermal expansion:

$$v_{T_e}^2 = M_e^2 kRT_t \quad \ldots\ldots [38]$$

in which $v_{t_e}$ is the velocity and $M_e$ the Mach number of the flow at the nozzle exit. The velocity of a gas at the end of an adiabatic expansion may, on the other hand, be represented by

$$v_{s_e}^2 = \frac{2kR}{k-1}T_s\left[1 - \left(\frac{p_e}{p_c}\right)^{\frac{k-1}{k}}\right] \quad \ldots\ldots [39]$$

The ratio of the isothermal to the adiabatic specific impulse will be equal to the ratio of the terminal gas velocities for the two types of expansions and will be given for both Case 1 and Case 2 by

$$I_t/I_s = M\left[\frac{\left(\frac{k-1}{2}\right)\frac{T_t}{T_s}}{1 - \left(\frac{p_e}{p_c}\right)^{\frac{k-1}{k}}}\right]^{1/2} \quad \ldots\ldots [40]$$

For the Case 1 isothermal expansion, both the temperature ratio and the Mach number at the nozzle exit are uniquely determined by the operating pressure ratio and may be replaced by their equivalent expressions in terms of pressure ratio with the following result:

$$I_t/I_s = \left[\frac{\frac{k-1}{k}\ln\left(\frac{p_c}{p_e}\right)}{\left\{1 + \frac{k-1}{k}\ln\left(\frac{p_c}{p_e}\right)\right\}\left\{1 - \left(\frac{p_e}{p_c}\right)^{\frac{k-1}{k}}\right\}}\right]^{1/2} \quad \ldots [41]$$

The comparison between the performance of an isothermal and an isentropic expansion operating at the same pressure ratio is presented in Fig. 4 as a function of pressure ratio. For the heat and mass addition process (Case 2), the specific impulse ratio is a function

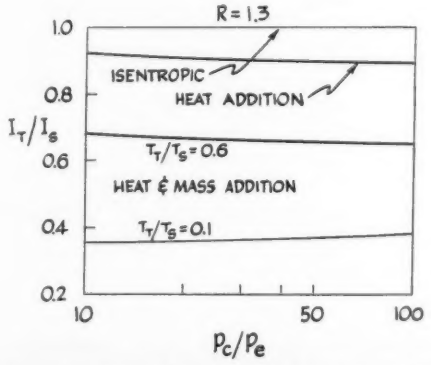


FIG. 4 RATIO OF ISOTHERMAL TO ADIABATIC SPECIFIC IMPULSE AGAINST PRESSURE RATIO FOR CORRECT EXPANSION.

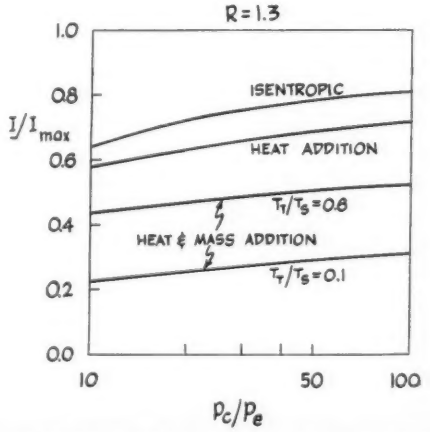


FIG. 5 THERMODYNAMIC EFFICIENCY OF EXPANSION AGAINST PRESSURE RATIO.

of the expansion temperature as well as the pressure ratio. This type of isothermal expansion is seen to be much inferior to the Case 1 expansion from the standpoint of propellant economy; moreover, it becomes progressively worse with decreasing temperature ratio over the range of values considered. Even the Case 1 process, however, is slightly inferior in performance to the isentropic expansion, its relative performance also decreasing with increasing pressure ratio for this range of values. Actually the specific impulse ratio for the Case 1 expansion eventually goes through a minimum and begins to increase at higher pressure ratios, approaching unity asymptotically. The curves for the Case 2 expansion also exhibit a different behavior at pressure ratios much higher than those plotted here; the temperature ratio curves cross over, and the specific impulse ratio increases with decreasing temperature ratio at a constant pressure ratio. However, the high pressure ratios at which these effects set in are beyond the range of practical interest.

It is instructive to compare the thermodynamic efficiencies of the energy conversion process in the various kinds of expansion. One measure of this efficiency is the ratio of the specific impulse attained at any pressure ratio to the maximum specific impulse obtainable (at an infinite pressure ratio). The expressions for this parameter as a function of pressure ratio are readily deduced from Equations [38] and [39] for the gas velocity and are as follows:

(*a*) Isentropic expansion

$$I/I_{\max} = \left[1 - \left(\frac{p_e}{p_c}\right)^{\frac{k-1}{k}}\right]^{1/2} \quad \ldots\ldots [42]$$

(*b*) Isothermal expansion, Case 1

$$I/I_{\max} = \left[\frac{\frac{k-1}{k}\ln\left(\frac{p_c}{p_e}\right)}{1 + \frac{k-1}{k}\ln\left(\frac{p_c}{p_e}\right)}\right]^{1/2} \quad \ldots\ldots [43]$$

(*c*) Isothermal expansion, Case 2

$$I/I_{\max} = M\left[\left(\frac{k-1}{2}\right)\frac{T_t}{T_s}\right]^{1/2} \quad \ldots\ldots [44]$$

The plot of the thermodynamic efficiency against pressure ratio for all the expansions, shown in Fig. 5, reveals that the isentropic expansion is the most efficient in its utilization of pressure for the conversion of heat into mechanical energy. The isothermal expansion involving heat and mass addition is significantly poorer in its pressure utilization than either of the other two processes and is adversely affected by decreasing temperature ratio.

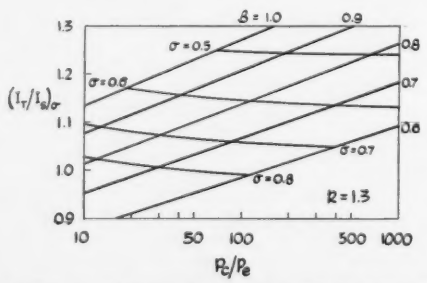


FIG. 6 RATIO OF ISOTHERMAL TO ADIABATIC SPECIFIC IMPULSE AGAINST PRESSURE RATIO. SITUATION IN WHICH MORE HEAT IS AVAILABLE THAN CAN BE UTILIZED IN AN ADIABATIC EXPANSION.

It is possible to conceive of at least one situation in which the performance of an isothermal jet engine can surpass that of an adiabatic engine, namely the situation in which more heat is available to the working fluid in the engine than can be utilized in an adiabatic process due to structural limitations of the combustion chamber and nozzle materials. Such a condition might arise in the use of high impulse rocket propellants, where adiabatic flame temperatures in the order of 5000 K are possible, or in the external addition of heat from a nuclear reactor which can supply a relatively limitless amount of energy. We shall complete our comparison of the isothermal and adiabatic expansion cycles with the analysis of this case. This will be carried out only for the Case 1 isothermal expansion, since the performance of the Case 2 expansion is too poor to warrant further consideration.

Let us now define the following quantities:

$T_L$, the limiting adiabatic chamber temperature (static and total are equal).

$\beta$, the ratio of the limiting isothermal expansion static temperature to the limiting adiabatic chamber temperature.

$T_{sL}$, the stagnation temperature of the isothermal flow at the nozzle exit for a static temperature of $\beta T_L$.

$\sigma$, the ratio of the limiting adiabatic chamber temperature to the stagnation temperature of the isothermal flow.

The value of $\beta$ can never exceed unity and will be fixed by the maximum permissible rate of heat transfer in the nozzle, which in turn will be proportional to the stream total temperature, all other things being equal. Hence the limitations of the nozzle material will set a maximum tolerable stream total temperature. Presumably this temperature will be lower than the adiabatic chamber temperature due to the greater value of the heat transfer coefficient in the nozzle as compared with the combustion chamber.

The parameter $\sigma$ is in effect a measure of the relative amounts of heat utilized in the adiabatic and isothermal expansions, respectively, expressed as the ratio of the two quantities. It is related to the parameter $\beta$ and the operating pressure ratio in the following way:

$$\sigma = \left[\beta\left(1 + \frac{k-1}{k}\ln\frac{p_c}{p_e}\right)\right]^{-1} \quad \ldots\ldots [45]$$

The relation between the stagnation temperature of the isothermal flow and the adiabatic limiting temperature is given by:

$$T_{sL} = \left[1 + \frac{k-1}{k}\ln\frac{p_c}{p_e}\right]\beta T_L \quad \ldots\ldots [46]$$

From the preceding two equations the exhaust velocity of the isothermal flow is found to be

$$v_t = [2c_pT_s(1 - \beta\sigma)]^{1/2} \quad \ldots\ldots [47]$$

while for the adiabatic flow the exhaust velocity is

$$v_e = \left[2c_p T_e \sigma \left\{1 - \left(\frac{p_e}{p_c}\right)^{\frac{k-1}{k}}\right\}\right]^{1/2} \quad \ldots\ldots\ldots [48]$$

The ratio of the isothermal to the adiabatic specific impulse for the case of excess heat available is then

$$(I_t/I_a)_\sigma = \left[\frac{\beta \frac{k-1}{k} \ln \frac{p_c}{p_e}}{1 - \left(\frac{p_e}{p_c}\right)^{\frac{k-1}{k}}}\right]^{1/2} \quad \ldots\ldots\ldots [49]$$

In Fig. 6 families of curves have been drawn which depict the variation of the specific impulse ratio with pressure ratio for a series of values of the parameter $\beta$. Lines of constant $\sigma$ have been cross-plotted on the same co-ordinate system to form a network which completely defines the performance of an isothermal rocket relative to an adiabatic rocket when excess heat is available.

It is evident that the performance increase obtained with an isothermal expansion, in the case of an unlimited energy source, is a function of the pressure ratio alone and may be read directly from the plots for the proper values of $\beta$. In the case where the total energy available is limited, the curves, entered at appropriate values of $\sigma$ and $\beta$, yield the pressure ratio necessary to utilize this amount of energy in an isothermal expansion and the associated increase in specific impulse. To illustrate, suppose that a certain propellant combination possesses an adiabatic flame temperature of 4400 K in the pressure range of interest and that the maximum chamber gas temperature the proposed rocket can tolerate is 3500 K. Let us further suppose that the maximum temperature that can be tolerated in the nozzle gas is 0.8 times this value, and that the specific heat ratio for the gases concerned is 1.3. In this example, $\sigma$ and $\beta$ are both equal to 0.8. Entering the network at these values, the pressure ratio required to utilize all the available chemical energy is found to be 12, and the increase in specific impulse of the isothermal expansion over the adiabatic expansion is approximately $2^1/_2$ per cent. If a higher pressure ratio is available for the expansion, the isothermal expansion temperature may be reduced, but the gain in specific impulse will not change.

### Conclusions

The preceding analysis has demonstrated that, in general, an isothermal expansion is a less desirable process than an adiabatic expansion for the conversion of chemical energy into mechanical energy in a jet propulsion device. The thermodynamic efficiency and performance of an isothermal expansion cycle are lower than those of an adiabatic cycle, and larger area ratios are required in the nozzle for the same pressure expansion ratio. These disadvantages, coupled with the formidable practical problems inherent in the attainment of an isothermal expansion, ordinarily outweigh any benefit of reduced operating temperatures.

(*Continued on page 287*)

# Effect of Local Variations in Mixture Ratio on Rocket Performance[1]

By DAVID ALTMAN[2] and JACK LORELL[3]

Jet Propulsion Laboratory, California Institute of Technology, Pasadena, Calif.

**The influence of local variations in mixture ratio in a rocket-motor combustion chamber on the motor performance is analyzed with regard to arbitrary modes of such variation.[4] The results of this analysis show that the effect in question can be evaluated by referring to a curve of theoretical specific impulse vs. weight fraction. In particular, if such a curve has a negative second derivative everywhere, local variations in mixture ratio can only decrease performance. If, on the other hand, there is a region with positive second derivative, then local variations in mixture ratio may improve performance; and if these variations could be controlled, the maximum performance so obtainable would be on the double tangent near the overall mixture-ratio point.**

## Nomenclature

| | | |
|---|---|---|
| $c$ | = | exhaust velocity |
| $c^*$ | = | characteristic velocity |
| $C_p$ | = | specific heat at constant pressure |
| $f$ | = | cross-sectional area in nozzle |
| $F$ | = | thrust |
| $I$ | = | specific impulse |
| $k$ | = | constant (cf. Equation [17]) |
| $\dot{m}$ | = | mass flow rate |
| $M$ | = | molecular weight of gases |
| $p$ | = | pressure |
| $r$ | = | mixture ratio (wt. oxidizer/wt. fuel) |
| $R$ | = | gas constant |
| $S$ | = | entropy |
| $T$ | = | temperature |
| $x_i$ | = | weight fraction of total propellant in $i$th element |
| $y(\rho)$ | = | $\rho_0$ distribution which maximizes specific impulse |
| $\eta$ | = | thermodynamic efficiency |
| $\lambda$ | = | Lagrange multiplier (cf. Equation [15]) |
| $\rho$ | = | weight fraction of oxidizer in propellant |

*Subscripts*

| | | |
|---|---|---|
| $c$ | = | chamber |
| $e$ | = | exit |
| $i$ | = | combustion element |
| $t$ | = | throat |

Received Oct. 6, 1951.

[1] This paper presents the results of one phase of research carried out at the Jet Propulsion Laboratory, California Institute of Technology, under Contract No. DA-04-405-Ord 18, sponsored by the Department of the Army, Ordnance Corps.

[2] Chief, Chemistry Section. Member ARS.

[3] Research Engineer, Analysis Section. Member ARS.

[4] The authors wish to express their appreciation to Dr. Martin Summerfield, formerly of this Laboratory, for suggesting this problem and for the interesting discussions with him during the analysis.

## I Thermodynamic Treatment

### (a) *Consideration of Thermodynamic Limitations*

THERMODYNAMICALLY there does not seem to be any objection to the attainment of an increased or decreased performance if there is nonuniform mixing of the fuel and oxidizer streams. Even if the total enthalpy of the combustion gas, relative to the elements at some base temperature, is a constant (in an adiabatic system) regardless of mixing, the distribution of energy among its various forms can be considerably changed, and hence the entropy and thermodynamic efficiency of the system altered. Depending upon which additional energy states are available, the entropy can be shifted up or down by mixing variations, and hence the work potential of the combustion gas is increased or decreased, respectively. Two simple illustrations will suffice to demonstrate this effect.

EXAMPLE 1: Consider a rocket motor $A$ operating with helium gas heated to 2000 K, and an adjacent motor $B$ identical in all respects except that half of the gas is at 1500 K and the other half at 2500 K. For the sake of argument, the difficulties in maintaining the sharp temperature boundary in the gas in motor $B$ may be disregarded since this boundary has no relation to the principle concerned. Now the specific impulse $I$ and the entropy $S$ are given by the following equations (for a nondissociating gas with constant specific heat):

$$I = \sqrt{\frac{2C_pT_c}{M}\left[1 - (p_e/p_c)^{R/C_p}\right]} = \sqrt{\frac{2C_pT_c}{M}\eta} \quad \ldots\ldots [1]$$

$$S = S_{300}^{\circ} + C_p \ln \frac{T_c}{300} - R \ln p_c \quad \ldots\ldots [2]$$

where

| | | |
|---|---|---|
| $T_c$ | = | chamber temperature |
| $p_c$ | = | chamber pressure |
| $p_e$ | = | exit pressure |
| $C_p$ | = | specific heat at constant pressure |
| $\eta$ | = | thermodynamic efficiency |
| $S_{300}^{\circ}$ | = | standard entropy at 300 K |

As is shown in Section I ($b$), the $I$ of motor $B$ is determined by taking the weighted average of the $I$ values corresponding to the two temperatures. Thus

$$I(B) = \frac{1}{2}\sqrt{\frac{C_p}{M}\eta}\,(\sqrt{1500} + \sqrt{2500}) \quad \ldots\ldots [3]$$

It is now evident that $I(A) > I(B)$ since $\sqrt{2000} > {}^1/_2(\sqrt{1500}+\sqrt{2500})$ and $\eta$ is the same for both motors.

Similarly, it is found that

$$S_A - S_B = C_p(\ln 2000 - {}^1/_2 \ln 1500 - {}^1/_2 \ln 2500)$$

$$= C_p \ln \frac{2000}{(1500 \times 2500)^{1/2}} > 0$$

Thus, for the case of a monatomic gas with constant specific heat in which only the translational energy states are activated, a nonuniform energy distribution will cause a lowering of the entropy and hence of performance.

EXAMPLE 2: An examination will now be made of a system in which other energy states besides translational are available. Consider a rocket motor $A$ containing hydrogen at 20.4 atm and 6000 K. At this temperature, equilibrium-constant data on $H_2$ show that it is about 92.5 per cent dissociated into atoms. Consider also a rocket motor $B$ identical with $A$ in all respects except that half of the gas has 12 kcal more heat per gram and the other half has 12 kcal less heat per gram. Equilibrium calculations show that the hotter half will attain a chamber temperature of 8000 K ($H_2$ is 100 per cent dissociated), an increase of 2000 K, whereas the cooler half will be 5450 K ($H_2$ is 75.5 per cent dissociated), showing a drop of only 550 K. This effect, which may be contrasted with that of the motor containing helium, results from the fact that a lowering of the temperature causes H atoms to recombine, thus liberating heat. A performance calculation carried out for the three temperatures 5450, 6000, and 8000 K yields the $I$ values (frozen expansion assumed for simplicity) of 1238, 1325, and 1550 sec, respectively. Thus the net $I$ observed for rocket $B$ would be ${}^1/_2$ (1238 + 1550) = 1394 sec, which represents about a 5 per cent increase in $I$ although the total heat content per gram of hydrogen in the chamber is the same in both cases. If equilibrium were assumed, the magnitude of the increase would have been diminished, but the general conclusion would be the same. The entropy difference between motors $A$ and $B$ is not significant in this case because the thermodynamic efficiencies of the two systems are different.

These two examples show that, when temperature variations are imposed on an adiabatic system, the propellant performance may be shifted up or down depending upon the availability of the various internal and chemical energy states of the molecules. In a rocket system such temperature variations may be accomplished through deviations in mixture ratio, but it would be necessary to know the equilibrium composition of each mixture-ratio element before conclusions could be drawn concerning whether performance was increased or decreased. Since the character of the $I$-$r$ plot depends on the thermodynamic distribution of energy in the combustion gas, conclusions concerning observed performance when inhomogeneous mixing occurs can be be drawn directly from such a curve.

### (b) *Performance of Rocket Containing Several Distinct Mixture Ratios in Combustion Gas*

It will be demonstrated here that the parameters $c^*$, $c$, and $I$ for the whole motor can be evaluated as weighted averages of the corresponding local parameters.[5] In carrying out this analysis, the following assumptions were made: (1) Each element at a given mixture ratio $r$ of oxidizer to fuel remains intact throughout expansion. (2) Friction and thermal conduction between filaments are negligible. (3) Each element reaches its minimum cross section at the throat and thus operates under the same constant pressure ratio. (4) Each element is in thermodynamic chemical equilibrium corresponding to its own composition.
Let

$x_i$ = weight fraction of total propellant in $i$th element
$f_i$ = throat area occupied by $i$th element
$\dot{m}_i$ = mass flow rate of $i$th element
$f_t$ = total throat area

The basic equations are

$$\dot{m}_i = x_i \dot{m} \quad [4]$$

$$c^*_i = \frac{p_c f_i}{\dot{m}_i} \quad [5]$$

$$c^* = \frac{p_c f_t}{\dot{m}} \quad [6]$$

The relation between $c^*$ and the quantities $c^*_i$ is obtained through the condition that

$$f_t = \sum_i f_i = \frac{1}{p_c} \sum_i \dot{m}_i c^*_i = \frac{\dot{m}}{p_c} \sum_i x_i c^*_i \quad [7]$$

Equations [6] and [7] can now be combined to yield

$$c^* = \sum_i x_i c^*_i \quad [8]$$

Similarly it can be shown that the exhaust velocities and hence $I$ should be averaged in the same way. If $F_i = \dot{m}_i c_i$ is the thrust contribution of the $i$th element, then

$$F = \sum_i F_i = \sum_i \dot{m}_i c_i = \dot{m} \sum_i x_i c_i = \dot{m} c \quad [9]$$

The last equality of Equation [9] shows that

$$c = \sum_i x_i c_i \quad [10]$$

Since it has been shown that the parameters $c^*$, $c$, and $I$ are evaluated by weighted averages, the problem remains to determine what arbitrary weighting shall be placed on the various mixture ratios in order to maximize the $I$. This problem is treated in Section II.

## II Mathematical Analysis

### (a) *Mathematical Formulation*

The problem of maximizing the specific impulse of a

[5] "Influence of Non-Uniform Mixing of Fuel and Oxygen on Characteristic Data of a Rocket Motor," by Carl Wagner, Fort Bliss, Texas, TR No. 22, Aug. 1947. In this report the influence of statistical deviations from uniform mixing is discussed, and the conclusion is reached that the effect on performance is least in the neighborhood of flat regions of the impetus-mixture ratio curve. This conclusion is implied as a special case of the present results.

rocket motor, as has been described earlier in this paper, can be interpreted mathematically as follows: Let $I(\rho)$ be a given function of $\rho$, single-valued, bounded, and nonnegative for $\rho$ on the interval 0 to 1. Then for each value of $\rho$ (for example, $\rho = \rho_0$) it is required to find a function $y(\rho)$ which satisfies the conditions

$$y(0) = 0 \text{ and } y(1) = 1 \quad [11]$$

$$y(\rho) \text{ increases monotonically with } \rho \quad [12]$$

$$\int_{\rho=0}^{1} \rho \, dy(\rho) = \rho_0 \text{ where } 0 \leq \rho_0 \leq 1 \quad [13]$$

and which maximizes the integral

$$I_1(\rho_0) = \int_{\rho=0}^{1} I(\rho) \, dy(\rho) \quad [14]$$

The function $I(\rho)$ corresponds, of course, to the curve of specific impulse vs. weight fraction for the given propellant system. The distribution function $y(\rho)$ is that fraction of the total propellant which is burned at mixture ratios corresponding to values of the weight fraction less than or equal to $\rho$. Thus, condition [11] states that none of the propellant is burned at a value of $\rho$ less than zero, whereas all of it is burned at values of $\rho$ less than or equal to unity. Condition [12] asserts that the fraction burned at a given mixture ratio is not negative. Condition [13] is the statement of conservation of mass. The integral to be maximized, $I_1(\rho_0)$, is the net specific impulse of the motor written as the weighted average of local specific impulses (cf. Section I (*b*)).

### (*b*) *Impossibility of Continuous and Differentiable Solution*

Since the problem involves maximizing an integral with regard to a variable function, the methods of the calculus of variations are applicable. However, as will be seen next, the Euler equation of the calculus of variations does not yield a useful solution. In fact, there is in general no continuous and differentiable solution of the type that satisfies the Euler equation. If there were such a solution, Euler's equation would take the form

$$\frac{d}{d\rho}\left[\frac{\partial}{\partial y'}(y'I + \lambda y)\right] - \frac{\partial}{\partial y}(y'I + \lambda y) = 0 \quad [15]$$

where $\lambda$ is a Lagrange multiplier, i.e., a constant.

Equation [15] reduces to

$$I' - \lambda = 0 \quad [16]$$

whence $I'$ is a constant. Thus a solution exists only if $I$ is linear in $\rho$; that is, of the form

$$I = \lambda\rho + k \quad [17]$$

In this case, Equation [14] becomes

$$\left.\begin{aligned} I_1(\rho_1) &= \int_0^1 (\lambda\rho + k)\, dy\,(\rho) \\ &= \lambda \int_0^1 \rho \, dy\,(\rho) + k \int_0^1 dy\,(\rho) \\ &= \lambda\rho_0 + k = I(\rho_0) \end{aligned}\right\} \quad [18]$$

That is, the maximized specific impulse function $I_1$ coincides with the given function $I$. Thus the only case for which the Euler equation yields a solution proves to be uninteresting.

### (*c*) *Geometric Derivation of Solution*

A direct method of attack yields better results. In fact, the general analytic solution to the problem as stated in Section II (*a*) can be given. The analytic solution, which involves considerable detail not relevant to the physical understanding of the problem, is given elsewhere.[6] The following geometric interpretation is, perhaps, more enlightening.

Consider the specific impulse function $I(\rho)$ shown in the accompanying sketch. It is apparent that the value of $I(\rho)$ at point $C$ is exceeded by the weighted average

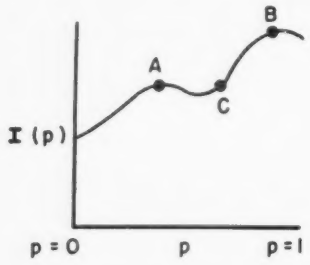


of the values of $I(\rho)$ at points $A$ and $B$. This weighted average, in fact, lies on the straight line connecting $A$ and $B$. On the other hand, the value of $I(\rho)$ at point $B$ cannot be exceeded by any weighted average because no chord of the curve lies above $B$.

Extrapolating these results gives the following criterion for increasing $I(\rho)$ by means of weighted averages. If, for any value of $\rho$ (for example, $\rho = \rho_0$), the curve $I(\rho)$ has a chord passing above $I(\rho_0)$ and has its ends on either side of $\rho_0$, the weighted average of the values of $I(\rho)$ at the ends of the chord exceeds $I(\rho_0)$. If no such chord can be found, $I(\rho_0)$ cannot be exceeded by weighted averages. It follows that the maximum weighted average is determined by the chord which is also tangent to $I(\rho)$ at its ends or, more generally, which lies above $I(\rho)$ over the whole range.

Thus the maximum specific impulse is obtained as a weighted average of the specific impulse at only two points. Averaging over more than two points cannot give further improvement.

## III Application to Several Propellant Systems

The results of Section II show that if the $I(\rho)$ curve is continuous everywhere, as is generally true for propellant systems investigated thus far, then the existence of a line touching at least two points of the $I(\rho)$ curve and lying above the curve defines a region in which $I(\rho_1) \geq I(\rho_0)$. This section is devoted to the examination of two typical $I(\rho)$ curves (calculated on basis of equilibrium expansion) in order to determine whether or not such tangent lines can be formed.

### (*a*) *RFNA-Aniline*

Fig. 1 is a plot of the specific impulse $I$ vs. the weight fraction $\rho$ of RFNA. At the $\rho$ values of 0.5 and 0.4,

[6] David Altman and Jack Lorell, Jet Propulsion Laboratory, Pasadena, Calif., PR No. 9-51, Jan. 15, 1951 (Restricted).

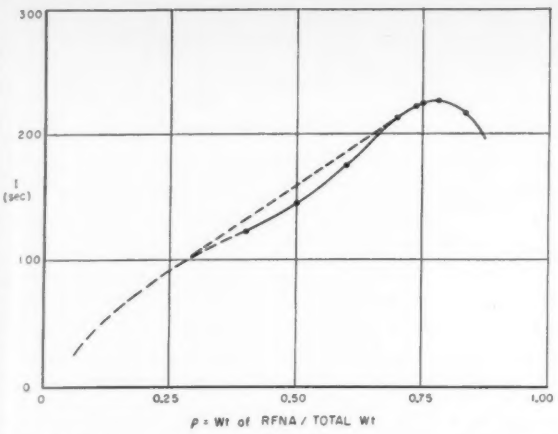


FIG. 1. SPECIFIC IMPULSE OF RFNA AND ANILINE VS. WEIGHT FRACTION OF RFNA

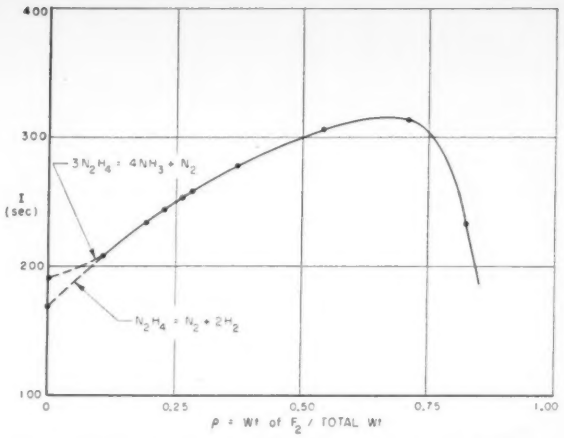


FIG 2. SPECIFIC IMPULSE OF $H_2l$ AND $F_2(l)$ VS. WEIGHT FRACTION OF $F_2$

the chamber temperatures are 1345 and 1230 K, respectively, allowing for the formation of carbon and methane. Other hydrocarbons were not considered because of the complexity of the calculations, although it is not believed that their omission will appreciably alter the results.

Since the $I$ curve should go approximately to zero at $\rho = 0$, a reasonable extrapolation shows a point of inflection near $\rho = 0.3$. This point permits the drawing of a tangent line between $\rho = 0.3$ and 0.7 maximizing $I$ in that interval. Thus, in the mixture-ratio range of 0.43 to 2.33, it is possible to observe performance above the theoretical as a result of inhomogeneous mixing.

**(b) $N_2H_4$-$F_2(l)$**

Fig. 2 is a graph of the specific impulse of $N_2H_4$ and $F_2(l)$ over a considerable range of $\rho$. The value of $I$ at $\rho = 0$ has the value for $N_2H_4$ as a monopropellant, corresponding to either of the reactions $N_2H_4 = N_2 + 2H_2$ or $3N_2H_4 = NH_3 + N_2$. The entire portion of this curve from $\rho = 0$ to 0.83 shows no region where $d^2I/d\rho^2 > 0$, and hence the maximum $I$ coincides with the curve.

## IV Conclusions

The results of this study have yielded the following practical conclusions:

1 Uniform equilibrium combustion throughout the cross section of a rocket motor does not necessarily yield the highest performance attainable at that mixture ratio unless it corresponds to the over-all maximum performance.

2 Nonhomogeneous mixing of propellant streams can either raise or lower $I$ depending on the shape of the $I$-$\rho$ curve. If $d^2I/d\rho^2 > 0$ for some value of $\rho$, nonuniform mixing will generally improve performance if the nonuniformities are not too large.

3 The region of possible improvement of performance by nonuniform mixing can be recognized quickly by examining an $I$-$\rho$ curve. If the curve is such that a straight line can be drawn touching the curve at two points but lying above the curve between these two points, then an improvement in performance is possible for values of $\rho$ between these two points. In fact, the new $I$-$\rho$ curve follows this straight line.

4 The facts presented in this paper point to a possible explanation of a common observation that combustion efficiencies in a given motor and injector are generally higher on the under-oxidized portion of the $I$-$\rho$ curve than near stoichiometric. Since all injectors have some degree of nonuniformity, the shape of the performance curve will influence the observed performance at a given mixture ratio.

# Servo-Stabilization of Combustion in Rocket Motors

H. S. TSIEN[1]

Daniel and Florence Guggenheim Jet Propulsion Center, California Institute of Technology, Pasadena, Calif.

**This paper shows that the combustion in the rocket motor can be stabilized against any value of time lag in combustion by a feedback servo link from a chamber pressure pickup, through an appropriately designed amplifier, to a control capacitance on the propellant feed line. The technique of stability analysis is based upon a combination of the Satche diagram and the Nyquist diagram. For simplicity of calculation, only low-frequency oscillations in monopropellant rocket motors are considered. However, the concept of servo-stabilization and method of analysis are believed to be generally applicable to other cases.**

THE phenomenon of rough burning in liquid-propellant rocket motor has been interpreted as the instability of the coupled system of propellant feed and combustion chamber by D. F. Gunder and D. R. Friant (1),[2] M. Yachter (2), M. Summerfield (3), and L. Crocco (4). The essential feature of these theories is the time lag between the instant of injection of the propellant and the instant when the propellant is burned into hot gas. Crocco has further improved on this concept by considering the time lag as an integrated effect of consecutive stages, each of which is controlled by the prevailing pressure in the combustion chamber. As a result of this new concept, Crocco showed the possibility of intrinsic instability with constant injection rate not influenced by the chamber pressure.

The present paper will first give a slightly more general formulation of Crocco's concept of time lag, allowing arbitrary pressure dependence of lag. Then the problem of intrinsic stability is discussed by applying a method suggested by M. Satche (5). This method is based upon a modification of the Nyquist diagram and is particularly useful for systems having time lag. For easy reference, this new diagram will be called the Satche diagram. The later sections of the paper will show the possibility of stabilizing the combustion by means of a feedback servo for all values of time lag. Such possibility of servo-stabilization was first mentioned by W. Bollay in his admirable paper (6) on the application of servomechanisms to aeronautics. The present study definitely shows the power of this idea.

## Time Lag in Combustion

Let $\dot{m}_b(t)$ be the mass rate of generation of hot gas by combustion at time instant $t$. Consider, for simplicity, a monopropellant motor. Then the mass rate of injection at $t$ can be denoted by $\dot{m}_i(t)$. Let $\tau(t)$ be the time lag for that parcel of propellant which is burned at the instant $t$. Then the mass burned during the interval from $t$ to $t + dt$ must be equal to the mass injected during the time from $t - \tau$ to $t - \tau + d(t - \tau)$. Thus

$$\dot{m}_b(t)dt = \dot{m}_i(t - \tau)d(t - \tau) \quad [1]$$

The mass of hot gas generated is either used to fill the combustion chamber by raising its pressure $p(t)$, or is discharged through the rocket nozzle. If the frequency of the possible oscillations in the chamber is small, then the pressure in the chamber can be considered as uniform, and as a first approximation (7) the rate of flow through the nozzle can be taken as proportional to the instantaneous chamber pressure $p(t)$. Thus if $\bar{\dot{m}}$ is the steady mass rate flow through the system, $\bar{M}_g$ is the average mass of hot gas in the chamber, and if the volume occupied by the unburned liquid propellant is neglected

$$\dot{m}_b\, dt = \bar{\dot{m}} \left(\frac{p}{\bar{p}}\right) dt + d\left(\bar{M}_g \frac{p}{\bar{p}}\right) \quad [2]$$

where $\bar{p}$ is the steady state pressure in the combustion chamber.

By following Crocco, the nondimensional variables for the chamber pressure and the rate of injection are defined as

$$\varphi = \frac{p - \bar{p}}{\bar{p}}, \quad \mu = \frac{\dot{m}_i - \bar{\dot{m}}}{\bar{\dot{m}}} \quad [3]$$

$\varphi$ and $\mu$ are then the fractional deviation of pressure and injection rate from the average. With Equation [3], $\dot{m}_b$ can be eliminated from Equations [1] and [2], and

$$\frac{\bar{M}_g}{\bar{\dot{m}}} \frac{d\varphi}{dt} + \varphi + 1 = \left(1 - \frac{d\tau}{dt}\right)[\mu(t - \tau) + 1] \quad [4]$$

To calculate the quantity $d\tau/dt$, Crocco's concept of pressure dependence of time lag has to be introduced. If the rate at which the liquid propellant is prepared for the final rapid transformation into hot gas is a function $(p)$, then the lag $\tau$ is determined by

$$\int_{t-\tau}^{t} f(p)\, dt = \text{const} \quad [5]$$

By differentiating Equation [5] with respect to $t$,

$$[f(p)]_t - [f(p)]_{t-\tau}\left(1 - \frac{d\tau}{dt}\right) = 0$$

The concept of small perturbation from the steady state will now be explicitly introduced: Assume that the deviation of the pressure $p$ from the steady state value $\bar{p}$ is small. Then $f(p)$ at the instant $t$ and $f(p)$ at the instant $t - \tau$ can be expanded as Taylor's series around $\bar{p}$. By taking only the first order terms,

Received February 22, 1952.

[1] Robert H. Goddard Professor of Jet Propulsion.

[2] Numbers in parentheses refer to the References on page 268.

$$[f(p)]_t = f(\bar{p}) + \bar{p}\left(\frac{df}{dp}\right)_{p=\bar{p}} \varphi(t)$$

$$[f(p)]_{t-\tau} = f(\bar{p}) + \bar{p}\left(\frac{df}{dp}\right)_{p=\bar{p}} \varphi(t-\tau)$$

Here $\tau$ is the lag at the average pressure $\bar{p}$, a constant now. Then

$$1 - \frac{d\tau}{dt} = 1 + \left(\frac{d \log f}{d \log p}\right)_{p=\bar{p}} [\varphi(t) - \varphi(t-\tau)] \quad [6]$$

By combining Equations [4] and [6], the following equation is obtained

$$\frac{d\varphi}{dz} + \varphi = \mu(z-\delta) + n[\varphi(z) - \varphi(z-\delta)] \quad [7]$$

where

$$n = \left(\frac{d \log f}{d \log p}\right)_{p=\bar{p}} \quad [8]$$

and

$$z = t/\theta_g, \quad \theta_g = \overline{M}_g/\overline{m} \quad [9]$$

If $n$ is a constant independent of $\bar{p}$, then $f(p)$ is proportional to $p^n$. This is the form of $f(p)$ assumed by Crocco. The present formulation of the problem is slightly more general in that $f(p)$ is arbitrary and the value of $n$ is to be computed by using Equation [8], and is a function of $\bar{p}$. $\theta_g$ is, of course, the gas transit time.

### Intrinsic Instability

Crocco called the instability of combustion with constant rate of injection the intrinsic instability. If the injection rate is constant and not influenced by the chamber pressure $p$, then $\mu \equiv 0$. Therefore the stability problem is controlled by the following simple equation obtained from Equation [7],

$$\frac{d\varphi}{dz} + (1-n)\varphi(z) + n\varphi(z-\delta) = 0 \quad [10]$$

Now let

$$\varphi(z) \sim e^{sz}$$

Then

$$s + (1-n) + ne^{-\delta s} = 0 \quad [11]$$

This is the equation for the exponent $s$.

Crocco determined the value of the complex number $s$ by studying the set of two equations for the real and the imaginary parts of Equation [11]. However, if the point of interest is whether the system is stable or not, one can use the well-known Cauchy theorem with advantage. Let

$$G(s) = e^{-\delta s} - \left[-\frac{1-n}{n} - \frac{s}{n}\right] \quad [12]$$

Then the question of stability is determined by whether $G(s)$ has zeros in the right half of the complex $s$-plane. This question itself can be in turn answered by watching the argument of $G(s)$ when $s$ traces a contour enclosing the right half $s$-plane. Specifically, let $s$ trace clockwise the contour consisting of the imaginary axis and a large half circle to the right of the imaginary axis (Fig. 1). If the vector $G(s)$ makes a number of complete clockwise

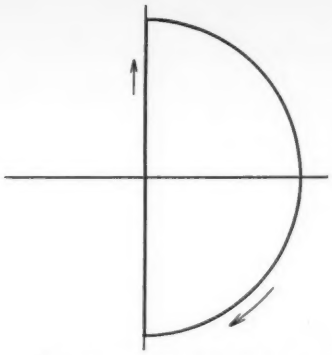

FIG. 1. CONTOUR TRACED BY THE VARIABLE $s$ FOR THE SATCHE DIAGRAM OR THE NYQUIST DIAGRAM

revolutions, then that number is, according to Cauchy's theorem, the difference between the number of zeros and the number of poles of $G(s)$ in the right half $s$-plane. Since $G(s)$ evidently has no poles in the $s$-plane, the number of revolutions of $G(s)$ is the number of zeros. Hence for stability, the vector $G(s)$ must not make any complete revolutions, as $s$ traces the specified contour. Therefore the stability question can be answered by plotting graphically $G(s)$ on the complex plane. This graph is, of course, the well-known Nyquist diagram.

A direct application of this method to $G(s)$ given by Equation [12] is, however, inconvenient for the complication caused by lag term $e^{-\delta s}$ (8). M. Satche (5), however, proposed a very elegant and ingenious method of treating such a system with time lag: Instead of $G(s)$, break it into two parts,

$$G(s) = g_1(s) - g_2(s) \quad [13]$$

where

$$g_1(s) = e^{-\delta s}$$

$$g_2(s) = -\frac{1-n}{n} - \frac{s}{n} \quad [14]$$

The vector $G(s)$ is thus a vector with vertex in $g_1(s)$ and its tail on $g_2(s)$. The graph of $g_1(s)$ is the unit circle for $s$ on the imaginary axis. For $s$ on the large half circle, $g_1(s)$ is within the unit circle. The graph of $g_2(s)$ is the straight line (Fig. 2) paralleled to the imaginary axis when $s$ is on the imaginary axis. When $s$ is on the large half circle, $g_2(s)$ is a half of a large circle closing the contour on the left. A moment's reflection will show that in order for the vector $G(s)$ not to make complete revolutions for any value of $\delta$, the

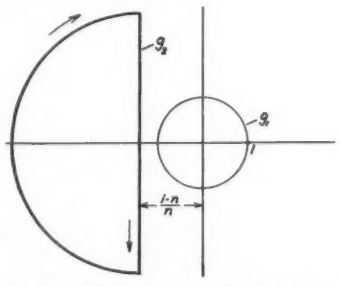


FIG. 2. STABLE SATCHE DIAGRAM FOR INTRINSIC OSCILLATIONS; $0 < n < 1/2$

$g_2(s)$ contour must lie completely out of the $g_1(s)$ contour. That is, for unconditional intrinsic stability

$$\frac{1-n}{n} > 1 \quad \text{or} \quad \frac{1}{2} > n > 0 \ldots\ldots\ldots [15]$$

When $n > 1/2$, the $g_1(s)$ contour and the $g_2(s)$ contour intersect. Stability is still possible, however, if for $g_2(s)$

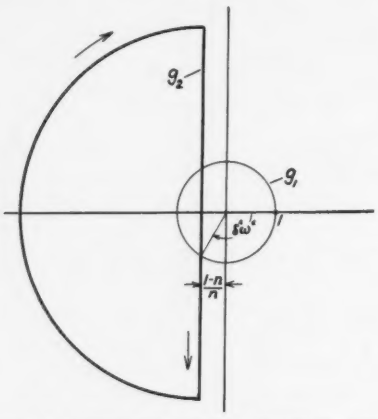


FIG. 3. UNSTABLE SATCHE DIAGRAM FOR INTRINSIC OSCILLATIONS; $n > 1/2$

within the unit circle (Fig. 3), $g_1(s)$ is to the right of $g_2(s)$. This condition is satisfied if

$$\cos(\delta\sqrt{2n-1}) > -\frac{1-n}{n}$$

Or if

$$\delta < \delta^*$$

where

$$\delta^* = \frac{1}{\sqrt{2n-1}} \cos^{-1}\left(-\frac{1-n}{n}\right) = \frac{1}{\sqrt{2n-1}}\left(\pi - \cos^{-1}\frac{1-n}{n}\right) \ldots [16]$$

When $\delta = \delta^*$, then with

$$\omega^* = \sqrt{2n-1} \ldots\ldots\ldots [17]$$

$G(i\omega^*) = 0$. Therefore when $\delta = \delta^*$, $\varphi$ has the oscillatory solution with the angular frequency $\omega^*$.

These results on intrinsic stability were obtained by Crocco. The present discussion with the Satche diagram, however, seems to be simpler. For the more complicated stability problem treated below with feed system and servo control, the solution is hardly practical without the Satche diagram.

### System Dynamics with Servo Control

Consider now a system including the propellant feed and a servo control represented by Fig. 4. In order to approximate the elasticity of the feed line, a spring load capacitance is put at the midway point between the propellant pump and the injector. The spring constant is to be computed from the feed-line dimensions.[3] Near the injector there is another capacitance controlled by the servo. The servo receives its signal from the chamber pressure pickup through an amplifier. If the feed system and the motor design are fixed by the designer, the question is whether it is possible to design an appropriate amplifier so that the whole system will be stable. Because there is no accurate information on the time lag of combustion, a practical design should specify unconditional stability, i.e., stability for any value of $\delta$.

Let $\dot{m}_0$ be the instantaneous mass flow rate out of the propellant pump, and $p_0$ be the instantaneous pressure at the outlet of pump. The average flow rate must be $\bar{m}$. The average pressure is $\bar{p}_0$. The pump characteristics can be represented by the following equation,

$$\frac{p_0 - \bar{p}_0}{\bar{p}_0} = -\alpha \frac{\dot{m}_0 - \bar{m}}{\dot{m}} \ldots\ldots\ldots [18]$$

If the time rate of change of mass flow is small, $\alpha$ is simply related to the slope of the head-volume curve of the pump at constant speed near the steady-state operating point. For constant pressure pump or the simple pressure feed, $\alpha$ is zero. For conventional centrifugal pumps, $\alpha$ is approximately 1. For displacement pumps, $\alpha$ is very large.

Let $\dot{m}_1$ be the instantaneous mass rate of flow after the spring loaded capacitance, $\chi$ the spring constant of the capacitance, and $p_1$ the instantaneous pressure at the capacitance. Then

$$\dot{m}_0 - \dot{m}_1 = \rho\chi \frac{dp_1}{dt} \ldots\ldots\ldots [19]$$

where $\rho$ is the density of the propellant, a constant.

In the following calculation, the pressure drop in the line by frictional forces will be neglected. Then the pressure difference $p_0 - p_1$ is due to the acceleration of the flow only. That is

$$p_0 - p_1 = \frac{l}{2A} \frac{d\dot{m}_0}{dt} \ldots\ldots\ldots [20]$$

where $A$ is the cross-sectional area of the feed line, a constant, and $l$ is the total length of the feed line. Similarly, if $p_2$ is the instantaneous pressure at the control capacitance.

$$p_1 - p_2 = \frac{l}{2A} \frac{d\dot{m}_1}{dt} \ldots\ldots\ldots [21]$$

If the mass capacity of the control capacitance is $C$, then

$$\dot{m}_1 - \dot{m}_i = \frac{dC}{dt} \ldots\ldots\ldots [22]$$

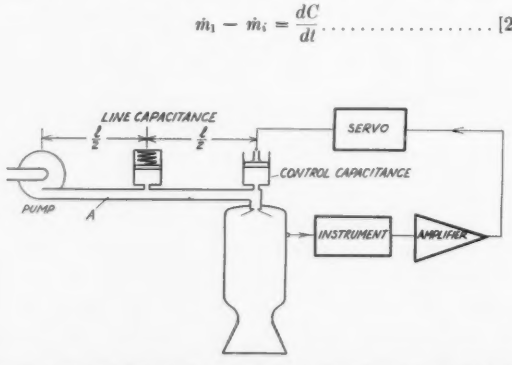


FIG. 4. SERVO-CONTROLLED LIQUID MONOPROPELLANT ROCKET MOTOR

[3] See the Appendix for details.

Since the control capacitance is very close to the injector, the inertia of the mass of propellant between the control capacitance and the injector is negligible. Then

$$p_2 - p = \frac{1}{2}\frac{\dot{m}_i^2}{\rho A_i^2} \quad \ldots\ldots [23]$$

where $A_i$ is the effective orifice area of the injector. $A^4$ can be eliminated from the calculation by noting that at steady state, the difference of pressures $\bar{p}_0$ and $\bar{p}$, or $\Delta\bar{p}$ is

$$\bar{p}_0 - \bar{p} = \Delta\bar{p} = \frac{1}{2}\frac{\bar{\dot{m}}^2}{\rho A_i^2} \quad \ldots\ldots [24]$$

Equations [18] to [24] describe the dynamics of the feed system. By a straightforward process of elimination of variables, a relation between $\dot{m}_i$, $p$, and $C$ is obtained. To express this relation in nondimensional form, the following quantities are introduced, following the notation of Crocco:

$$P = \frac{\bar{p}}{2\Delta\bar{p}}, \quad E = \frac{2\Delta\bar{p}}{\bar{\dot{m}}\theta_g}\rho\chi, \quad J = \frac{l\dot{m}}{2\Delta\bar{p}A\theta_g} \quad \ldots\ldots [25]$$

and

$$\kappa = C/\bar{\dot{m}}\theta_g \quad \ldots\ldots [26]$$

where $\theta_g$ is the gas transit time given by Equation [9]. Then the nondimensional equation relating $\varphi$, $\mu$, and $\kappa$ is

$$P\left\{1 + E\left(P+\frac{1}{2}\right)\frac{d}{dz} + \frac{JE}{2}\frac{d^2}{dz^2}\right\}\varphi + \left[\left\{1+\alpha\left(P+\frac{1}{2}\right)\right\} + \left\{\alpha E\left(P+\frac{1}{2}\right)+J\right\}\frac{d}{dz} + \left\{\frac{\alpha JE}{2}\left(P+\frac{1}{2}\right)+\frac{JE}{2}\right\}\frac{d^2}{dz^2} + \frac{J^2E}{4}\frac{d^3}{dz^3}\right]\mu + \left[\alpha\left(P+\frac{1}{2}\right)\frac{d}{dz} + J\frac{d^2}{dz^2} + \frac{\alpha JE}{2}\left(P+\frac{1}{2}\right)\frac{d^3}{dz^3} + \frac{J^2E}{4}\frac{d^4}{dz^4}\right]\kappa = 0 \ldots [27]$$

where $z$ is the nondimensional time variable defined by Equation [9].

The dynamics of the servo control are specified by the composite of the instrument characteristics of the pressure pickup, the response of the amplifier, and the properties of the servo. Since it is not the purpose of the present paper to discuss the detailed design of the servo control, the over-all dynamics of the servo control are represented by the following operator equation:

$$F\left(\frac{d}{dz}\right)\varphi = \kappa \quad \ldots\ldots [28]$$

where $F$ is the ratio of two polynomials with the denominator of higher order than the numerator.

Equations [7], [27], and [28] are the three equations for the three variables $\varphi$, $\mu$, and $\kappa$. Since they are equations with constant coefficients, the appropriate forms for the variables are

$$\varphi = ae^{sz}, \quad \mu = be^{sz}, \quad \kappa = ce^{sz} \quad \ldots\ldots [29]$$

By substituting Equation [29] into Equations [7,] [27], and [28], three homogeneous equations for $a$, $b$, and $c$ are obtained. In order for $a$, $b$, $c$ to be nonzero, the determinant formed by their coefficients must vanish. This condition can be written as follows:

$$[s+(1-n)]\left[\frac{J^2E}{4}s^3 + \frac{JE}{2}\left\{1+\alpha\left(P+\frac{1}{2}\right)\right\}s^2 + \left\{\alpha E\left(P+\frac{1}{2}\right)+J\right\}s + \left\{1+\alpha\left(P+\frac{1}{2}\right)\right\}\right] + e^{-\delta s}\left\{\frac{nJ^2E}{4}s^3 + \left[\frac{nJE}{2}\left\{1+\alpha\left(P+\frac{1}{2}\right)\right\} + \frac{JEP}{2}\right]s^2 + \left[n\left\{\alpha E\left(P+\frac{1}{2}\right)+J\right\} + \alpha EP\left(P+\frac{1}{2}\right)\right]s + \left[n\left\{n+\alpha\left(P+\frac{1}{2}\right)\right\} + P\right] + sF(s)\left[\frac{J^2E}{4}s^3 + \frac{\alpha JE}{2}\left(P+\frac{1}{2}\right)s^2 + Js + \alpha\left(P+\frac{1}{2}\right)\right]\right\} = 0 \ldots [30]$$

This is the equation for determining the exponent $s$. $F(s)$ is now recognized as the over-all transfer function of the servo-control link. The complete system stability depends upon whether Equation [30] gives roots that have positive real parts.

### Instability Without Servo Control

The system characteristics without the servo control can be simply obtained from the basic Equation [30] by setting $F(s) = 0$. Let it be assumed that the polynomial multiplied into $e^{-\delta s}$ has no zero in the positive half $s$-plane, as is usually the case. Then Equation [30] can be divided by that polynomial without introducing poles in the positive half $s$-plane into the resultant function. That is, for the Satche diagram, one has again

$$G(s) = g_1(s) - g_2(s), \qquad g_1(s) = e^{-\delta s}$$

$g_1(s)$ is thus again the "unit circle." $g_2(s)$ is now much more complicated:

$$g_2(s) = -\left[\frac{s}{n} + \frac{1-n}{n}\right]\frac{\frac{J^2E}{4}s^3 + \frac{JE}{2}\left\{1+\alpha\left(P+\frac{1}{2}\right)\right\}s^2 + \left\{\alpha E\left(P+\frac{1}{2}\right)+J\right\}s + \left\{1+\alpha\left(P+\frac{1}{2}\right)\right\}}{\frac{J^2E}{4}s^3 + \frac{JE}{2}\left\{1+\alpha\left(P+\frac{1}{2}\right)+\frac{P}{n}\right\}s^2 + \left\{\alpha E\left(P+\frac{1}{2}\right)\left(1+\frac{P}{n}\right)+J\right\}s + \left\{1+\alpha\left(P+\frac{1}{2}\right)+\frac{P}{n}\right\}} \quad \ldots [31]$$

The intercept of $g_2(s)$, when $s$ is pure imaginary, is given by setting $s = 0$ in Equation [31], i.e.,

$$g_2(0) = -\frac{1-n}{n}\frac{1+\alpha\left(P+\frac{1}{2}\right)}{1+\alpha\left(P+\frac{1}{2}\right)+\frac{P}{n}} \quad \ldots\ldots [32]$$

Since all the parameters $n$, $\alpha$, $P$ are positive, the magnitude of $g_2(0)$ is now smaller than the magnitude of $g_2(0)$ given by Equation [14] for the intrinsic stability problem. Thus the effect of the feed system is to move the $g_2(s)$ curve toward the unit circle of $g_1(s)$ in the Satche diagram. For instance, for $n = 1/2$, $g_2(s)$ is just tangent to the unit circle for the intrinsic system without considering the propellant feed. But with the propellant feed system, $g_2(s)$ contour will intersect the

unit circle and the system will become unstable, for time lag $\delta$ exceeds a certain finite value. The influence of the feed system is thus always destabilizing. This is further confirmed by considering the asymptote of $g_2(s)$ for large imaginary $s$, obtained from Equation [31]. That is

$$g_2(s) \sim -\left[\frac{s}{n} + \left(\frac{1-n}{n} - \frac{2P}{Jn^2}\right) + \ldots.\right], \qquad |s| \gg 1 \ldots [33]$$

Therefore, for large imaginary $s$, $g_2(s)$ approaches asymptotically a line parallel to the imaginary axis at a distance

$$\frac{1-n}{n} - \frac{2P}{Jn^2}$$

to the left of the imaginary axis. The effect of the feed system is again to move $g_2(s)$ toward the unit circle.

It is thus evident that for the parameter $n$ near $1/2$ or larger than $1/2$, it would be impossible to design the system for unconditional stability. In the Satche diagram, $g_1(s)$ contour and $g_2(s)$ will always intersect without a servo control.

### Complete Stability with Servo Control

If the polynomial $H(s)$

$$H(s) = \frac{J^2E}{4}s^3 + \left[\frac{JE}{2}\left\{1 + \alpha\left(P + \frac{1}{2}\right)\right\} + \frac{JEP}{2n}\right]s^2 + \left[\alpha E\left(P + \frac{1}{2}\right) + \frac{\alpha EP}{n}\left(P + \frac{1}{2}\right)\right]s + \left[1 + \alpha\left(P + \frac{1}{2}\right) + \frac{P}{n}\right] + \frac{1}{n}sF(s)\left[\frac{J^2E}{4}s^3 + \frac{\alpha JE}{2}\left(P + \frac{1}{2}\right)s^2 + Js + \alpha\left(P + \frac{1}{2}\right)\right] \ldots [34]$$

which multiplies into $e^{-\delta s}$ in Equation [30], has no poles and zeros in the right half $s$-plane, then the occurrence zeros of the expression in Equation [30] in the right half $s$-plane can be determined from the Satche diagram with

$$g_1(s) = e^{-\delta s}$$

and

$$g_2(s) = -\left[\frac{s}{n} + \frac{1-n}{n}\right]\left[\frac{J^2E}{4}s^3 + \frac{JE}{2}\left\{1 + \alpha\left(P + \frac{1}{2}\right)\right\}s^2 + \left\{\alpha E\left(P + \frac{1}{2}\right) + J\right\}s + \left\{1 + \alpha\left(P + \frac{1}{2}\right)\right\}\right] \Big/ H(s) \ldots [35]$$

As $s$ traces the contour of Fig. 1, $g_1(s)$ is again a unit circle. Therefore, if simultaneously the $g_2(s)$ contour is completely outside the unit circle, there can be no root of Equation [30] in the right half $s$-plane. In other words, if the transfer function $F(s)$ of the servo-control link is so designed as to place the $g_2(s)$ contour completely out of the unit circle (Fig. 5), then the system is stabilized for all time lags.

As an example, take

$$n = \frac{1}{2}, \quad P = \frac{3}{2}, \quad J = 4, E = \frac{1}{4}, \quad \alpha = 1$$

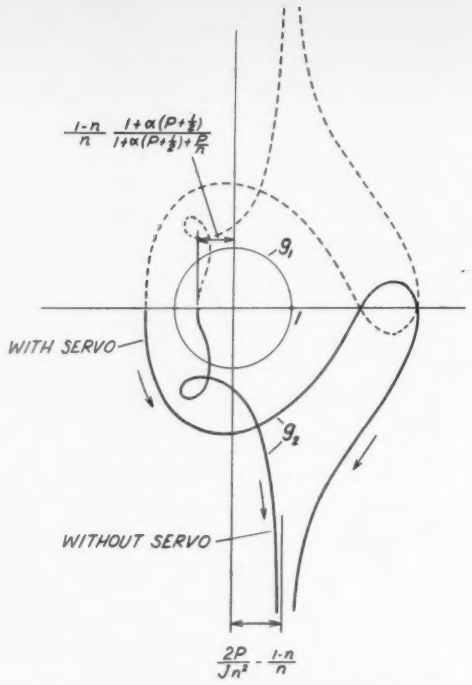


FIG. 5. SATCHE DIAGRAM FOR THE ORIGINAL AND FOR THE SERVO-STABILIZED SYSTEM

Then without the servo control, the $g_2(s)$ is

$$g_2(s) = -\frac{1}{2}\frac{(2s+1)(2s^3+3s^2+9s+6)}{s^3+3s^2+6s+6}$$

Of primary interest is the behavior of $g_2(s)$ when $s$ is a pure imaginary number $i\omega$, $\omega$ real. Thus

$$g_2(i\omega) = -\frac{1}{2}\frac{(6-21\omega^2+4\omega^4)(6-3\omega^2)+\omega^2(21-8\omega^2)(6-\omega^2)}{(6-3\omega^2)^2+\omega^2(6-\omega^2)^2} - \frac{1}{2}i\omega\frac{(21-8\omega^2)(6-3\omega^2)-(6-21\omega^2+4\omega^4)(6-\omega^2)}{(6-3\omega^2)^2+\omega^2(6-\omega^2)^2}$$

This contour for $\omega \geq 0$ is plotted in Fig. 6. It is evident that for sufficiently large values of time lag, the system will be unstable. On the other hand, if the $g_2(s)$ contour can be changed by the servo control to, say,

$$g_2(s) = -2\frac{(s+2)(s+3)}{(s+6)}$$

Then, as plotted in Fig. 6, the new $g_2$ contour is completely outside of the unit circle of $g_1(s)$. Therefore the system is now unconditionally stable. A straightforward calculation from Equations [31] and [35] shows that the required transfer function $F(s)$ for the servo link is

$$F(s) = -4.875\frac{(s+1.0528)(s^2+0.7164s+2.6304)}{s(s+2)(s+3)(s+0.5332)(s^2+0.4668s+3.7511)}$$

The servo link has thus the character of an integrating circuit. If, with given response of the chamber pressure pickup and of the servo for the control capacitance, an amplifier could be designed to give an over-all transfer function close to that specified above, the combustion can be stabilized by such a servo control.

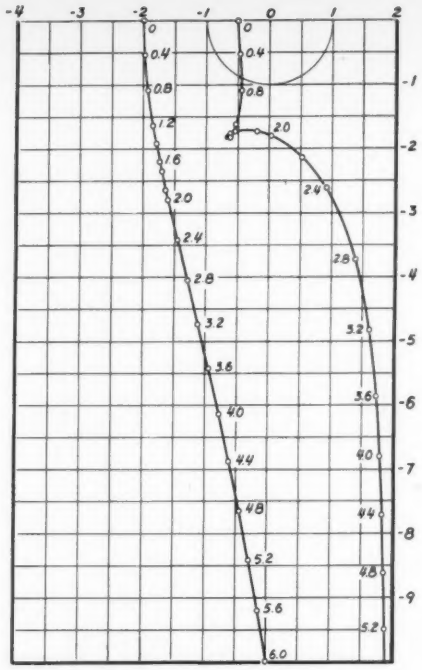

FIG. 6. SATCHE DIAGRAM FOR THE ORIGINAL AND FOR THE SERVO-STABILIZED SYSTEM

$P = {}^3/_2, J = 4, E = {}^1/_4, \alpha = 1$

($g_2(i\omega)$ without servo intersects the unit circle; $g_2(i\omega)$ with servo is outside the unit circle. Numbers beside points are the value of $\omega$.)

As the second example, take

$$n = \frac{1}{2}, P = \frac{3}{2}, J = 4, E = \frac{1}{4}, \alpha = 0$$

Since $\alpha = 0$, the feed pressure $p_0$ is thus constant with even variable flow of propellant. The case then corresponds to that of a simple pressure feed. Without the servo control,

$$g_2(s) = -\frac{1}{2}\frac{(2s+1)(2s^3+s^2+8s+2)}{s^3+2s^2+4s+4}$$

When $s$ is pure imaginary,

$$g_2(i\omega) = -\frac{1}{2}\frac{(4-2\omega^2)(2-17\omega^2+4\omega^4)+\omega^2(4-\omega^2)(12-4\omega^2)}{(4-2\omega^2)^2+\omega^2(4-\omega^2)^2} - \frac{1}{2}i\omega\frac{(4-2\omega^2)(12-4\omega^2)-(4-\omega^2)(2-17\omega^2+4\omega^4)}{(4-2\omega^2)^2+\omega^2(4-\omega^2)^2}$$

This contour of $g_2$ is plotted in Fig. 7. It is evident that without servo control the combustion will be unstable for sufficiently long time lag. In fact, the system is even less stable than the system considered in the first example: It will become unstable at shorter time lag. The part of the $g_2$ contour near $\omega = 2$ is of special interest. Near $\omega = 2$, the contour comes so close to the unit circle of $g_1$ that if the value of time lag $\delta$ is such as to make $g_1$ and $g_2$ for $\omega \sim 2$ very close to each other, then an almost undamped oscillation at $\omega \sim 2$ can occur. This critical value of $\delta$ is evidently smaller than the critical $\delta$ determined from the true intersection of $g_2$ with the unit circle at $\omega \sim 0.65$. Such near instability at smaller values of time lag can be easily overlooked in the analytic treatment of the stability condition by Crocco, and yet such possible instability should not be dismissed. This, perhaps, indicates the superiority of the present graphical method.

For unconditional stability, $g_2$ should be displaced out of the unit circle, to, say, the same "stable" contour as in the first example. The required transfer function $F(s)$ is calculated to be

$$F(s) = -4.875\frac{(s+0.8126)(s^2-0.04337s+2.6506)}{s^2(s+2)(s+3)(s^2+4)}$$

The required servo link must then have the character of double integrating circuit. Furthermore, the transfer function has two purely imaginary poles at $\pm 2i$. This unrealistic requirement on the amplifier comes from the original feed-system dynamics and is due to the neglect of frictional damping in the feed line. In any actual system, the frictional damping in the feed line will remove these purely imaginary poles of the required transfer function $F(s)$ and replace them by two complex conjugate poles.

## Stability Criteria

In the preceding discussion of servo-stabilization, it is assumed that the polynomial $H(s)$, Equation [34], has no pole or zero in the right half $s$-plane. This is, however, not necessarily the case. In general then, one should first investigate the number of zeros and poles of $H(s)$ in the right half $s$-plane. To do this, it

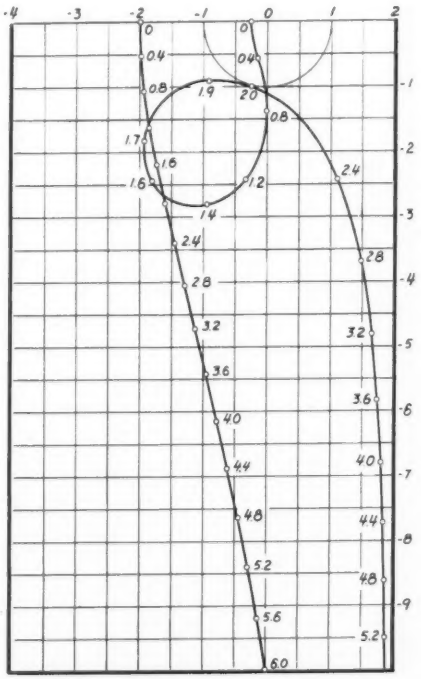

FIG. 7. SATCHE DIAGRAM FOR THE ORIGINAL AND FOR THE SERVO-STABILIZED SYSTEM

$P = {}^3/_2, J = 4, E = {}^1/_4, \alpha = 0$

($g_2(i\omega)$ without servo intersects the unit circle; $g_2(i\omega)$ with servo is outside the unit circle. Numbers beside points are the value of $\omega$.)

should be recognized that the polynomial in Equation [34] before the factor $F(s)$ usually does not have zeros in the right half $s$-plane. Therefore instead of studying $H(s)$, one can study the ratio of $H(s)$ and that polynomial. That is, the number of zeros and poles of $H(s)$ in the right half $s$-plane is the same as the number of zeros and poles of the following function

$$1 + K(s) = \frac{H(s)}{\frac{J^2E}{4}s^3 + \left[\frac{JE}{2}\left\{1 + \alpha\left(P + \frac{1}{2}\right)\right\} + \frac{JEP}{2n}\right]s^2 + \left[\alpha E\left(P + \frac{1}{2}\right) + \frac{\alpha EP}{n}\left(P + \frac{1}{2}\right)\right]s + \left[1 + \alpha\left(P + \frac{1}{2}\right) + \frac{P}{n}\right]} \quad \ldots [36]$$

where

$$K(s) = \frac{\frac{1}{n}sF(s)\left[\frac{J^2E}{4}s^3 + \frac{\alpha JE}{2}\left(P + \frac{1}{2}\right)s^2 + Js + \alpha\left(P + \frac{1}{2}\right)\right]}{\frac{J^2E}{4}s^3 + \left[\frac{JE}{2}\left\{1 + \alpha\left(P + \frac{1}{2}\right)\right\} + \frac{JEP}{2n}\right]s^2 + \left[\alpha E\left(P + \frac{1}{2}\right) + \frac{\alpha EP}{n}\left(P + \frac{1}{2}\right)\right]s + \left[1 + \alpha\left(P + \frac{1}{2}\right) + \frac{P}{n}\right]} \quad \ldots [37]$$

According to the Nyquist criterion, the number of poles and zeros for $1 + K(s)$ in the right half $s$-plane can be found by plotting the Nyquist diagram of $1 + K(s)$ with $s$ tracing the contour of Fig. 1. In fact, if $1 + K(s)$ or $H(s)$ has $r$ zeros and $q$ poles in right half $s$-plane then $K(s)$ will carry out $r-q$ clockwise revolutions around the point $-1$, as $s$ traces the contour of Fig. 1. Hence the necessary information on $H(s)$ can be obtained by plotting the Nyquist diagram of $K(s)$.

When one divides the Equation [30] by $H(s)$ in order to obtain $g_1(s)$ and $g_2(s)$ as given by Equation [35], $g$ zeros and $r$ poles are introduced in the right half $s$-plane. The g poles of $K(s)$ must come from $F(s)$, since the polynomial in the denominator of Equation [37] has no zero in the right half $s$-plane. Therefore the original expression in Equation [30] also has $g$ poles in the right half $s$-plane. Hence in order for the original expression in Equation [30] to have no zero in the right half $s$-plane, $g_2(s)$ must make $-q + (q - r) = -r$ clockwise revolutions around the unit circle. In order for stability to be unconditional, i.e., stable for all time lag, the $g_2(s)$ contour should never intersect the unit circle. Therefore the general unconditional stability criteria are, first, $g_2(s)$ contour completely outside of the unit circle; and, second, $g_2(s)$ making $r$ counterclockwise revolutions around the unit circle as $s$ traces the conventional contour enclosing the right half $s$-plane. These are the criteria for stability with the Satche diagram. To determine $r$, one has to use the Nyquist diagram of $K[s]$, Equation [37]. Thus the stability problem for the general case requires both the Satche diagram and the Nyquist diagram (Fig. 8).

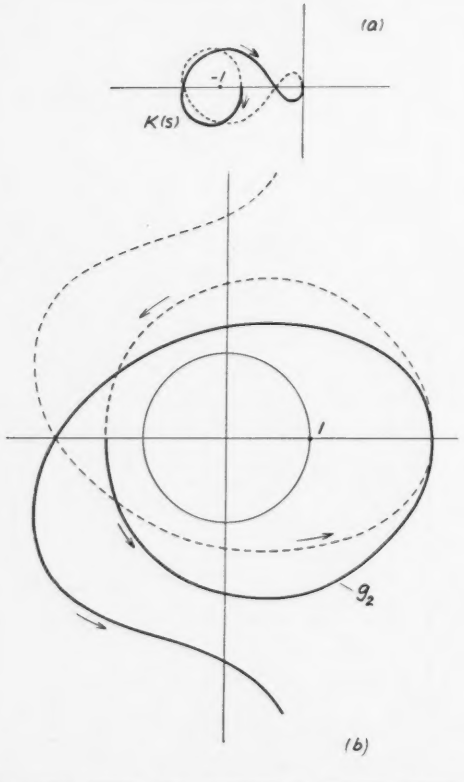


FIG. 8. FULL CURVE FOR POSITIVE $\omega$; DOTTED CURVE FOR NEGATIVE $\omega$.
($a$) Nyquist diagram for $K(s)$, with two zeros for $1 + K(s)$ in right half $s$-plane. ($b$) Corresponding stable Satche diagram.

## Concluding Remarks

In the previous sections of this paper, the theoretical possibility of completely stabilizing the combustion for any value of time lag by servo control is demonstrated. The great flexibility of electronic amplifier seems to indicate that this theoretical possibility can be always realized. On the other hand, without the servo link, unconditional stability is shown to be generally impossible. Therefore the concept of feedback servo is indeed a powerful tool in controlling the behavior of a time-lag system. It is to be realized, of course, that the proposed scheme is but one among many. No attempt is made here to give an exhaustive treatment of all possible schemes. The best scheme is certainly to be determined by detailed considerations on all aspects of the engineering problem, such as the possibility of high-frequency acoustic oscillations which are not considered here. The main purpose here is to give a general discussion of the concept together with a suggested general method of analyzing the stability by the Satche diagram.

(*Continued on page 268*)

# Longitudinal Vibrations of Gas at Ambient Pressure in a Rocket Thrust Chamber[1]

I. ELIAS[2]
University of California, Los Angeles, Calif.

ROBERT GORDON[3]
Aerojet Engineering Corporation, Azusa, Calif.

**An analysis is presented for the determination of the natural frequency in longitudinal vibration of a static gas mass at ambient pressure contained in a rocket thrust chamber. The technique used is the Rayleigh-Ritz method of equating the kinetic energy to the work done in a conservative system, and determining the natural frequencies from the solution of the differential equations defining the energy relationship of the system. A comparison of the expression derived from the theory and that of the one-quarter wave length oscillator is made and the relationship indicated. Tests were made to determine the resonant frequency of thrust chambers filled with air at normal temperature and pressure. Results from these tests with thrust chambers of three different configurations are presented in substantiation of the theoretical results.**

## Introduction

THE idea has been advanced that unstable combustion in the rocket motor is a manifestation of one or more of the possible modes of vibration of the gas mass contained in the chamber being excited into resonance. This theory, in order to be pursued, requires two pieces of information: (1) The frequencies associated with the various possible modes of vibration, which are best investigated under nonrocket-operating conditions, i.e., with ambient air in the system; and (2) the average temperature and molecular weight of the gases throughout the combustion chamber under combustion conditions. Knowing the natural frequencies under ambient conditions, they can then be corrected for the acoustic velocity related to the gas properties at the conditions existing in the combustion chamber. A comparison of these calculated frequencies with those measured by experiment will then serve as a check of the theory.

The normal modes of vibration of any enclosure are determined by the geometry which describes that enclosure. For the case of the rocket motor thrust chamber, its geometry lends itself best to the use of cylindrical co-ordinates for a proper definition. Consequently, there are three types of modes of vibration possible; namely those in the radial, circumferential, and longitudinal direction; or symbolically, $r$, $\theta$, and $y$. Those vibrations in the r and $\theta$ direction are quite adequately covered by the classical acoustic theory describing the oscillations in a cylinder (1).[4] However, the analysis for the longitudinal modes is not strictly applicable in view of the deviation of the rocket motor geometry from that of a constant area channel.

The literature on acoustics is quite meager on the subject of resonances in variable area ducts. A. T. Jones (2) has treated the case of longitudinal resonances in a channel consisting of two cylindrical tubes of different diameters connected by a conical section. Richardson (3) has performed an analysis, assuming a cavity as a resonator, and has derived an expression for the fundamental mode of oscillation as a function of the cavity volume and neck dimensions. This is an extension of the classical analysis (4) contained in acoustic literature pertaining to resonators characterized by having a throat with diameter small compared to the cavity diameter. Richardson's work is broader in that it is not limited by this requirement on the throat-to-cavity ratio. However, it was felt that none of these analyses could be applied satisfactorily to the rocket motor thrust chamber.

At first it seemed possible to apply the theory developed for resonances in a conical horn to this problem. The rocket motor can be broken up into two sections: (1) One section consisting of two horns with their throats adjacent to each other, thus accounting for the converging, diverging portion of the chamber, and (2) a second section consisting of a cylinder corresponding to the combustion chamber proper. The natural frequency of the entire system can then be determined by matching impedances at the two interior boundaries in accordance with transmission line theory. However, it was considered more desirable to analyze the problem directly and develop a theory based on fundamental physical principles rather than adopt secondarily derived expressions. The theory as developed is presented below.[5]

## Theory

The Rayleigh-Ritz method (5) of determining the gravest mode of oscillation of a conservative system essentially consists of four steps: (1) Assume a form of

Received Feb. 15, 1952.

[1] This work was done for the U. S. Air Force, Wright Air Development Center, early in 1951.

[2] Graduate student, Physics Department. Formerly Development Engineer, Aerojet Engineering Corporation, Azusa, Calif.

[3] Head, Projects Department, Liquid Engine Division. Member ARS.

[4] Numbers in parentheses refer to the References on page 268.

[5] Based on an approach suggested by Dr. Theodore von Kármán.

elastic displacement of the system. (2) Compute the potential energy of the system at the maximum displacement. (3) Compute the kinetic energy of the system at the neutral position, i.e., position of zero potential energy. (4) Equate the two expressions for energy.

If the system being analyzed contains potential energy at the time of maximum kinetic energy or kinetic energy at the time of maximum potential energy, then it is necessary to use differences of potential and kinetic energy rather than absolute values of these two properties. For example, if this technique were being used to analyze the behavior of a pendulum, then the difference of the potential energies would be the difference in elevation of the pendulum bob from the extreme of the swing to the neutral position, rather than the elevation of the bob above some arbitrary plane. In a similar manner, when considering the energies in a vibrating air column, one must use the difference in pressures between the maximum and minimum compression and the difference in volume between the same points. The potential energy, $U$, is thus equal to the work done by a mass of gas undergoing expansion from its maximum to minimum pressure. This is then one half the change in pressure times the change in volume, which can be written as follows (7):

$$U = -\int \frac{1}{2}\,\Delta p \Delta\left(\frac{1}{\rho}\right) dm$$

which becomes, after performing the indicated differentiation, and using the relationship

$$\frac{\Delta\rho}{\rho} = -\frac{\Delta V}{V}$$

$$U = \int \frac{1}{2}\,\frac{\Delta p}{\Delta\rho}\left(\frac{\Delta\rho}{\rho}\right)^2 dm = \int \frac{1}{2}\,\frac{\Delta p}{\Delta\rho}\left(\frac{\Delta V}{V}\right)^2 \rho S dx$$

and since $\Delta p / \Delta\rho = a^2$, where $a$ = acoustic velocity (assumed constant)

$$U = \frac{a^2}{2}\int \left(\frac{\Delta V}{V}\right)^2 \rho S dx \qquad [1]$$

Now to determine $\frac{\Delta V}{V}$:

Consider the expansion of a mass of gas, $dm$, through a duct of variable area; then the relations depicted in Fig. 1 hold where

$\xi$ = displacement of the given mass of gas
$S$ = cross-sectional area at position $x$
$\Delta x$ = thickness of slab of the given mass of gas
$\rho$ = gas density
$V$ = volume of given mass of gas

Volume before expansion $= S\Delta x$. Volume after expansion

$$= \left(S + \frac{\partial S}{\partial x}\xi\right)\left(\Delta x + \frac{\partial \xi}{\partial x}\Delta x\right)$$

$$= S\Delta x + S\Delta x\,\frac{\partial \xi}{\partial x} + \xi\Delta x\,\frac{\partial S}{\partial x} + \xi\Delta x\,\frac{\partial \xi}{\partial x}\,\frac{\partial S}{\partial x}$$

Rearranging the above expression and dropping the higher order terms, we obtain

$$\simeq S\Delta x\left[1 + \frac{1}{S}\,\frac{\partial(\xi S)}{\partial x}\right]$$

Then

$$\frac{\Delta V}{V} = \frac{S\Delta x\left[1 + \frac{1}{S}\,\frac{\partial\,(\xi S)}{\partial x}\right] - S\Delta x}{S\Delta x} = \frac{1}{S}\,\frac{\partial(\xi S)}{\partial x}$$

Then substituting into [1]

$$U = \frac{a^2}{2}\int \frac{\rho}{S}\left[\frac{\partial(\xi S)}{\partial x}\right]^2 dx \qquad [2]$$

The density $\rho$ at any position $x$ in the duct is

$$\rho = \rho_0 + \Delta\rho = \rho_0\left(1 - \frac{\rho}{\rho_0}\,\frac{\Delta V}{V}\right)$$

$$= \rho_0\left(1 - \frac{\rho}{\rho_0}\,\frac{1}{S}\,\frac{\partial(\xi S)}{\partial x}\right)$$

Then substituting into [2]

$$U = \frac{\rho_0 a^2}{2}\int \frac{1}{S}\left[\frac{\partial(\xi S)}{\partial x}\right]^2 dx - \frac{\rho a^2}{2}\int \left[\frac{1}{S}\right]^2\left[\frac{\partial(\xi S)}{\partial x}\right]^3 dx$$

The second term is dropped due to its higher order and consequent insignificance relative to the first term. (This is equivalent to assuming nearly incompressible flow, that is, small oscillations.) The final expression for the potential energy then becomes

$$U = \frac{\rho_0 a^2}{2}\int \frac{1}{S}\left[\frac{\partial(\xi S)}{\partial x}\right]^2 dx \qquad [3]$$

The kinetic energy of the system is

$$T = \int \frac{1}{2}\,v^2 dm = \int \frac{1}{2}\,v^2 \rho S dx \qquad [4]$$

Assuming plane wave motion through the duct, and assuming that the velocity will vary sinusoidally with time; then at any $x$

$$v = v_0 \sin \omega t = \left(\frac{d\xi}{dt}\right)$$

for any normal mode. The displacement is:

$$\xi = -\frac{v_0}{\omega}\cos \omega t$$

In establishing the limits of integration, we note that the kinetic energy will be a maximum at time $t = \frac{\pi}{2}\,\frac{1}{\omega}$; i.e., when the velocity is the greatest. It is this inte-

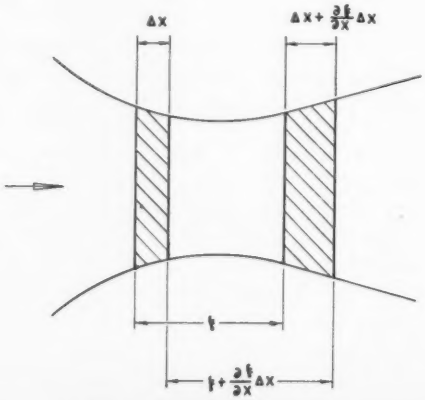


FIG. 1 VARIABLE AREA DUCT

grated maximum $T$ which is equated to the potential energy $U$. It follows, then, that

$$\xi_m = -\frac{v_0}{\omega} \cos \omega t \Big|_0^{\pi/2\omega} = \frac{v_m}{\omega}$$

$$v_m^2 = (\omega \xi_m)^2$$

The expression for the maximum kinetic energy becomes

$$T = \frac{\omega^2}{2} \int \frac{\rho}{S} (S\xi_m)^2 dx \quad \ldots\ldots [5]$$

The variation in $\rho$ may again be neglected as shown in the development for the potential energy expression. Summarizing then, the expressions for the maximum kinetic and potential energies are

$$T = \frac{\rho_0 \omega^2}{2} \int_0^L \frac{1}{S} (S\xi_m)^2 dx \quad \ldots\ldots [6]$$

$$U = \frac{\rho_0 a^2}{2} \int_0^L \frac{1}{S} \left[\frac{d(S\xi_m)}{dx}\right]^2 dx \quad \ldots\ldots [7]$$

where the limits of integration extend over the length of the cavity for the geometry shown in Fig. 2.

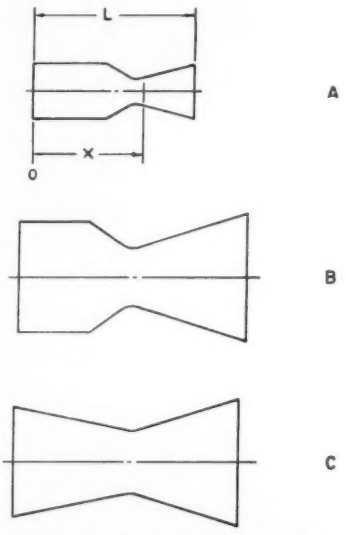


FIG. 2 THRUST CHAMBER GEOMETRIES

It remains now to relate $S$ and $\xi_m$ to $x$ in order to perform the above indicated integrations.

Since both $S$ and $\xi_m$ are functions of $x$, the equation becomes complicated mathematically. Therefore, assume a series solution

$$S\xi_m = \sum_{n=1}^{\infty} A_n \sin\left(\frac{n\pi}{2} \frac{x}{L}\right) \quad \ldots\ldots [8]$$

where the $n$'s define the characteristic values as determined by the boundary conditions of the particular configuration. The geometry under consideration has an open end,[6] and consequently only odd values of $n$ are valid. Considering only the first and third harmonics,

$$S\xi_m = A_1 \sin\left(\frac{\pi}{2} \frac{x}{L}\right) + A_3 \sin\left(\frac{3\pi}{2} \frac{x}{L}\right)$$

[6] The effect of this assumption is discussed later on in the paper.

The functions of $S\xi_m$ shown in Equations [6] and [7] are

$$(S\xi_m)^2 = \left[A_1 \sin\left(\frac{\pi}{2} \frac{x}{L}\right)\right]^2 + 2A_1A_3 \sin\left(\frac{\pi}{2} \frac{x}{L}\right) \sin\left(\frac{3\pi}{2} \frac{x}{L}\right) + \left[A_3 \sin\left(\frac{3\pi}{2} \frac{x}{L}\right)\right]^2 \ldots [9]$$

$$\left[\frac{d}{dx}(S\xi_m)\right]^2 = \left[\frac{\pi}{2L} A_1 \cos\left(\frac{\pi}{2} \frac{x}{L}\right)\right]^2 + 6\left(\frac{\pi}{2L}\right)^2 A_1A_3 \cos\left(\frac{\pi}{2} \frac{x}{L}\right) \cos\left(\frac{3\pi}{2} \frac{x}{L}\right) + \left[\left(\frac{3\pi}{2L}\right) A_3 \cos\left(\frac{3\pi}{2} \frac{x}{L}\right)\right]^2 \ldots [10]$$

Then, substituting [9] into [6] and introducing the constants $S_t$ for the minimum duct cross-sectional area, and $L$ for the length of the duct

$$T = \frac{\rho_0 \omega^2}{2} \frac{L}{S_t} [A_1^2 K_1 + 2A_1A_3K_2 + A_3^2 K_3] \ldots\ldots [11]$$

where

$$\left.\begin{aligned} K_1 &= \int_0^1 \frac{1}{S/S_t} \sin^2\left(\frac{\pi}{2} \frac{x}{L}\right) d\left(\frac{x}{L}\right) \\ K_2 &= \int_0^1 \frac{1}{S/S_t} \sin\left(\frac{\pi}{2} \frac{x}{L}\right) \sin\left(\frac{3\pi}{2} \frac{x}{L}\right) d\left(\frac{x}{L}\right) \\ K_3 &= \int_0^1 \frac{1}{S/S_t} \sin^2\left(\frac{3\pi}{2} \frac{x}{L}\right) d\left(\frac{x}{L}\right) \end{aligned}\right\} \ldots [12]$$

and substituting [10] into [7]

$$U = \frac{\rho_0 a^2}{2} \frac{L}{S_t} \left[\left(\frac{\pi}{2L}\right)^2 A_1^2 K_4 + 6\left(\frac{\pi}{2L}\right)^2 A_1A_3K_5 + \left(\frac{3\pi}{2L}\right)^2 A_3^2 K_6\right] \ldots [13]$$

where

$$\left.\begin{aligned} K_4 &= \int_0^1 \frac{1}{S/S_t} \cos^2\left(\frac{\pi}{2} \frac{x}{L}\right) d\left(\frac{x}{L}\right) \\ K_5 &= \int_0^1 \frac{1}{S/S_t} \cos\left(\frac{\pi}{2} \frac{x}{L}\right) \cos\left(\frac{3\pi}{2} \frac{x}{L}\right) d\left(\frac{x}{L}\right) \\ K_6 &= \int_0^1 \frac{1}{S/S_t} \cos^2\left(\frac{3\pi}{2} \frac{x}{L}\right) d\left(\frac{x}{L}\right) \end{aligned}\right\} \ldots [14]$$

The integrals $K_1 \ldots K_6$ are dimensionless and can be evaluated by graphical integration or by numerical methods for the particular geometry being considered. The system is conservative and therefore $T = U$. Since $T - U = 0$ must be true for all values of the two parameters $A_1$ and $A_3$, it follows:

$$\frac{\partial(T-U)}{\partial A_1} = \frac{\partial(T-U)}{\partial A_3} = 0$$

Then, conducting the above indicated operations, we obtain

$$\frac{\partial(T-U)}{\partial A_1} = \rho_0 \omega^2 \frac{L}{S_t} [A_1K_1 + A_3K_2] - \rho_0 a^2 \frac{L}{S_t} \left[\left(\frac{\pi}{2L}\right)^2 A_1K_4 + 3\left(\frac{\pi}{2L}\right)^2 A_3K_5\right] \ldots [15]$$

$$\frac{\partial(T-U)}{\partial A_3} = \rho_0 \omega^2 \frac{L}{S_t} [A_1K_2 + A_3K_3] - \rho_0 a^2 \frac{L}{S_t} \left[3\left(\frac{\pi}{2L}\right)^2 A_1K_5 + 9\left(\frac{\pi}{2L}\right)^2 A_3K_6\right] \ldots [16]$$

From [15] and [16], obtain

$$A_1\left[\omega^2 K_1 - \left(\frac{\pi a}{2L}\right)^2 K_4\right] = A_3\left[3\left(\frac{\pi a}{2L}\right)^2 K_5 - \omega^2 K_2\right] \quad \ldots [17]$$

$$A_1\left[\omega^2 K_2 - 3\left(\frac{\pi a}{2L}\right)^2 K_5\right] = A_3\left[9\left(\frac{\pi a}{2L}\right)^2 K_6 - \omega^2 K_3\right] \ldots [18]$$

The ratio of the two constants, $A_1/A_3$, can thus be obtained from [17] or [18]. It is seen that two different values of $A_1/A_3$ are obtained. As will be seen later, two frequencies are obtained. The equation $v = v_0 \sin \omega t$ which was utilized in the derivation to establish the kinetic energy implies a single frequency along the channel for any normal mode. However, there will be different frequencies for the different normal modes. Each value of $A_1/A_3$ describes a different normal mode. (The obtaining of multiple frequencies is discussed in greater detail in Reference (8)). The calculated values of $A_1/A_3$ differ by large amounts. One value of $A_1/A_3$ may be considered to define $f_1$, while the other defines $f_3$.

At this point, it is convenient to introduce the substitution, $(\pi a/2\omega L)^2 = \theta$.

Then forming the fraction [17]/[18]

$$\frac{K_1 - \theta K_4}{K_2 - 3\theta K_5} = \frac{3\theta K_5 - K_2}{9\theta K_6 - K_3} \quad \ldots [19]$$

A quadratic expression in $\theta$ is obtained which upon solution becomes

$$\theta = -\frac{6K_2K_5 - K_3K_4 - 9K_1K_6}{18(K_4K_6 - K_5^2)} \pm \frac{\sqrt{(6K_2K_5 - K_3K_4 - 9K_1K_6)^2 - 36(K_4K_6 - K_5^2)(K_3K_1 - K_2^2)}}{18(K_4K_6 - K_5^2)} \quad \ldots [20]$$

Two values of $\theta$ are obtained, $\theta_1$, and $\theta_2$, which thus define two values of $\omega$. Then, recalling the substitution made earlier, $(\pi a/2\omega L)^2 = \theta$, and solving for $\omega$ (and neglecting the negative value), obtain

$$\omega_1 = \frac{\pi a}{2L\sqrt{\theta_1}} \qquad \omega_2 = \frac{\pi a}{2L\sqrt{\theta_2}}$$

or since, $\omega = 2\pi f$

$$f_1 = \frac{a}{4L\sqrt{\theta_1}} \qquad f_3 = \frac{a}{4L\sqrt{\theta_2}} \quad \ldots [21]$$

Note that $\theta$ is a constant which is determined solely by the geometry being considered, When $\theta = 1$, the expression for the $^1/_4\,\lambda$ oscillator is obtained. Therefore, $\sqrt{\theta}$ can be interpreted as a correction factor to the chamber length, $L$, which will make the $^1/_4\,\lambda$ formula applicable.

Furthermore, the value of $\sqrt{\theta}$ is independent of $L$, provided the dimensionless function $S/S_t = F(x/L)$ is the same for the configurations being considered. This function may be used, therefore, as a definition of acoustic similarity.

## Discussion

### 1. *Theoretical*

Calculations based on the analysis developed above were made to predict the natural frequency at ambient conditions of three thrust chambers of different configuration. Two are of the conventional rocket motor design consisting of a cylindrical section followed by a converging-diverging nozzle. A third is characterized by a conical section to the throat of the nozzle, followed by a diverging section. For purposes of this discussion, these chambers will be designated as Chambers A, B, and C, and they are shown schematically in Fig. 2. Results of the calculations are presented in Table 1.

TABLE 1

| Chamber | A | B | C |
|---|---|---|---|
| $f_1$ Calculated by Equation [21] | 127 | 96 | 102 |
| $f_3$ Calculated by Equation [21] | 576 | 384 | 359 |
| $f_1$ Calculated by Equation [23] | 142 | .. | .. |
| $f_3$ Calculated by Equation [23] | 573 | .. | .. |
| $f_1$ Experimental | 125 | 98 | 102 |

These calculations were carried through with only two terms in the series expansion, as shown previously, thus producing values for the fundamental and first overtone. It is of interest to note that the overtone is not a harmonic of the fundamental. This is in contrast to the condition for constant area pipes, where the natural frequencies in longitudinal resonance form a harmonic series.

As can be seen from the analysis, a specific application of the method involves the evaluation of six integrals when two terms are used in the series expansion. If three terms are used, there are twelve integrals developed, or generally $n(n + 1)$ expressions need to be evaluated where $n$ is the number of terms considered in the series expansion. Each of these expressions requires either graphical or numerical calculation methods for their solution—procedures which are admittedly tedious and time-consuming. Attempts to obtain a solution which is completely analytical have been unsuccessful to date.

In an attempt to simplify the method, an analysis has been conducted with only one term in the expansion for the particular tone required, i.e.,

$$S\xi_m = A_1 \sin\left(\frac{\pi}{2}\frac{x}{L}\right); \qquad S\xi_m = A_3 \sin\left(\frac{3\pi}{2}\frac{x}{L}\right) \ldots [22]$$

Resulting expressions for the frequencies are thus obtained which require only two integrals to be evaluated, or specifically,

$$f_1 = \frac{a}{4L}\sqrt{\frac{K_4}{K_1}}; \qquad f_3 = \frac{a}{4L}\sqrt{\frac{K_6}{K_3}} \quad \ldots [23]$$

where the subscripts are those identifying the integrals in [12] and [14]. Calculations carried through with this method give values for the fundamental which are 12 per cent higher than when both terms are used in the expansion. There is negligible deviation for the third harmonic. The results obtained from experimentation (which will be discussed later and are shown in Table 1) show satisfactory agreement with the frequencies calculated using two terms in the series expansion. Therefore, to obtain a satisfactory degree of accuracy, it is recommended that the lengthier set of calculations be performed.

Attention must be directed to one point. In the analysis, an assumption is made that plane wave motion exists throughout the chamber. Obviously, this as-

sumption is not rigorously correct since the sloping walls of the converging-diverging nozzle must distort the plane wave. However, it seems reasonable that the effect of the converging section on the plane wave front emanating from the cylinder will be offset by the effect of the diverging section on the resultant spherical wave. These two effects conceivably may combine to make valid a plane wave analysis for the over-all wave propagation. Certainly, the agreement obtained between the experimental and theoretical values show that the assumption of plane wave motion does not introduce enough error to make this approach invalid.

*2. Experimental Results*

Experimental results obtained from testing with the three afore-mentioned chambers are also included in Table 1. Values for the third harmonic cannot be presented due to the inconclusiveness of the experimental data obtained. The experimental technique consisted of vibrating the air mass contained in the chamber by means of a high impedance sound source driven by an audio oscillator. Resonances were detected by noting the increased output of a microphone located in the chamber as the driving frequency was swept through the audio range. Care was taken that the microphone be sufficiently small to avoid distorting the sound field present in the chamber. As can be seen by comparison with the calculated values, satisfactory agreement exists between experimental and theoretical values.

## Comparison with Organ Pipe Theory

It is interesting to compare the theory developed for the organ pipe with that developed in this paper for variable area ducts. One difference has already been indicated earlier, namely, the higher frequencies for the variable area duct are not integral values of the fundamental, as is the case for the constant area duct. It has been shown in Equation [21] that the final expression for the frequency is related to the $^1/_4$ wave-length expression by a geometrical factor, $\sqrt{\theta}$. Then, taking the chamber as a constant area duct with the same length leads to a frequency of 152 cps for Chamber A and 108 cps for Chambers B and C. A comparison of these frequencies with those calculated from the theory results in values for $\sqrt{\theta} = 1.2$, 1.13, and 1.06 for Chambers A, B, and C, respectively. It is obvious that, although Chambers B and C are of equal length, thus possessing the same frequencies when the $^1/_4\ \lambda$ expression is applied, different values for $\sqrt{\theta}$ would be obtained as a result of their considerably different internal geometries.

The theory pertaining to oscillations in a tube, from which the $^1/_4\ \lambda$ formula is derived, assumes that a true antinode exists at the open end. This is not strictly correct, however, in that the air beyond the open end is also in vibration, which consequently makes the effective length greater than the actual length. Experimenters in acoustics have observed that end corrections to the physical length are required in order to reconcile the $^1/_4\ \lambda$ formula with test results. Values used vary from .6R to .8R (where R is the radius of the tube) depending upon the nature of the flange at the exit. Therefore, for a proper test of the applicability of the $^1/_4\ \lambda$ expression to the longitudinal resonances in rocket motor thrust chambers, it is necessary that end corrections be applied. This has been done for the three chambers, using an intermediate value of 0.7 of the radius of the exit, as the length to be added to the geometrical length of each chamber. The resultant frequencies obtained are 135 cps for Chamber A and 90 cps for Chambers B and C. For comparison, Table 2 shows the values discussed above.

TABLE 2

| Chamber | A | B | C |
|---|---|---|---|
| $f_1$ Calculated by $^1/_4\ \lambda$ formula | 152 | 108 | 108 |
| $\sqrt{\theta}$ | 1.20 | 1.13 | 1.06 |
| $f_1$ Calculated by $^1/_4\ \lambda$ formula with end correction | 135 | 90 | 90 |

It may be argued that end corrections should be applied as well to the expression for the frequency derived in this paper. However, a value for the end correction for a flared tube has not been firmly established. Two experimenters in acoustics, Mokhtar and Messih (6), have shown recently in their work on conical pipes that the end correction is less than that of a cylindrical pipe having the same radius as the mouth, without advancing any quantitative results. A frequency obtained by the Rayleigh-Ritz method is higher than the true frequency, the degree of error depending on the lack of similarity between the assumed and true forms of elastic displacement. Neglect of the end correction also increases the calculated frequency. It would appear, therefore, that the calculated frequency of Equation [21] should be higher than the measured frequencies. However, the error in the Rayleigh-Ritz method is usually small. Den Hartog (5) analyzes the frequency of a vibrating string by this method, utilizing three assumed forms of elastic displacement. The resulting relative frequencies are as follows:

| Form of Displacement | Relative Frequency |
|---|---|
| Sinusoidal (true form) | 1.00 |
| Parabolic | 1.006 |
| Triangular | 1.102 |

It is believed that the assumption of sinusoidal motion for gas vibrations cannot be far in error. The agreement between the experimentally obtained and theoretically calculated results indicates that end corrections for the three chambers considered would be small. A possibility does exist that the lack of end correction and the assumption of plane waves in the convergent and divergent sections of the duct give rise to compensating errors.

## Application to Operating Rocket Thrust Chambers

It remains now to relate the preceding theory which was developed for the nonoperating ambient condition with the operating thrust chamber. There are differences between the two conditions which must be

considered further, the most apparent being as follows:

(1) A nonplanar sonic boundary exists in the throat of the rocket nozzle.

(2) The gas contents of the thrust chamber are flowing at high velocity, whereas in the derivation no through-flow velocity was assumed.

(3) The distribution of the RT function throughout the chamber is not constant and therefore the acoustic velocity is not constant.

(4) Supersonic flow exists near and downstream of the throat. This will demand consideration of compressibility effects.

(5) The oscillations of chemical energy release and entropy with time as a result of combustion under oscillating pressure will affect the conservation of the potential and kinetic energy within the system, one of the basic assumptions of the derivations.

An extension of the theory developed should include the factors listed above. It is hoped to extend the above theory and to present data on the experimental results of firing tests on the thrust chambers, the dimensions of which were used to calculate the values presented in this paper.

### References


1 "Vibration and Sound," by P. M. Morse, McGraw-Hill Book Company, Inc., New York, Toronto, London, 2nd edition, 1948, pp. 398–401.

2 "Resonance in Certain Non-Uniform Tubes," by A. T. Jones, *Journal of the Acoustic Society of America*, vol. 10, 1939, pp. 167–172.

3 "The Amplitude of Sound Waves in Resonators," by E. G. Richardson, *Proc. Physical Society of London*, vol. 40, December 1927 to August 1928, pp. 206–220.

4 "The Theory of Sound," by Rayleigh, Dover Publications, New York, 1st American edition, 1945, vol. II, pp. 170–172.

5 "Mechanical Vibrations," by J. P. Den Hartog, McGraw-Hill Book Company, Inc., New York and London, 3rd edition, 1947, pp. 178–185.

6 "The Acoustic Characteristics of Conical Pipes," by M. Mokhtar and G. Messih, *Physical Society of London*, vol. 62, 1949, pp. 793–799.

7 "The Theory of Sound," by Rayleigh, Dover Publications, New York, 1st American edition, 1945, vol. II, p. 17.

8 "Vibration Problems in Engineering," by S. Timoshenko, D. Van Nostrand, Inc., New York, 2nd edition, 1947, pp. 370–376.


---

## Servo-Stabilization of Combustion in Rocket Motors

(*Continued from page 262*)

It is of interest to point out that stabilization by servo control is only one phase of the general concept of feedback link. The opposite case of destabilization could be of importance also. For instance, consider the so-called valveless pulsejet. It is not always possible to operate the engine with the desired pulsation. With a feedback servo linking the combustion chamber pressure pickup through an amplifier to the fuel line, the system can be destabilized at the desired operating frequency and thus operate the engine at that frequency of pulsation. This application of servo-destabilization gives the valveless pulsejet a new flexibility and an extended range of operation. Therefore it seems worth while to explore carefully all possible applications of feedback control to systems with time lag.

### APPENDIX

*Calculation of Parameters J and E*

If $L^*$ and $c^*$ are the characteristic length and the characteristic velocity of the motor, and if $T_c$ is the chamber temperature, $R$ the gas constant, the transit time $\theta_g$ is $\theta_g = L^*c^*/RT_c$.

To calculate $J$ and $E$ defined by Equation [25], it is more convenient to use the average propellant velocity $v$ in the feed line. Thus $\bar{m} = \rho A v$.

Thus, according to Equation [25]

$$J = \frac{1}{2}\rho v \left(\frac{l}{\theta_g}\right) \Big/ \Delta\bar{p}$$

A consistent set of units would be $\rho$ in slugs per cubic foot, $v$ in feet per second, $l$ in feet, $\theta_g$ in seconds, and $\Delta\bar{p}$ in pounds per square foot.

If $d$ is the diameter of the feed line, $h$ its thickness, and $E'$ Young's modulus of the tube material, then $\chi$, the change in volume of the feed line per unit rise in pressure, is

$$\chi = l\pi \left(\frac{d}{2}\right)^2 d \Big/ E'h$$

Therefore Equation [25] gives

$$E = \frac{2\Delta\bar{p}}{E'} \left(\frac{d}{h}\right) \frac{l/\theta_g}{v}$$

A consistent set of units would be $\Delta\bar{p}$ in pounds per square inch, $E'$ in pounds per square inch, $l$ in feet, $\theta_g$ in seconds, and $v$ in feet per second.

### References


1 "Stability of Flow in a Rocket Motor," by D. F. Gunder and D. R. Friant, *Journal of Applied Mechanics*, vol. 17, September 1950, pp. 327–333.

2 Discussion of above paper, by M. Yachter, *Journal of Applied Mechanics*, vol. 18, March 1951, pp. 114–115.

3 "A Theory of Unstable Combustion in Liquid Propellant Rocket Systems," by M. Summerfield, JOURNAL OF THE AMERICAN ROCKET SOCIETY, vol. 21, September 1951, pp. 108–114.

4 "Aspects of Combustion Stability in Liquid Propellant Rocket Motors, Parts I and II," by L. Crocco, JOURNAL OF THE AMERICAN ROCKET SOCIETY, vol. 21, November 1951, pp. 163–178; vol. 22, January-February 1952, pp. 7–16.

5 Discussion by M. Satche on "Stability of Linear Oscillating Systems with Constant Time Lag," by H. I. Ansoff, *Journal of Applied Mechanics*, vol. 16, December 1949, pp. 419–420.

6 "Aerodynamic Stability and Automatic Control," by W. Bollay, *Journal of the Aeronautical Sciences*, vol. 18, 1951, pp. 569–623, particularly p. 605.

7 "The Transfer Functions of Rocket Nozzles," by H. S. Tsien, JOURNAL OF THE AMERICAN ROCKET SOCIETY, vol. 22, May-June 1952, pp. 139–143.

8 See, for instance, "Stability of Linear Oscillating Systems with Constant Time Lag," by H. I. Ansoff, *Journal of Applied Mechanics*, vol. 16, June 1949, pp. 158–164.

# Manned Flight at the Borders of Space[1]

## *The Human Factor of Manned Rocket Flight*

HEINZ HABER[2]

Institute of Transportation and Traffic Engineering, University of California, Los Angeles, Calif.

**A functional border between atmosphere and space is defined as a level at which the atmosphere fails as a supporting medium, and space-equivalent conditions begin. Depending upon a particular kind of function the corresponding limit is located at a certain altitude. The major functions of the atmosphere for man and craft are the following: Contributing to respiration, preventing boiling of body fluids, sustaining combustion of fuel, absorbing heavy primaries of cosmic radiation, absorbing solar UV-radiation, supplying aerodynamic lift, supplying diffuse daylight, absorbing meteors, interacting thermally with the craft, and interfering by air drag over long periods of time (permanence of satellite orbits). Depending upon the nature of a particular function, the functional borders so defined are more or less extended regions. The various functional borders of space lie in the region between 10 and 120 miles of altitude. The significance of the above mentioned factors for manned rocket flight is discussed with special emphasis upon problems of aero-medical and space-medical nature. The use of the term "aeropause" for the border region between atmosphere and space is proposed.**

THE upper boundary of the atmosphere is commonly identified with that region of the exosphere where the upper most geophysical phenomena, namely the highest aurora, are occasionally observed. In terms of this concept, the limit of the terrestrial atmosphere is located at about 600 miles above the surface of the earth. The peak of the highest rocket trajectories attained so far—250 miles—lies yet within the boundaries of the atmosphere. For all practical purposes of rocket engineering, however, the atmosphere ceases to exist at an altitude of 110–120 miles. Unmanned rocket craft are routinely reaching beyond the physically effective regions of the atmosphere, and manned flights in the border region of the atmosphere are being made in experimental rocket airplanes. Flights at very high altitudes, i.e., in excess of 10 miles, are still short in duration; nevertheless, the technical means available in aviation of today make it necessary to investigate the medical and psychological problems peculiar to flight in the border area between the terrestrial atmosphere and space.

Since the geophysical concept of the borders of the atmosphere is of little use in aviation medicine and space medicine, a new concept must be found. This new concept must be adapted to the uses of rocketry and aviation medicine, in other words, it must be based on the functions which the atmosphere fulfills for craft and men. In a series of papers, Haber (1, 2)[3] and Strughold et al. (3) attempted to develop such a new concept by introducing the "functional borders between atmosphere and space." A functional border is defined as a certain level above the ground at which the atmosphere fails as a supporting medium. Depending on the nature of the various functions, the borders are located at different altitudes. They are found in the area between 10 and 120 miles of altitude. In these regions of the atmosphere the conditions of conventional aviation gradually blend into those of actual space flight.

From this point of view the following functional borders can be listed:

TABLE 1

| | Function | Altitudes, miles |
|---|---|---|
| 1 | Contributing to respiration | 10 |
| 2 | Preventing boiling of body fluids | 12 |
| 3 | Sustaining combustion of fuel | 13–15 |
| 4 | Absorbing heavy primaries of cosmic radiation | 13–23 |
| 5 | Absorbing solar ultraviolet radiation between 210 and 300m$\mu$ (Hartley band of $O_3$) | 22–28 |
| 6 | Supplying aerodynamic lift | 50–60 |
| 7 | Supplying diffuse daylight | 60–90 |
| 8 | Absorbing meteors | 65–95 |
| 9 | Interacting thermally with the craft | 100–115 |
| 10 | Interfering by air drag over long periods of time (permanence of satellite orbit) | 120 |

In addition to these data it may be mentioned that the presence of ozone above the 8-mile level can result in toxic concentrations of this gas in the cabin air, if the pressurization of the cabin is maintained by compressing ambient air. Fortunately, ozone is easily intercepted by means of simple filters.

Of course, the functional borders so defined are more or less extended regions. Especially the functions mentioned under 6, 9, and 10 are dependent upon the velocity of the craft, and the altitude data given are related to a velocity of the order of 5 miles/second. This velocity must be attained in order to establish a craft in a permanent satellite orbit around the planet.

In the following, those functions of the atmosphere that have a bearing on the human factor of manned rocket flight will be discussed briefly.

Received July 24, 1952.

[1] Paper presented at the Fall Meeting of the AMERICAN ROCKET SOCIETY, Chicago, Ill., Sept. 9, 1952.

[2] Associate Physicist.

[3] Numbers in parentheses refer to the Bibliography on page 276.

### *A The Function of Contributing to Respiration*

Quantitative information as to the extent to which the atmosphere can maintain the oxygen supply of the body is obtained through experiments on explosive decompression. In experiments of this kind, a test subject is transposed, within fractions of a second, from an environment of normal or slightly reduced oxygen pressure to a state of acute oxygen need such as would be found at higher altitudes. If a subject is brought abruptly from normal oxygen pressure to that found at 5 miles the first psychophysiological disturbances can be observed after about two minutes; after another minute the subject becomes entirely helpless, and loses consciousness. The interval during which he is still capable of acting is called the "time of useful consciousness" after Armstrong (4), or "time reserve" after Strughold (5). This characteristic time span is reduced to about 80 seconds at 6 miles, and it is further reduced with increasing height, and finally reaches an asymptotic value of about 15 seconds at a height of 9 to 10 miles. Fig. 1 shows the time of useful

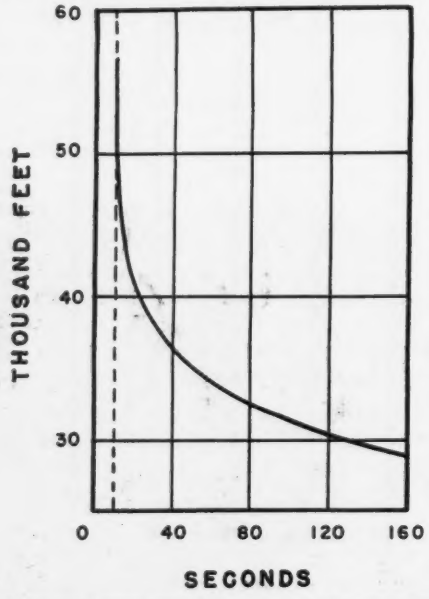


FIG. 1 TIME OF USEFUL CONSCIOUSNESS AT VARIOUS LEVELS OF ALTITUDE

consciousness as a function of altitude according to measurements carried out by Luft, Clamann, and Opitz (6). In experiments made in the low-pressure chamber at simulated altitudes up to 12 miles, the time of useful consciousness remained constant at an average of 15 seconds. There is no reason to assume that the minimum time span of 15 seconds will become any shorter at still greater heights. The height of the critical level in the atmosphere—about 10 miles where we first observe the minimum time reserve—can be derived from an analysis of the alveolar gases. The constitution of the air in the lungs differs from ambient air. In average atmospheric air of 760 mm Hg, about 580 mm are provided by $N_2$, 150 mm by $O_2$, 23 mm by water vapor, and 7 mm by A. The rare constituents of free air, such as the other inert gases and $CO_2$, are omitted in this listing. The approximate values for alveolar air at sea level are: 560 mm $N_2$, 106 mm $O_2$, 47 mm water vapor, 40 mm $CO_2$, and 7 mm A. At higher altitudes the partial pressures of the individual gases in free air fall off in exactly the same rate as the total pressure, since the atmosphere is being kept mixed thoroughly throughout. (The gravitational separation of atmospheric gases existing in the 22–30 miles layer and above, Ref. 7, can be omitted in this discussion.) Alveolar air, however, behaves differently. If air of a lowered total pressure is breathed, the partial pressures of nitrogen and oxygen in the lungs are likewise lowered proportionally; the partial pressures of water vapor and carbon dioxide, however, remain practically constant at about 80 to 87 mm Hg. This is because water vapor and carbon dioxide inside the lungs originate from the blood through continuous evaporation and exhalation. At increasing heights, water vapor and carbon dioxide occupy an ever-increasing percentage of the alveolar air. Obviously, the air inside the lungs will consist exclusively of these two components as soon as the pressure of the ambient air falls to 80 to 87 mm, a value which is reached at an altitude of about 9 to 10 miles. At this altitude no additional oxygen can enter the lungs because their capacity is exclusively claimed by water vapor and carbon dioxide. The function of the atmosphere to contribute to man's respiratory needs comes to an end at an altitude of about 10 miles.

### *B The Function of Preventing Boiling of Body Fluids*

At a somewhat greater altitude the barometric pressure of the atmosphere can no longer prevent the body fluids from boiling. The boiling point of body fluids is reached at an altitude where the barometric pressure becomes equal to the water vapor pressure at body temperature, i.e., 47 mm Hg at 98.6 F. The critical level where boiling of body fluids sets in, lies at about 12 miles of altitude. Armstrong (8) has studied the boiling of body fluids in a low pressure chamber by exposing animals to a barometric pressure below 47 mm Hg. The first manifestations of boiling of body fluids appeared as rapid bubbling of the saliva around the mouths of the animals. After a delay of several seconds, ballooning of the animal skin was observed which is attributed to the formation of water vapor bubbles in the soft tissue. Boiling of blood in the lungs must also be expected upon lowering the barometric pressure below the critical value of 47 mm Hg.

### *C The Function of Absorbing Heavy Primaries of Cosmic Radiation*

Originally, the cosmic ray particles were thought to consist exclusively of protons, i.e., the nuclei of hydrogen atoms. In 1948, Freier, Lofgren, Ney, and Oppenheimer (9) presented evidence to the fact that primary cosmic radiation contains also nuclei of heavier atoms. Bradt and Peters (10) determined the abundance ratio of different nuclear species in primary

cosmic radiation. Their results indicate that the following ratios exist: H:He:Heavier nuclei = 79:20:1. This frequency distribution can be expected to correspond approximately to the cosmic abundance of the chemical elements. Owing to the tremendous energy of the cosmic primaries ($\sim$ 2 BeV per nucleon), they are characterized by an enormous energy dissipation in passing through matter. This energy dissipation, which is dependent upon velocity and nuclear charge of the individual particles, determines the penetrating power of the particles. Consequently, the lower limits to which a certain percentage of the primaries can penetrate exhibit a certain stratification according to atomic number and energy of the particles.

About one half of the primary protons penetrate down to an altitude of approximately 12.5 miles. The lower limit of the heavy primaries is found at about 12 miles. Above this level their number increases considerably reaching a saturation at an altitude of about 23 miles. The air blanket above this latter level has no appreciable effect on the density and nature of the incoming particles of cosmic radiation.

Because cosmic rays are a highly ionizing type of radiation, their possible hazard to man exposed to them at greater altitudes must be investigated. The biological effectiveness of cosmic radiation was studied theoretically by Krebs (11), Schaefer (12, 13, 14), and Muller (15). Krebs gave special emphasis to the possible effects of the so-called star phenomenon. A primary particle entering the atmosphere from outer space carries such a high energy that specific hitherto unknown phenomena are produced in the processes of collision between a cosmic ray particle and a target nucleus. The cosmic ray particles create an explosion or "evaporation" of nuclei resulting in a complete disintegration of nuclei. The fragments shooting away from the site of the nuclear event imprint themselves on the emulsion of a photographic plate producing star-like formations. A typical star is shown in Fig. 2. According to Hornbostel and Salant (16), the frequency of stars with 4 or more prongs is about 2000 per cubic centimeter per day, at an altitude of 17 miles. Krebs estimates that the total of the prongs produced in the tissue of an individual exposed to cosmic radiation outside the air blanket is equivalent to a concentration of $6.2 \times 10^{-12}$ grams radium elements per cubic centimeter. Comparing this figure with the natural occurrence of radioactive materials found in human tissue, Krebs concludes that "the radiation delivered by the cosmic ray stars at the top of the atmosphere comes very close to the amounts of radioactive energies which today are considered to be in no way harmless to tissue . . . the possibility for biological effects of cosmic radiation becomes, to a certain degree, reality."

Hermann J. Schaefer has evaluated the present-day knowledge of cosmic radiation in terms of the hazard to health. He was the first to point out that the heavy particles of cosmic radiation must be expected to be particularly effective, even though their number is small compared to that of primary protons. A detailed analysis by Dr. Schaefer of the biological aspects of the heavy primaries of cosmic radiation is given elsewhere in the JOURNAL (see pages 277–283 in this issue).

### *D The Function of Absorbing Ultraviolet Solar Radiation*

The existence of ozone in the atmosphere in quantities sufficient to entirely block the passage of ultraviolet radiation from the sun was first assumed by Hartley (17), the discoverer of the absorption band of ozone between 210 and 300 m$\mu$, that bears his name. The absorption of ozone begins at about 300 m$\mu$, and soon becomes so effective that the solar spectrum is cut off abruptly at 286.3 m$\mu$, as reported by Goetz (18). The maximum of ozone absorption lies at 255 m$\mu$, where the absorption coefficient $\alpha_{10}$ was found to be as high as 123/cm. A layer of ozone at standard pressure and temperature, having a thickness of 0.002 cm, reduces the flux density of an incident beam of ultraviolet light to about one half. This shows that ozone is a more effective absorber than all metals.

The bulk of atmospheric ozone is found in the layer between 9 and 25 miles of altitude. The mean total amount of ozone corresponds to a layer of 3-mm thickness at STP. The existence of this small amount of ozone in the atmosphere is nevertheless of great biological importance. It provides an extremely effective blanket against those parts of ultraviolet radiation

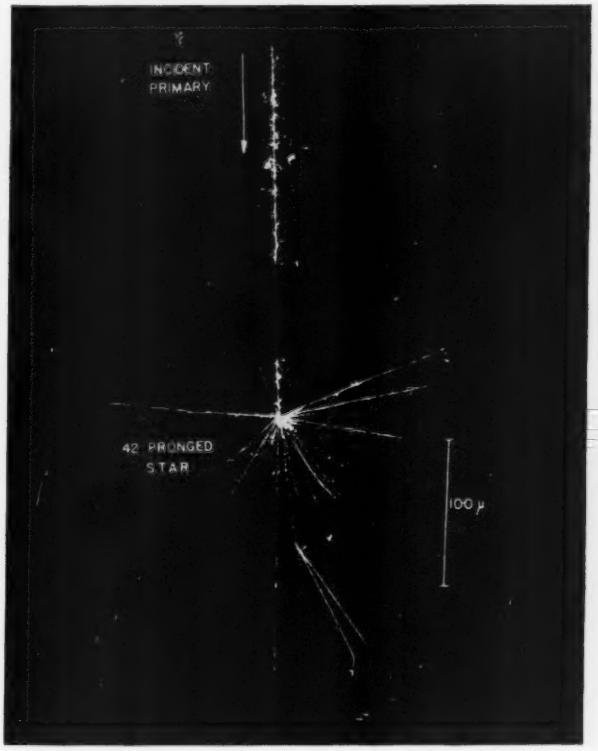


FIG. 2 TYPICAL COSMIC-RAY STAR

(From H. L. Bradt and B. Peters, Ref. 10. Courtesy of Dr. M. F. Kaplon, Dept. of Physics, The University of Rochester, Rochester, N. Y.)

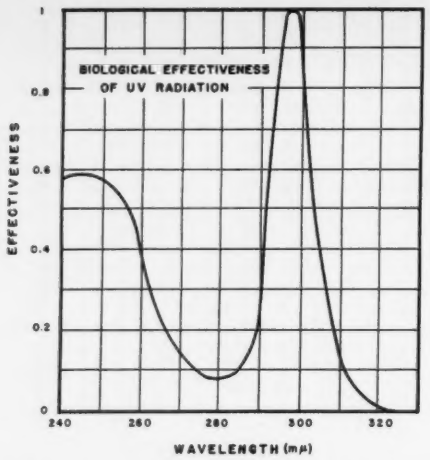


FIG. 3. BIOLOGICAL EFFECTIVENESS OF UV RADIATION

that have a pronounced effect upon the skin and the eyes by causing erythema of the skin and conjunctivitis. Fig. 3 shows the erythema producing effectiveness in arbitrary units as a function of wave length. The values given were adopted by the International Illumination Commission in 1937 (19). On the basis of these data, and by use of recent results of ozone investigations, Buettner (20) has estimated that erythema of the skin within and above the ozone layer is produced 10 to 50 times as fast as at sea level. Protection against ultraviolet radiation, therefore, is mandatory at altitudes in excess of 15 miles. Fortunately, window materials capable of absorbing these kinds of radiation are available. Upon massive irradiation by ultraviolet rays, however, most materials become turbid and discolored. Quartz, for instance, becomes brownish if exposed to large amounts of UV-radiation of a wave length smaller than 250 mμ.

### *E The Function of Supplying Aerodynamic Lift and Drag*

It appears as though the final disappearance of aerodynamic lift at greater altitudes is of interest only to the engineer. It can be shown, however, that the absence of aerodynamic lift and drag will be responsible for a medical problem of far-reaching consequences. For, in the absence of aerodynamic and propelling forces, the crew of a high-flying rocket craft will be transposed into the state of weightlessness.

Following the reasoning of Haber (21), weight of a body can be identified with the vectorial sum of all external forces acting on the body. The same definition can be applied to the concept of "apparent weight" or "*g*-forces" used in aviation medicine which are usually defined as the sum of the force of gravity and the forces of inertia inherent to accelerated motion, according to the equation

$$W_a = F_g + F_i \quad \ldots\ldots [1]$$

where $W_a$ is the apparent weight of the body, $F_g$ the force of gravity, and $F_i$ the forces of inertia. Using the principle of d'Alembert

$$F_g + F_i + F_e = 0 \quad \ldots\ldots [2]$$

where $F_e$ is the vectorial sum of all external forces, the apparent weight or *g*-forces can simply be written as

$$W_a = -F_e \quad \ldots\ldots [3]$$

The external forces comprise friction, aerodynamic lift and drag, propelling forces from an engine, and all elastic forces involved in the situation of a body being fully or partially supported. As can be derived immediately from Equation [3], a body becomes weightless if it coasts freely outside the range of the mechanically effective parts of the atmosphere.

Owing to the decreasing support which the atmosphere provides at increasing altitudes, states of reduced weight and weightlessness become increasingly more dominant in modern aviation. There can be no doubt that the phenomenon weightlessness is about to become an outstanding aeromedical problem as aviation progresses. So far, only the problems of increased body weight were of aeromedical import. Now we have reached a point where investigations of external forces acting on the body must extend into the range of reduced weight down to the complete lack of weight.

The problems related to increased body weight (*g*-forces greater than 1) concern primarily the interference of additional forces with the mechanical factors of circulation, respiration, dislocation of organs, body movements and their consequences. All these disturbances are, in one way or another related to elastic deformations of the body and its parts. These disturbances, up to a certain limit, vary approximately in proportion to the increase of body weight. Consequently, the elimination of body weight will probably have no decisive or even lethal effects upon the physiological functions mentioned previously. The transition from the condition of normal weight into the state of weightlessness removes the normal elastic stress exerted upon the body by its support, and there are no major indications of a possible failure of the previously enumerated body functions in the absence of this stress. The correctness of this kind of reasoning was proved by experiments with monkeys and mice in V-2 and Aerobee rockets, carried out by Henry and Ballinger (22). In several experiments of this kind, test animals were carried aloft in research rockets and subjected to the state of weightlessness during the free-flight period, lasting between 2 to 3 minutes. The rate of pulse and breathing, and breathing movements were recorded during these tests, and only slight disturbances were observed.

In contrast to the functions of purely mechanical nature, the mechanical sense organs of the body do not react to alterations of the stimulating forces in a linear relationship. They follow a logarithmic relationship which is described by the Weber-Fechner law. Therefore, we must conclude that changes of mechanical excitation in the absence of a basic stress will probably have pronounced effects on man's ability to cope with the mechanical factors of his environment in the state of weightlessness. According to Gauer and Haber (23), and Haber and Gerathewohl (24), we must expect disturbances in the function of orientation, in the proper

execution of body movements, and in the harmony of the coordination between the various components of man's mechano-receptor system. The disturbing occurrence of optical illusions, akin to the oculo-gravic illusion (33), cannot be excluded. Our empirical knowledge of the possible physiological and psychophysical consequences of weightlessness is rather fragmentary—in fact, it is practically nil. This fact constitutes a challenge to aeromedical, or better, to space-medical research.

### *F The Function of Supplying Diffuse Daylight*

The brightness of the daylight sky at a particular point of observation depends upon the zenith distance of the sun, the difference in azimuth between the sun and the point of observation, the mean reflectivity of the earth, and—which is of particular interest here—the sky brightness depends on altitude. Haber (25) has computed the brightness of the daylight sky as a function of altitude by using the theory of Tousey and Hulburt (26). In Fig. 4 is depicted the zenith brightness in millilamberts as a function of altitude. As can be seen from the graph, the brightness of the sky at a height of 20 miles is about $^1/_{30}$ of its value at sea level. Fig. 5 shows the extension of zenith brightnesses up to altitudes of 90 miles. Although the theory of Tousey and Hulbert was not designed to stand an extrapolation to such great heights, the data given can be expected to be a fairly good approximation. According to Fig. 5, the light of the sky vanishes completely only at very great altitudes. At heights in excess of 85 miles the zenith brightness approaches that of a moonless night at sea level. From there on the blackness of space is complete.

The absence of diffuse illumination provided by the atmosphere poses a visual problem. When looking down from a high-flying craft, the eye meets brightnesses of varying degrees, depending upon the features of the landscape and meteorological conditions. Looking up, the daylight sky appears as the only source of light. Most features of the ground, the clouds and other sunlit objects are rather bright. Their brightnesses lie in the range between 300 and 10,000 millilamberts. In contrast to these values, the brightness of the sky is rather low even at moderate altitudes, and decreases further at higher levels. Owing to these conditions strong contrasts of simultaneously perceived brightnesses are produced.

The brightness contrast is expressed by the following ratio:

$$C = \frac{B_t - B_b}{B_b} \quad [4]$$

where $B_t$ is the brightness of the target, and $B_b$ the brightness of the background or surrounding. Guth (27) has established contrast levels which produce an initial momentary sensation judged to be at the borderline between comfort and discomfort (*BCD*). The critical contrast values depend upon the brightness of the target, the solid angle ($Q$) subtended by the target, and the brightness of the background in the following fashion:

$$BCD = 108 \cdot B_b^{0.44}(Q^{-0.21} - 1.28) \quad [5]$$

whereby the brightnesses are given in footlamberts (1 footlambert = 1.0764 millilambert). From the data of Guth it can be concluded that viewing of objects at higher altitudes will be anything but comfortable. Even at moderate altitudes, objects having a reflectance as low as 20 or 30% surpass the threshold of comfort, if they are illuminated by the sun when

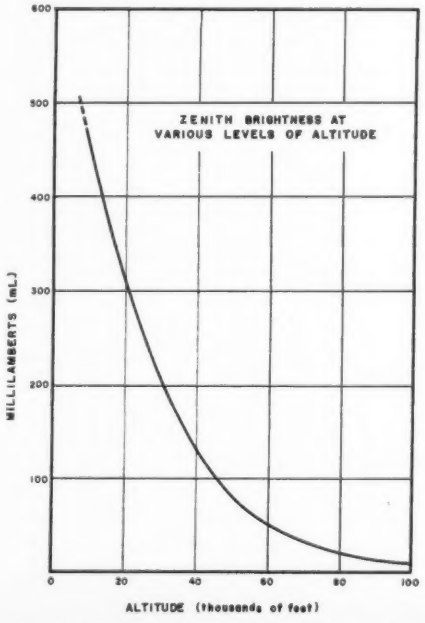


FIG. 4. ZENITH BRIGHTNESS AT VARIOUS LEVELS OF ALTITUDE

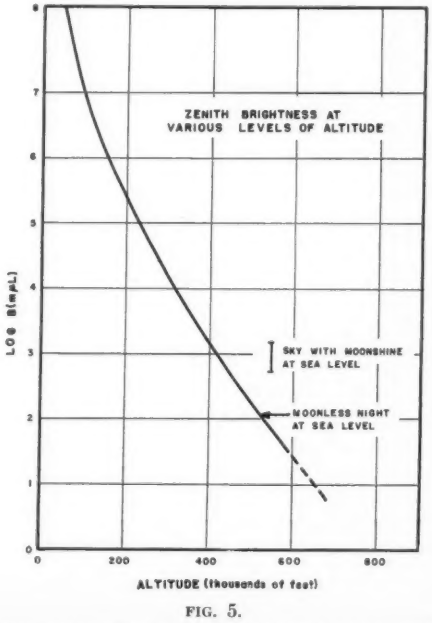


FIG. 5.
ZENITH BRIGHTNESS AT VARIOUS LEVELS OF ALTITUDE

viewed before the background of the sky. For an object the size of the wing of an aircraft, the comfort threshold is exceeded at a height of 10,000 feet, even if the reflectance of the wing surface is only 25%. At a height of 20 miles, sunlit objects as small as the disk of the moon appear too bright for comfort, if their reflectance is larger than 10%.

Far more discomfortable brightness contrasts will be encountered inside of the cabin of a high flying ship where sunlit patches will be seen adjacent to deep shadows. Owing to the small illumination of the waning light of the sky, the interior of a cabin will be rather dark. Reading of instruments will be impossible unless they are illuminated artificially. These conditions will undoubtedly cause visual discomfort, fatigue, or even disabling glare. Cibis (28) has suggested the use of light-diffusing panels covering a certain section of the window area. In this way, the interior of the ship would be shielded against direct sunlight. At the same time, such a device would provide a sufficient amount of comfortably diffuse illumination from the panel that substitutes for the loss of diffuse illumination normally afforded by the light of the sky.

### *G The Function of Absorbing Meteors*

The hazards arising from possible impacts with meteors is of particular space-medical interest. Even moderately large meteors can easily puncture the hull of a high-flying ship—an event which would result in a very rapid explosive decompression of the crew. At altitudes accessible to man with present-day means, no hazard from meteors exist, since meteors are vaporized and annihilated at great altitudes. The great majority of meteors ranging between fine meteoric dust and particles weighing a gram or more, are absorbed before reaching the 60-mile level. Above 90 miles of altitude, however, a ship would run the same risk of being hit by meteors as in interplanetary space, except for the protection afforded by the shielding bulk of the earth.

### *H The Function of Interacting Thermally with the Craft*

One of the most intriguing problems of modern aviation is the generation of an envelope of hot air around a fast-flying aircraft owing to aerodynamic heating. This is not the place to discuss the many aspects of the "heat barrier" which our high-speed aircraft encounter. Relative to our subject we are primarily interested in the quesion at what altitude aerodynamic or friction heating can be expected to cease. This question has been answered by Saenger (29), who has studied the stability of a satellite vehicle at various levels of altitude. He has found that, at a height of 80 miles, a satellite would lose over 6 miles of altitude per revolution as a consequence of air drag. The altitude loss per revolution would be only 3 feet, if the satellite would circle at a height of 112 miles. Somewhere in the range between 80 and 110 miles of of altitude, air drag and, simultaneously, skin heating for velocities of the order of 5 miles per second will become negligible.

The temperature problems of rocket flight, however, persist even at greater altitudes. Beyond the border of thermal interaction between atmosphere and craft, the skin temperature will be determined by the exchange of radiation between the exterior of the craft on the one side, and the sun, the earth, and the cosmos on the other. Buettner (30, 31) has studied this problem in detail by calculating equilibrium temperatures of various metals and other substances. The equilibrium temperatures are calculated by equating the rate of absorbed radiant energy to the radiation losses of the body in space. The latter is proportional to the fourth power of temperature (Stefan-Boltsmann law) and to the emissivity of the body's surface in the infrared. The surprising result obtained by Buettner was the fact that all metals become excessively hot under conditions of radiative equilibrium in space, even if they are highly polished and reflecting. The high temperatures are caused by the poor emissivity of the metals in the infrared. A few of Buettner's data are given in Table 2.

TABLE 2 EQUILIBRIUM TEMPERATURES OF VARIOUS MATERIALS IN SPACE, °F

| Material | Illuminated by sun | Illuminated by "full earth" |
|---|---|---|
| Black (soot) | 252 | 154 |
| White (MgO) | −60 | 9 |
| Aluminum | 802 | 563 |

The figures show that only gleaming white materials such as magnesium oxide can serve as surface coatings, if a manned craft is exposed to the field of thermal radiation in space.

From the standpoint of aviation medicine and space medicine the temperature problem has a further important aspect. It is the problem of survival in cases of failure of cooling systems—in other words: What is

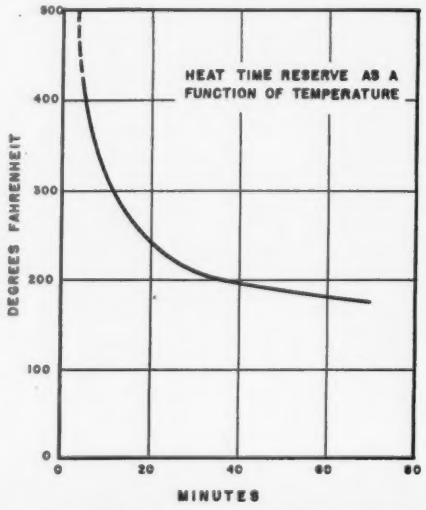


FIG. 6. HEAT TIME RESERVE AS A FUNCTION OF TEMPERATURE

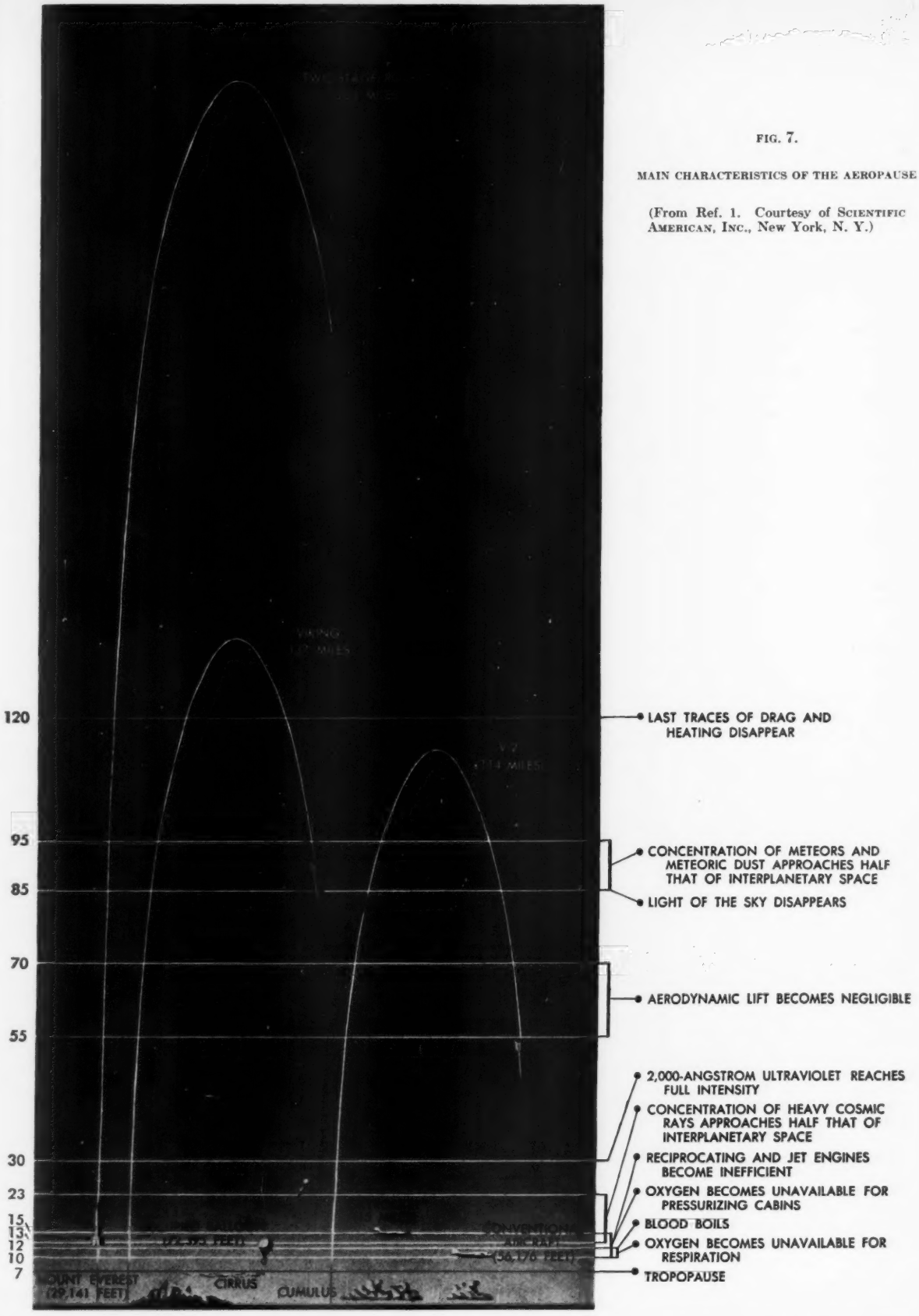


FIG. 7.

MAIN CHARACTERISTICS OF THE AEROPAUSE

(From Ref. 1. Courtesy of SCIENTIFIC AMERICAN, INC., New York, N. Y.)

the time reserve of an individual more or less suddenly exposed to a hot environment? By "heat time reserve" one understands the time span that elapses between the beginning of the exposure to heat and the moment when heat collapse must be anticipated. Naturally, one must expect the heat time reserve to be dependent upon many factors such as type of clothing, profuseness of sweating, precooling of the subject, and the like. In one of his recent papers, Buettner (31) has compiled some average data which are given in Fig. 6.

### *I The Function of Interfering by Air Drag Over Long Periods of Time*

Saenger has shown that at an altitude of 120 miles air drag has completely vanished. Beginning at this height, the establishment of a permanent satellite orbit would be possible, although a somewhat greater height would be indicated for practical purposes to allow for a certain eccentricity of the satellite orbit. Nevertheless, the 120-mile level can be considered the mechanical border of space. This line is of space medical interest insofar as above this level the state of weightlessness can be maintained for any length of time. Above an altitude of 120 miles—which, incidentally, is only about 3% of the earth's radius—the environment of space is complete.

Above an altitude of 120 miles there are only three factors of terrestrial origin that make the environment of the craft different from that found at any other point of interplanetary space: (1) The bulk of the earth which shields off half the number of meteors and cosmic ray particles. (2) The magnetic field of the earth which deflects cosmic ray particles below a certain magnetic rigidity, if they approach the earth in or near the equatorial plane. (3) The solar radiation reflected by the earth and its atmosphere, and the infrared radiation emitted by the earth proper.

The problems which arise in the operation of manned vehicles at very high altitudes and eventually in free space are of an extremely diverse and complex nature. Their solution requires contributions from meteorology, geophysics, astronomy and astrophysics, cosmic ray physics, aerodynamics, radiobiology, physiology, aviation medicine, space medicine, bioclimatology, and human engineering. Owing to these many different fields, difficulties in semantics are frequently encountered. Particularly, the term "upper atmosphere" is inadequate and misleading, since it conveys different meanings in the various fields such as meteorology, geophysics, and aviation medicine. For the common benefit it appears expedient to coin a new term for designating those regions of the atmosphere where, in terms of manned rocket flight, the conditions of conventional aviation blend into those of actual space flight. To this end, Buettner (32) proposed the term "aeropause." The aeropause is defined as that region of the atmosphere where its various functions for man and craft begin to cease and space-equivalent conditions are gradually approached. The concept of the aeropause appears to be quite useful in modern aviation and rocketry. It circumscribes the area characterized by certain factors of environment that are distinctly different from those found in the area of conventional aviation or of space. The aeropause encompasses the region between the 10- and 120-mile levels. The main characteristics of the aeropause are depicted in Fig. 7.

## Bibliography


1 "Flight at the Borders of Space," by H. Haber, *Scientific American*, vol. 186, 1952, no. 2, p. 20.

2 "Phasing and Coordination of Medical Research with Technical and Environmental Development," by H. Haber. Contribution to "Physics and Medicine of the Upper Atmosphere," edited by C. S. White and O. O. Benson, Jr., The University of New Mexico Press, Albuquerque, N. M., 1952.

3 "Where Does Space Begin? Functional Concept of the Boundaries between Atmosphere and Space," *Journal of Aviation Medicine*, vol. 22, 1951, p. 342.

4 "Principles and Practices of Aviation Medicine," by H. G. Armstrong, William and Wilkins Co., Baltimore, Md., 1952, p. 243.

5 "Die Zeitreserve," by H. Strughold, *Z. Biologie*, vol. 3, 1939, p. 55.

6 "The Latency of Hypoxia on Exposure to Altitudes above 50,000 Feet," by U. C. Luft, H. G. Clamann, and E. Opitz, *Journal of Aviation Medicine*, vol. 22, 1951, p. 117.

7 The Constitution of the Stratosphere," by R. Penndorf, *Bulletin of the American Meteorological Society*, vol. 27, 1946, p. 343.

8 "Principles and Practices of Aviation Medicine," by H. G. Armstrong, Williams and Wilkins Co., Baltimore, Md., 1952, p. 345.

9 "Evidence for Heavy Nuclei in the Primary Cosmic Radiation," by P. Freier, E. F. Lofgren, E. P. Ney, and F. Oppenheimer, *Physical Review*, vol. 74, 1948, p. 213.

10 "The Heavy Nuclei of the Primary Cosmic Radiation," by H. L. Bradt and B. Peters, *Physical Review*, vol. 77, 1950, p. 54.

11 "The Possibility of Biological Effects of Cosmic Rays in High Altitudes, Stratosphere, and Space," by A. T. Krebs. MDF RL Project No. 6-64-12-08-(7), Medical Department Field Research Laboratory, Fort Knox, Ky., April 29, 1950.

12 "Evaluation of Present-Day Knowledge of Cosmic Radiation in Terms of the Hazard to Health," by H. J. Schaefer, *Journal of Aviation Medicine*, vol. 21, 1950, p. 375.

13 "Further Evaluation of Present-Day Knowledge of Cosmic Radiation in Terms of the Hazard to Health," by H. J. Schaefer, Project No. NM 001 059.13.02, U. S. Naval Air Station, School of Aviation Medicine, Pensacola, Fla., August 15, 1951.

14 "The Biologic Effects of Cosmic Radiation," by H. J. Schaefer. Contribution to "Physics and Medicine of the Upper Atmosphere," edited by C. S. White and O. O. Benson, Jr., The University of New Mexico Press, Albuquerque, N. M., 1952.

15 "The Genetic Effects of Cosmic Radiation," by H. J. Muller. Contribution to "Physics and Medicine of the Upper Atmosphere," edited by C. S. White and O. O. Benson, Jr., The University of New Mexico Press, Albuquerque, N. M., 1952.

16 "High Energy Events at High Altitudes," by J. Hornbostel and E. O. Salant, *Physical Review*, vol. 76, 1949, pp. 468, 859, 984.

17 "On the Absorption Spectrum of Ozone," by W. N. Hartley, *Chemical News*, vol. 42, 1880, p. 268.

18 "Das atmosphaerische Ozon," by F. W. P. Goetz, vol. 1 of the series, "Ergebnisse der kosmischen Physik," Akad. Verlagsges., Leipzig, 1931, p. 180.

19 Commission internationale de l'eclairage: C. R. 9. Session, Berlin, 1935, Cambridge, 1937. Com 41 d'études sur le rayonnement UV, pp. 596–625.


(*Continued on page 283*)

# Exposure Hazard from Cosmic Radiation at Extreme Altitude and in Free Space[1]

HERMANN J. SCHAEFER[2]

U. S. Naval School of Aviation Medicine, Pensacola, Fla.

**Recordings in the lower stratosphere have furnished, in recent years, direct pictorial evidence for the so-called heavy nuclei component of the primary cosmic radiation. This discovery places the problem of a possible exposure hazard for humans in the region of the primary radiation on a new basis.**

**The heavy primaries are characterized by an extremely high specific ionization and by a large radial spread of the ionization dosage around the particle tracks. Both qualities are apt to endow them with a greatly increased biological effectiveness which cannot be measured adequately in terms of ordinary biological dosage units.**

**The geomagnetic field exerts strong, deflecting forces on the charged primaries. This influence is strongest in the equatorial plane and weakest along the polar axes. The minimum energy of the primary spectrum, therefore, shows a marked latitude dependence and the exposure hazard can be expected to be substantially higher in the polar cap than in the equatorial belt. This holds especially since the low-energy particles which represent the most harmful type occur only at high latitudes.**

**For interplanetary space a conclusive answer with regard to the exposure hazard cannot yet be given since no experimental data on the genuinely "primary" spectrum outside any shielding magnetic field are available, and since the existence of a heliomagnetic field which would screen off low-energy primaries from the full region inside the earth's orbit is also a doubtful issue.**

## 1 Introduction

FROM outer space a very penetrating ionizing radiation whose origin is completely unknown is coming to the earth. Ever since this radiation was discovered and its extraterrestrial origin clearly recognized in 1912, cosmic ray research has been presenting atomic physics with a never-ending series of startling new phenomena. Some of these discoveries, of paramount importance for our understanding of the binding forces of the atom nucleus, have been made in most recent years, and to predict that more such discoveries are still to come seems rather trite especially if one considers that, at present, complete ignorance must be admitted with regard to any reasonable explanation of the origin of cosmic radiation.

Rather early in this development it had been conjectured that cosmic radiation might have some influence on living matter, and this problem has been a controversial issue ever since. This discourse is not intended to deal with this problem in its general meaning, but is limited to the question of what possible effects on the human organism might result from an exposure in the region of the primary cosmic radiation at the upper end of and outside the terrestrial atmosphere where the radiation intensity is about 150 times higher than at sea level.

## 2 Nature of the Primary Cosmic Radiation

A revolutionary change in the concepts of the primary cosmic radiation has taken place since 1948. In that year, P. Freier and collaborators (1)[3] could present the first pictorial evidence for the so-called heavy nuclei component of the primary radiation. This new component has since been studied systematically in several investigations (2, 3, 4, 5), and rather accurate information on the composition of the primary radiation is now available.

The old concept (before 1948) that the primary radiation consisted mainly if not exclusively of high energy protons had to be abandoned on the basis of the new high-altitude recordings. It is now well established that the primary radiation consists of atom nuclei of many of the elements of the Periodic System, and their relative abundance seems rather similar to the abundances of the elements in the universe as astro-spectroscopy and the study of meteorites reveal them.

The most startling quality of the heavy nuclei is their extremely high kinetic energy. It exceeds by far the energies which can be obtained from any natural or artificial terrestrial radiation source. Due to this excessively high energy these nuclei become stripped of all their orbital electrons as soon as they penetrate any absorber, i.e., they turn into multiply charged ions. This means since nuclei as heavy as iron (atomic number Z-26) or even tin (Z-50) have been identified in the primary radiation, that 26-fold or even 50-fold ionized nuclei occur in the heavy component Now, since the ionizing power of a high energy particle increases with the square of its charge, it is seen that the heavy primaries of cosmic radiation must have an extremely high energy dissipation along their paths in any absorber. It is this quality which represents the specific hazard of an exposure in the region of the primary cosmic radiation.

Received July 7, 1952.

[1] Paper presented at the Fall Meeting of the AMERICAN ROCKET SOCIETY in Chicago, Ill., September 9, 1952.

[2] Biophysicist; member of the staff.

[3] Numbers in parentheses refer to the Biblography on page 283.

In talking of the extremely high energies of the cosmic ray primaries one must clearly distinguish between the over-all energy of the total incoming cosmic ray flux and the energy of the individual particle. It is only the latter which exceeds by many ten powers all other radiations available. The former is very small even in the lower stratosphere, where no attenuation due to absorption has occurred. That means more precisely, the number of incoming particles per unit time and per unit cross section is very small. Due to this circumstance, cosmic ray research faces the unfortunate double difficulty that, while experimentation with the primary radiation can only be performed in the gondolas of pilot balloons or in the warheads of rockets, prolonged exposure times are required to produce measurable effects.

## 3 The Influence of the Geo- and Heliomagnetic Fields

Before proceeding to the presentation of quantitative data on the mass and energy spectrum of the primary radiation, another phenomenon has to be briefly discussed, namely, the influence of the geomagnetic field on the primaries. As is well known, the Earth is a magnet and its magnetic dipole field extends far beyond the ionosphere into empty space. The cosmic ray primaries, being positively charged particles, suffer from deflection in this field, and it requires a certain minimum kinetic energy for a cosmic ray particle to reach the Earth at all. Moreover, since the deflecting influence of the geomagnetic field is strongest for particles traveling in the equatorial plane and weakest along the magnetic axis, this minimum energy for reaching the Earth can be expected to show a marked latitude dependence. The experimental data give indeed a full, quantitative corroboration of this theoretical conclusion for the latitude range from zero (equator) to about 55°N. Table 1 gives the minimum energy necessary for completely ionized nuclei to reach the Earth at vertical incidence for different latitudes.

TABLE 1 GEOMAGNETIC CUT-OFF VALUES FOR CHARGED PRIMARIES APPROACHING THE EARTH FROM OUTER SPACE[a]

| | Geomagnetic latitude | | | |
|---|---|---|---|---|
| Particle type | 55° | 41° | 30° | 0° |
| A = Z (Protons) | 1.0 BeV | 4.0 | 7.3 | 13.8 |
| A = 2Z (He and heavier) | 0.3 | 1.6 | 3.3 | 6.5 |

[a] The table gives the minimum kinetic energy in billion electron-volts required for atom nuclei to reach the earth at vertical incidence for different latitudes. A, Atomic weight; Z, Atomic number.

It is seen from these data that, due to the screening influences of the geomagnetic field, low-energy particles are entirely excluded from reaching the Earth. It remains under these circumstances an open question whether such low-energy particles are present or not in the genuinely "primary" spectrum of cosmic radiation in free space far away from any heavenly body with its shielding magnetic field.

Closely connected with this question is the controversial issue of the existence of a magnetic field of the Sun (7, 8). It has been mentioned previously that the latitude dependence of the cosmic ray intensity follows the prediction of the geomagnetic theory only to about 55°N. Beyond that latitude a further strong increase should be expected theoretically. Actually, however, a knee is observed in the curve and the intensity remains constant toward higher latitudes, at least, as far as the recordings available at present are conclusive. This behavior of the intensity curve has been tentatively attributed to the influence of the heliomagnetic field whose field strength at the Earth's orbit is assumed, according to this hypothesis, to equal in screening strength the geomagnetic field at 55°N and take over the shielding function from this point to higher latitudes.

It might be emphasized once more that this hypothesis is far from being well established. No clear experimental decision can be given at present whether the Sun has a magnetic field and what its intensity and configuration in particular might be. Consequently, we also do not know whether the absence of the low-energy cosmic ray primaries is a secondary effect due to magnetic shielding or an intrinsic quality of the cosmic radiation itself. More detailed high-altitude recordings close to the geomagnetic poles are needed for the solution of this problem.

For the radiobiological consequences, this uncertainty is especially unfortunate since the main threat of an exposure hazard rests upon the low-energy part of the spectrum, as will be discussed in detail later.

## 4 The Energy and Mass Spectrum of the Primary Radiation

The full energy spectrum of the primaries is a continuum which extends from the geomagnetic cut-off energies given above to extremely high values. One of the highest energies so far directly measured has been found in a primary alpha particle recorded by M. F. Kaplon and collaborators (9). Its kinetic energy can be analyzed rather accurately because this particle has released, in the stack of photographic plates, a nuclear disintegration comprising 72 fragments which can be followed through many subsequent plates so that the total energy balance can be thoroughly computed. The kinetic energy of this particle equals $8 \times 10^{12}$ electron-volts, i.e., 8000 billion electron-volts.

Such rare giants in the primary radiation are the starting point of the so-called large cosmic ray showers. These are avalanches of many thousands, or even millions, of simultaneously occurring particles sometimes covering, at sea level, areas of a mile or more in diameter. The showers gradually develop in cascades of successive nuclear disintegrations from such primaries of extremely high energy. Though the complicated mechanism of shower production has been thoroughly investigated and very well clarified in its different phases, the main question of where the primary particles collect their tremendous energy stays completely unsolved.

Besides the energy spectrum, the mass spectrum of

the cosmic ray primaries is of interest. Table 2 gives the quantitative data on it as they follow from the recordings. It should be mentioned that one must clearly distinguish between the particle number with which the different components are represented in the spectrum and the energy which they carry. It is a well-established fact, which is so far not yet understood in its causation, that the heavy primaries carry equal amounts of energy *per nucleon;*[2] i.e., the average energy of a heavy particle is larger than the one of a lighter particle by the ratio of the atomic weight. Thus, the percentage of the total energy carried by the heavy components is considerably larger than the percentage of the particle number, as is shown from Table 2. This remarkable phenomenon might help some day to shed light on the acceleration mechanism and the origin of the cosmic ray primaries.

TABLE 2 MASS SPECTRUM OF THE PRIMARY COSMIC RADIATION ON TOP OF THE ATMOSPHERE AT DIFFERENT LATITUDES[a]

| | Geomagnetic latitude | | | |
|---|---|---|---|---|
| Particle type | 55° | 41° | 30° | 0° |
| Protons | 12,600 | 4560 | 2510 | 1350 |
| He | 1,820 | 723 | 327 | 163 |
| C, N, O | 91 | 38 | 18 | 8.8 |
| $Z > 10$ | 27 | 15 | 6.2 | 3.1 |

[a] The table gives the number of particles per second traversing a horizontal surface of 1 square meter under any angle, i.e., incoming from the full hemisphere.

## 5 The Transition Effect

Though the discussion here is limited to the situation on top of and outside the atmosphere, it might be permitted to outline briefly the situation in the lower stratosphere and in the troposphere. The high-energy primaries when entering the air blanket undergo different types of collision processes in which their energy is transmitted to secondary particles. As a consequence, the composition of the cosmic radiation in the lower regions is completely different from the primary radiation. At 70,000 ft, practically all primaries are extinguished and the secondaries (mesons, neutrons, photons, electrons, positrons, and secondary protons and alpha particles) are the exclusive carriers of the energy flux. In each collision of a primary particle several to many such secondaries are generated. Thus, the number of particles increases substantially in the initial layers of the air blanket until finally at greater depths the absorption processes outweigh this multiplication and the particle numbers decrease. It is seen that at a certain altitude a maximum particle density must occur. This happens at about 70,000 ft.

Parallel to the maximum number of particles the rate of energy dissipation per unit mass of absorber passes also through a maximum. In radiobiological terms, the ionization dosage in living tissue also goes through a maximum. Fig. 1 gives the numerical data for this relationship.

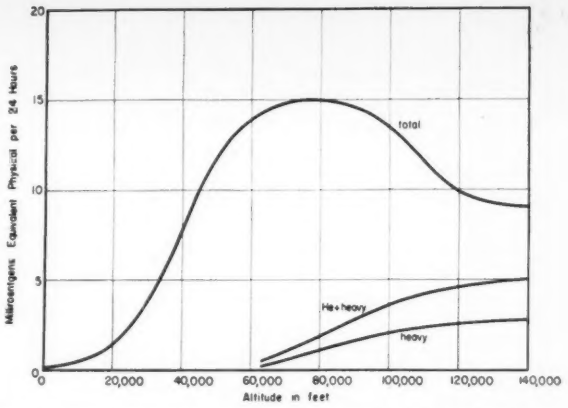


FIG. 1 IONIZATION DOSAGE IN LIVING TISSUE FROM COSMIC RADIATION AT NORTHERN LATITUDES

The phenomenon that the rate of energy dissipation of a radiation in an absorber passes through a maximum is called transition effect. The transition effect of the cosmic radiation plays an important role in the evaluation of the actual exposure hazard of human beings in a ship. The values of the total dosage in Fig. 1 are correct only for an infinitesimally small sample of living tissue far apart from any additional masses of a greater density. They probably still will be correct for an object of the size of a mouse. But as soon as a larger mass is involved, for instance a rocket ship, local transition effects will develop and the ionization dosage in the surroundings will be much higher. Fig. 1 shows that the dosage multiplication factor due to the transition effect in the rarefied air beyond 75,000 ft equals about 2. It can be expected that for denser materials this value will be markedly exceeded. These relationships quite generally have to be kept in mind as soon as one starts calculating actual figures for the ionization dosage in any kind of ship. It would be a gross mistake to assume the numerical values of Fig. 1. They merely represent the lower limit for very small objects.

## 6 The Radiobiological Aspects

The crucial point in the problem of a possible exposure hazard at high altitudes, however, is not connected to this phenomenon but is of a very different nature. As has been seen from the brief analysis of the transition processes which occur when the primary radiation interacts with the air blanket, a continuous change in the types of particles which carry the energy flux and produce the ionization takes place from the top of the atmosphere to deeper regions. As far as the heavy component of the primary radiation is concerned, Fig. 2 gives the numerical data for their gradual extinction.

The primaries transfer their energy mainly to mesons, alpha particles, neutrons, protons, and electrons. This change in the type of ionizing particle has decisive importance for the biological effectiveness of the cosmic

[2] Nucleon is a general term for proton and neutron. Since modern theory of the intra-nuclear forces assumes that protons and neutrons exchange their identities in the nuclear bond, it was useful to introduce a common name for both particles.

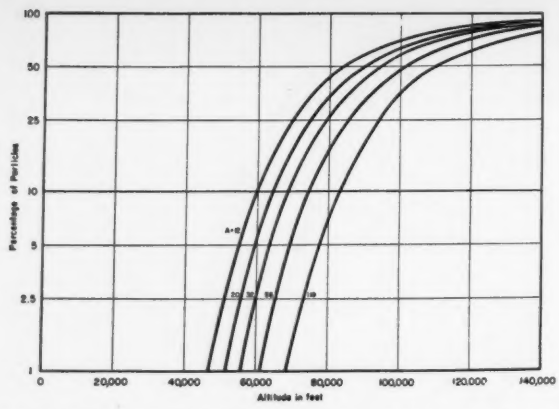


FIG. 2 DEPTH OF PENETRATION FOR HEAVY NUCLEI OF PRIMARY COSMIC RADIATION

ray energy flux because these secondaries differ greatly in specific ionization from the heavy primaries.

The specific ionization of a radiation is a measure of the density of ionization along the path of the individual ionizing particle. It is usually given by the number of ion pairs per unit path length. The specific ionization varies greatly for different types of particles. Moreover, it varies greatly for the same particle for different kinetic energies. A fair first approximation is given by the general rule that the specific ionization is proportional to the square of the charge of the particle and inversely proportional to the square of its velocity.

It is a well-established fact in radiobiology that the specific ionization is a factor which greatly influences the quantity of effect of a radiation exposure. The same total ionization dosage, say 500 roentgen units, administered once with gamma rays (low specific ionization) and once with alpha rays (high specific ionization), will produce a very different degree of radiation damage. For the so-called long-term low-dosage damage with which we deal in prolonged or often repeated exposures to very low intensities, this difference amounts to a factor of about 20 for alpha radiation, meaning that alpha radiation is twenty times as effective as gamma radiation. To take into account this difference in the biological effectiveness of the same ionization dosage of different types of radiations, the original definition of the roentgen unit has been amended by introducing the differentiation in two units, the roentgen-equivalent-physical and the roentgen-equivalent-man, the former giving the ionization dosage, the latter giving the biologically effective dosage.

The specific ionization of the heavy primaries of the cosmic radiation covers a wide range from values below that for alpha rays to values far above it. Under these aspects it is seen that the right-hand part of the curve of the total ionization in Fig. 1 represents, with regard to the biological effect, something completely different from the left-hand part. On the right side of the ionization maximum of 70,000 ft, the heavy component is participating in the production of the total ionization dosage. The actual biological dosage in this region, therefore, can be expected to be considerably higher than in the corresponding region below 70,000 ft.

The high values of specific ionization are not the only characteristic feature of the heavy primaries. In addition, profound differences exist with regard to the spatial distribution of the ionizations along the particle tracks. Fig. 3 might demonstrate this more clearly. It shows a heavy nucleus and an alpha track recorded in the same nuclear emulsion plate and microphotographed at the same magnification. Though the photo emulsion is not suited to furnish accurate quantitative information, Fig. 3 shows clearly the much larger spread of the ionization events in the cross section of the heavy nucleus track. The reason for this phenomenon is the high kinetic energy of the heavy nucleus which results in correspondingly higher kinetic energies transmitted to the secondary electrons which the heavy nucleus particle produces in collisions with absorber atoms. This large radial spread of the ionization dosage around the heavy nuclei tracks is a novel phenomenon, since no other artificial or natural radiation source furnishes these excessively high kinetic energies. It is, therefore, not yet possible to appraise the biological significance in all its consequences.

As has been mentioned already, the specific ionization varies greatly with the velocity of the particle obeying roughly an inverse square law. It is due to this fact that the low-energy part of a heavy track represents the most harmful section with regard to the exposure hazard. Fig. 4 demonstrates such a terminal section of a heavy track in nuclear emulsion. The left-hand part shows the track section of a heavy nucleus of Z 20 at 15 billion e-volts kinetic energy. The upper part of the central section shows the same track at 1.25 billion e-volts kinetic energy. The track here is in its terminal phase and passes through the so-called ionization peak and thin-down part before coming to a final stop. The scale at the upper left gives the magnification; 1 division equals 10 microns. It has to be kept in mind, how-

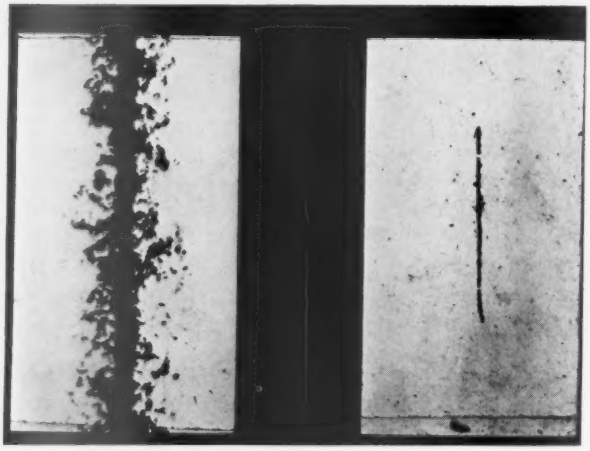

FIG. 3 NUCLEAR EMULSION TRACKS OF A HEAVY NUCLEUS AND AN ORDINARY ALPHA TRACK

Both pictures were taken from the same plate and at the same magnification. Vertical length of the visual field: 82 microns. (Recorded by P. Freier and E. P. Ney, University of Minnesota.)

ever, that Fig. 4 shows the track in nuclear emulsion. If it had traversed living tissue, the length of the track, because of the considerably lower absorptive power of living tissue, would have to be increased by about a factor 4. Fig. 4 demonstrates strikingly that the ionization peak and thin-down part are the specifically harmful phases of the entire track.

Besides the energy dissipation by ionization due to collisions with orbital electrons, heavy nuclei can undergo another type of collision process, namely, with the nuclei of absorber atoms. This process often is called catastrophic absorption because, in such a collision, usually the total energy of the projectile nucleus is transformed in one elementary act and a total disruption of both the projectile and the target nucleus occurs.

If such a nuclear collision takes place in an atom of heavy atomic weight (silver or bromine) in photographic emulsion, the fragments of the nuclear explosion form a starlike pattern. Microphotographs of such disintegration stars in emulsions give an impressive pictorial demonstration of the large energies involved. Fig. 5 gives an example of such a high-energy event recorded in the lower stratosphere by H. Yagoda (4). One can distinguish in the picture a narrow cone consisting of many mesons, a somewhat wider cone of similar composition, and several noncollimated heavier fragments.

FIG. 4 NUCLEAR EMULSION TRACK OF A HEAVY NUCLEUS OF Z-20

The left section shows the track at 15 billion e-volts kinetic energy. The center and right-hand sections (travel direction downward) show the terminal part. The kinetic energy at the uppermost point of the center section is 1.25 billion e-volts. Scale at upper left: 1 division—10 microns. (Pilot balloon recording of P. Freier and E. P. Ney, University of Minnesota.)

In a discussion of possible effects on living matter one should clearly remember, however, that the special emulsions used for such recordings contain more than 80 per cent in weight of silver bromide, whereas living tissue contains heavier atoms only to a negligible percentage. Disintegration stars released in tissue, therefore, can consist only of a small number of prongs. Columns of such an extremely dense ionization as is seen in the initial part of the narrow meson cone in Fig. 5 are not likely to occur in living matter from disintegration stars.

The probability for a nuclear encounter quite generally is incomparably smaller than for a collision with some orbital electrons resulting in ordinary ionization. This ratio is of the order of $10^9$. That means a heavy nucleus before undergoing a catastrophic absorption produces on the average about $10^9$ ionizations before being annihilated in a nuclear collision. It is seen from this relationship, even without entering into mathematical detail, that high-energy heavy nuclei passing through an absorber have a higher chance to be eliminated by catastrophic absorption before reaching the ionization peak and thin-down phase in the terminal part of their track than low-energy nuclei. This consequence has important bearing for the exposure hazard. As has been seen above, the geomagnetic cut-off values vary considerably with lati-

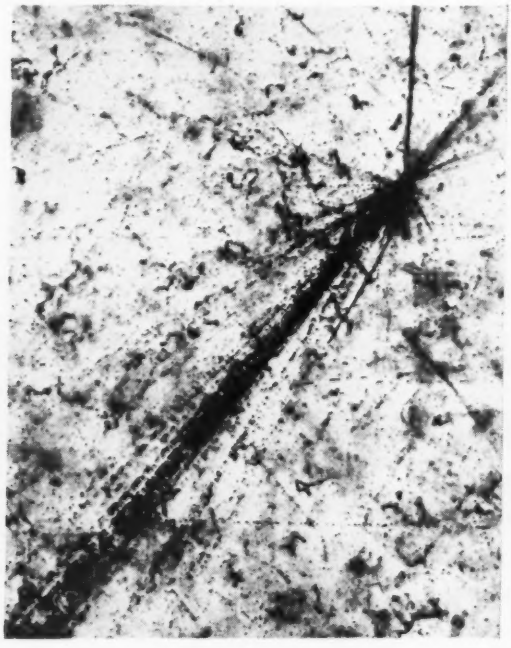

FIG. 5 NUCLEAR DISINTEGRATION OF A SILVER OR BROMINE NUCLEUS OF PHOTOGRAPHIC EMULSION RELEASED BY A HIGH ENERGY PARTICLE OF PRIMARY COSMIC RADIATION

(Recording of H. Yagoda, Laboratory of Physical Biology; National Institute of Health)

tude. The numerical values for this relationship happen to be just in the critical range so that, for the lowest energy at which heavy nuclei can reach the earth in the equatorial belt up to about 30°, the probability for catastrophic collision is practically unity, whereas at about 50° N this probability has decreased to about 0.85. That means that practically no particles in the equatorial belt reach the ionization peak. They are all eliminated beforehand by catastrophic absorption. At 50° N, however, about 15 per cent of all incoming heavy nuclei escape nuclear collisions and pass through the ionization peak. The detailed latitude curve for this relationship has yet to be investigated more thoroughly, but it seems safe to conclude on the basis of the present experimental data that the most harmful type of the heavy primaries, those which pass through the ionization peak with its excessively high specific ionization, seems to be limited to northern latitudes and the polar cap.

Whether this greatly increased hazard due to the low-energy heavy primaries is fairly constant in the entire region from 55°N to the pole, or whether the heavy component at extreme altitudes does not follow the general leveling-off of the total intensity, remains an open question. It can only be hoped that the modern tools for high-altitude sounding will be more extensively used in the near future at the geomagnetic north pole itself to clarify this unknown part of the problem and the controversial issue of the Sun's magnetic field.

## 7 The Exposure Hazard in the Interplanetary Region

Still more vague and uncertain is the situation with regard to the interplanetary regions at greater distances from the Earth. The highest direct Geiger counter telescope recordings extend to an altitude at about 150 kilometers. They indicate that in the range between 40 and 150 kilometers the total intensity of the primary cosmic radiation is constant. This information, however, does not contain any details in regard to the composition of the radiation.

For still larger distances from the earth the intensity of all components can be expected to increase slowly to twice their stratospheric values, due to the fact that the influence of the shadow of the earth gradually vanishes. For an observer in the upper stratosphere, the Earth still covers very nearly the full hemisphere and, therefore, screens off half of the cosmic ray intensity. This simple geometric relationship is plotted in Fig. 6. The actual intensity can be expected to increase somewhat steeper and to higher values than those in the figure because at increasing distances from the earth the shielding influence of the geomagnetic field gradually decreases.

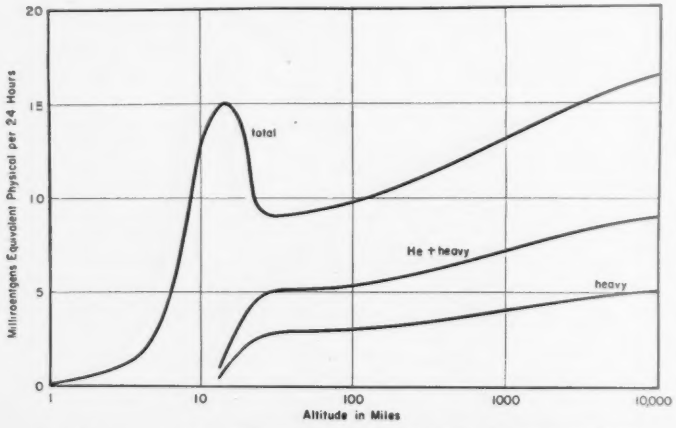


FIG. 6 IONIZATION DOSAGE IN LIVING TISSUE FROM COSMIC RADIATION

## 8 Conclusions

All these conclusions concerning the situation beyond the altitude of 150 kilometers which represents at the moment the limit of the zone directly accessible for measurements are, of course, guesswork. The unknown magnitude is the lower part of the energy spectrum of the primary cosmic radiation, and we have seen that it is just this part which is most important for the problem of a possible exposure hazard. Thus, very disappointingly, the present state of knowledge can only be summarized in three "if" statements:

(1) If there is no such thing as a lower end in the genuinely primary spectrum and only the geomagnetic field produces artificially the cut-off edges in the spectrum which we actually observe, it can be assumed that radiation hazards in regions outside the shielding influence of the geomagnetic field will be prohibitively great.

(2) If the hypothesis of the heliomagnetic field taking over the shielding function at 50°N latitude should prove true, exposure of humans seems feasible—though with a rather marked deterioration of the mean life expectancy due to the radiation damage—in that part of interplanetary space in which the protection due to the heliomagnetic field is effective. This would certainly be true for the full space inside the Earth's orbit, but it would be rather questionable whether the "safe" zone would extend outward to Mars' orbit.

(3) If already in the genuinely primary spectrum the low-energy heavy nuclei are absent, exposure of humans seems practicable everywhere in space with the restriction concerning chronical radiation damage mentioned before. What the actual figure for the abbreviation of the lifetime or the other possible types of radiation injury from exposure of humans to low-energy heavy nuclei will be cannot yet be sharply defined. The heavy nuclei component of the primary cosmic radiation is a new phenomenon not only for the cosmic ray physicist but all the more for the radiobiologist. Its exploration is for the latter unequally more difficult since he has to deal with reactions in living matter which, for full development and manifestation, require periods of months and large-scale statistical experimentation. To perform

such experimentation in the lower stratosphere is both expensive and time-consuming.


### Acknowledgment

The author wishes to express his gratitude to Drs. E. P. Ney and P. Freier for permitting the reproduction of Figs. 3 and 4, and to Dr. H. Yagoda for Fig. 5.


### Bibliography

The following references are selected merely to introduce the interested reader to the vast literature. Wilson's monograph (6) is the latest complete survey of the whole field but requires a full knowledge of modern theoretical physics. For a short outline of the field, the nonmathematical reader might better resort to Leprince-Ringuet's monograph (10).


1 "The Heavy Component of Primary Cosmic Radiation," by P. Freier, E. J. Lofgren, and F. Oppenheimer, *Physical Review*, vol. 74, 1949, pp. 1818–1827.

2 "The Heavy Nuclei of the Primary Cosmic Radiation," by H. L. Bradt and B. Peters, *Physical Review*, vol. 77, 1950, pp. 54–70.

3 "Intensities of Heavy Cosmic-Ray Primaries by Pulse Ionization Chamber Measurements," by J. A. Van Allen, *Physical Review*, vol. 84, 1951, pp. 791–797.

4 "The Emission of Slow Positive or Negative Mesons from Nuclear Disruptions Produced by Cosmic Radiation," by H. Yagoda, *Physical Review*, vol. 85, 1952, pp. 891–900.

5 "The Energy Spectrum of Primary Cosmic Radiation," by M. F. Kaplon, B. Peters, H. L. Reynolds, and D. M. Ritson, *Physical Review*, vol. 85, 1952, pp. 295–309.

6 "Progress in Cosmic Ray Physics," by J. G. Wilson, North-Holland Publishing Company, Amsterdam; Interscience Publishers, Inc., New York, 1952, 557 pp.

7 "The Apparent Absence of Low Energy Cosmic Ray Primaries," by J. A. Van Allen and S. F. Singer, *Nature*, 1952 (in press).

8 "The Increase in the Primary Cosmic Ray Intensity at High Latitudes and the Non-Existence of a Detectable Permanent Solar Magnetic Field," by M. A. Pomerantz, *Physical Review*, vol. 77, 1950, pp. 830–837.

9 "Evidence for Multiple Meson and Gamma-Ray Production in Cosmic-Ray Stars," by M. F. Kaplon, B. Peters, and H. L. Bradt, *Physical Review*, vol. 76, 1949, pp. 1735–1736.

10 "Cosmic Rays," by L. Leprince-Ringuet, Prentice-Hall, Inc., New York, 1950, 290 pp.


## Manned Flight at the Borders of Space


*(Continued from page 276)*



20 "Effects of Cosmic, Ultra-Violet and Heat Radiation at 50,000 to 100,000 Feet," by K. J. K. Buettner. Paper presented at the June 1952 meeting of the Aero-Medical Engineering Association University of California, Los Angeles, Calif.

21 "Gravity, Inertia and Weight," by H. Haber. Contribution to "Physics and Medicine of the Upper Atmosphere," edited by C. S. White and O. O. Benson, Jr., The University of New Mexico Press, Albuquerque, N. M., 1952.

22 "Animal Experiments in Rockets," by J. P. Henry and J. Ballinger. Paper presented at the session of the Space-Medical Association of the American Aero-Medical Association, Washington, D. C., March 1952.

23 "Man under Gravity-free conditions," by O. Gauer and H. Haber, German Aviation Medicine World War II, vol. 1, p. 641; U. S. Government Printing Office, Washington, D. C.. 1950.

24 "Physics and Psychophysics of Weightlessness," by H. Haber and S. J. Gerathewohl, *Journal of Aviation Medicine*, vol. 22, 1951, p. 180.

25 "The Light of the Sky and Related Problems," by H. Haber. Paper presented at the June 1952 Meeting of the Aero-Medical Engineering Association, University of California, Los Angeles, Calif.

26 "Brightness and Polarization of the Daylight Sky at Various Altitudes above Sea Level," by R. Tousey and E. O. Hulburt, *Journal of the Optical Society of America*, vol. 37, 1947, p. 78.

27 "Brightness Relationships for Comfortable Seeing," by S. K. Guth, *Journal of the Optical Society of America*, vol. 41, 1951, p. 235.

28 "A Discussion of Retinal Adaptation Applicable to Visual Problems Encountered by Man in Flight at Increasing Altitude," by P. A. Cibis. Contribution to "Physics and Medicine of the Upper Atmosphere," edited by C. S. White and O. O. Benson, Jr., The University of New Mexico Press, Albuquerque, N. M., 1952.

29 "The Laws of Motion in Space Travel," by E. Saenger, *Interavia*, vol. 4, 1949, p. 416.

30 "Bioclimatology of Manned Rocket Flight," by K. J. K. Buettner. Contribution to "Space Medicine," edited by J. P. Marbarger, The University of Illinois Press, Urbana, Ill., 1951.

31 "Thermal Aspects of Travel in the Aeropause; Part I: Thermal Radiation," by K. J. K. Buettner. Contribution to "Physics and Medicine of the Upper Atmosphere," edited by C. S. White and O. O. Benson, Jr., The University of New Mexico Press, Albuquerque, N. M., 1952.

32 "The Aeropause," by K. J. K. Buettner and H. Haber, *Science*, vol. 115, 1952, p. 656.

33 "Apparent Rotation of a Fixed Target Associated with Linear Acceleration in Flight," by B. Clark and A. Graybiel, *American Journal of Ophthalmology*, vol. 32, 1949, p. 549.


# Letters to the Editor

**This section of the Journal is open to letters not exceeding 600 words in length (or one and one-half columns) devoted to brief research reports or technical discussions of papers previously published. Such letters are published without editorial review, usually within two months of the date of receipt. The style and manner of submission of letters are the same as for regular contributions. (See inside back cover.)**

# Jet Propulsion News*

C. F. WARNER, Purdue University, *Associate Editor*

with the assistance of W. G. BOHL

## Rockets and Missiles

ACCORDING to an article by G. L. Christian in *Aviation Week*, a scale model of one of the Navy's tailless delta-wing aircraft is being flight-tested by means of rocket power. The model, equipped with telemetering apparatus, is attached near the tail of a standard 5-in. military rocket. The extensive telemetering equipment built by Bendix Aviation Corporation records continuously such in-flight information as ram air pressure, longitudinal acceleration and deceleration, yaw and pitch acceleration, and amplitude and frequency of wing vibrations. The use of the relatively inexpensive rocket-powered model eliminates the need for wind tunnel tests. The model, approximately 12 ft long with a span of 4 ft, reaches a flight Mach number of over 1 in approximately two seconds and has a flight time of twenty seconds.

✦ ✦ ✦

THE Navy has announced that its Douglas Skyrocket established a new world altitude record for piloted aircraft of higher than 79,000 ft during its June 15, 1951, flight. The flight was checked and certified by the National Advisory Committee for Aeronautics. A speed of 1238 mph has also been confirmed.

✦ ✦ ✦

IT has been reported that the Borg-Warner Corporation has obtained a patent for the design of a rocket-ramjet missile motor. The use of nitroaliphatic rocket propellants by supplying additional oxygen are said to contribute to a more stable flame front. The patent claims that the use of these oxidizers increases the thrust and efficiency of the ramjet.

✦ ✦ ✦

THE Northrop Decelerator, designed to "determine the tolerances of the human body's resistance to decelerative forces so that better equipment can be provided for emergency and crash landings," employs from one to four Aerojet 5 AS-1000 solid rockets, each rated at 5000 lb-sec of impulse, to reach its maximum speed. The Decelerator consists of a sled riding on a 2000-ft long track. At 150 mph, brakes are applied which slow the sled to 70 mph in a distance of 25 ft in a mere 0.16 sec. Both dummies and human volunteers have been used in the tests. The decelerative force is applied in a 50-ft section of the 2000-ft track, where 45 brakes, each with four brake shoes, are remotely applied by instruments developed especially for use with the sled. Much of the equipment tested has already proved its usefulness in saving lives.

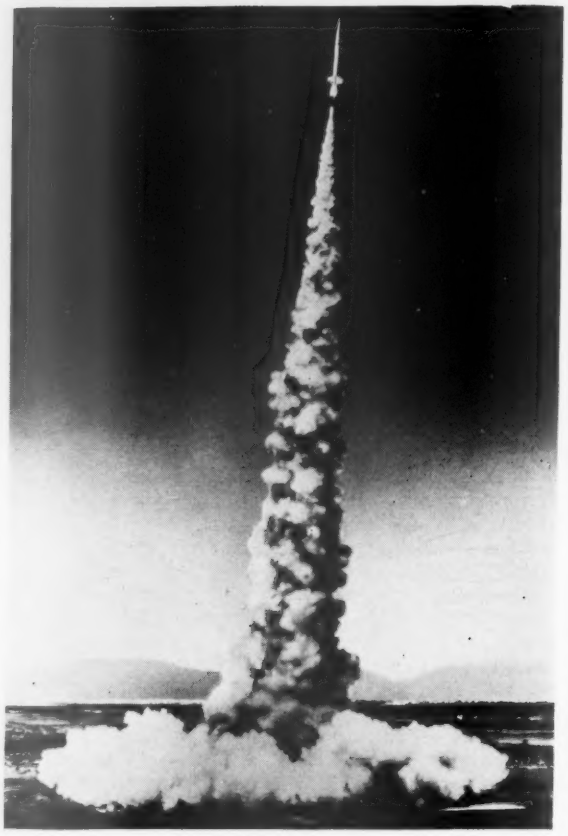

FIG. 1 AEROJET AEROBEE SOUNDING ROCKET LEAVING THE LAUNCHING TOWER UNDER TREMENDOUS THRUST FROM ITS SOLID PROPELLANT BOOSTER ROCKET

✦ ✦ ✦

A CONTRACT for production of missile motor components of a type recently developed by Aerojet Engineering Corporation has been awarded by Aerojet to Ryan Aeronautical Company. This is the second Aerojet rocket project for which Ryan has been selected as a productive source. Previously Ryan built major components of the Aerobee high-altitude sounding rocket. Currently, Ryan is also building complete rocket motors for surface-to-surfaee missiles under a production contract from Firestone Tire and Rubber Company. Ryan also supplied this rocket motor under previous experimental contracts to Douglas Aircraft. The motor was developed by the Caltech Jet Propulsion Laboratory.

* The information reported in this Section has been selected from approved news releases originating with the Department of Defense, private manufacturers, universities, etc., and from published news accounts in journals and newspapers. The reports are considered generally reliable, although no attempt has been made to verify them.

IT has been reported that, under Britain's large unpublicized guided missile program, missiles are being built by six major aircraft or engine manufacturers. Several Australian-built target drones powered by British Armstrong Siddeley Adder turbojets have been flown successfully. Several models of ramjets and expendable engines are to be tested soon at the Australian Woomera range. Since test flights are restricted by short ranges and weather in England, a joint British-Australian proving ground was started in Australia in 1947. This area, known as the Long Range Weapons Establishment, extends 1200 miles into the open desert.

✦ ✦ ✦

McDONNELL Aircraft Company, in a report on 17 airplane, helicopter, and guided missile models, revealed that it has been manufacturing for the U. S. Navy a self-propelled armor-piercing radio-controlled pilotless bomb designated the RTV-2 Gargoyle.

✦ ✦ ✦

A NEW altitude record of 80 miles was recently established for the Aerojet AEROBEE free-flight sounding rocket in launchings at the proving grounds in New Mexico. By making it possible to investigate the upper atmosphere for conditions of temperature, composition, density, magnetic-field, cosmic ray intensity, x-ray intensity, winds aloft, etc., the AEROBEE has been the medium for obtaining valuable scientific data heretofore unavailable. Since initial launchings in 1947, it has been the most widely used and least expensive research sounding rocket available for transporting scientific instrumentation on nearly vertical flight.

Carrying a nominal pay load of 150 lb, the AEROBEE vehicle is powered by a bipropellant liquid rocket and is initially accelerated by a large JATO booster rocket, which detaches and falls away upon cessation of booster thrust (Fig. 1). After reaching a high velocity during powered flight, the AEROBEE coasts to the zenith altitude, at which time nose ejection may be accomplished for parachute recovery of the nose section. Launched from a tower 150 ft in height, the AEROBEE is stabilized with fixed fins. The vehicle is 20 ft long and 15 in. in diam, the booster rocket adding another 6 ft to the over-all length.

## Aircraft

THE USAF has announced the existence of three new jet fighters, the North American XF-100, the McDonnell XF-101 Voodoo, and the Convair XF-102, and a light bomber, the Douglas RB-66.

✦ ✦ ✦

AMERICA'S latest answer to air invasion, an almost automatic jet warplane armed with radar and rockets to outshoot enemy bombers, is now in production at Lockheed Aircraft Corporation. The new airplane, the Starfire F-94C, built for USAF, carries twenty-four 2.75-in. rockets housed in a ring of firing tubes around the nose. Different views of this fighter-intercepter are shown in Figs. 2, 3, and 4.

FIG. 2 THE ALL-ROCKET-ARMED LOCKHEED F-94C STARFIRE

Radar and an electrical "copilot" enable the Starfire to spot the enemy miles away, lock onto the target, track, close, aim, and open fire without pilot assistance. The main duties of the pilot and radar operator are to take the plane off, maneuver to the general target area as guided by ground radar watchers, switch on the "electronic crew" at the proper time, monitor operation of the piloting and rocket-control apparatus during attack, and then land. The automatic pilot with unlimited maneuverability was developed by the Westinghouse Electric Corporation. With the autopilot at the controls, the plane will be able to take the steepest dives, turns, rolls, and loops with ease.

The Starfire, with its 1200 lb of electronic gear, is powered by a Pratt and Whitney J-48-P-5, 6250-lb thrust jet engine equipped with an afterburner. A ribbon parachute, stowed in a tail compartment, can be released just as the ship lands, to halt it in a short space. The take-off weight is more than 20,000 lb; it has a length of 41 ft and a span of $37\frac{1}{2}$ feet.

✦ ✦ ✦

A RADICALLY new flying-boat hull bottom, affixed to the wing and full crown of a World War II vintage seaplane, is currently being taxi- and flight-tested on and over the waters of the Chesapeake Bay. Designated as research model M-270, the hull embodies in full scale the result of years of extensive towing tank and wind tunnel tests, according to a joint announcement by

FIG. 3 THE F-94C WITH ROCKET DOORS OPEN


FIG. 4 THE STARFIRE IN FLIGHT

the U. S. Navy and the Glenn L. Martin Company. For years, flying boat engineers have envisioned larger slimer hulls to provide superior aerodynamic seaplane shapes as well as more efficient structural bodies. These shapes are likewise dictated through the necessity of having more efficient hulls in which to use jet engines, as these will give seaplanes of the future much greater speed. Fig. 5 shows a model of the M-270 in the towing tank at Stevens Institute of Technology.

✦ ✦ ✦

ACCORDING to *Interavia*, the Russians are flight-testing a two-jet swept-wing bomber designated the Type 150. The new bomber, designed by a group of German engineers under the leadership of Dr. B. Baade, formerly of the Junkers works, is said to have a span of 102 ft, a length of 82 ft, and to be powered by two 11,000-lb thrust Lulkov axial-flow turbojet engines. The bomber is reported to have a speed of 620 mph.

✦ ✦ ✦

IT is reported that a French process has been developed for building supersonic aircraft wings from prestressed concrete. An experimentally developed wing by Bregault is cheaper and easier to build than a conventional wing. The new wing is also reported to have greater strength.

## Turbojet Engines

BRISTOL has developed a twin-spool compressor jet engine—the Olympus—in the 10,000-lb thrust class. It is claimed to be the world's most economical and most powerful jet engine at this stage of development. The engine is able to accelerate from idling to full power in two seconds and is said to have a fuel rate of 0.766 lb/lb thrust/hr. The Olympus has a frontal diameter of only 40 in., a length of 124 in., and weighs 3250 lb. Under its agreement with Bristol, Wright Aeronautical has had an Olympus under test at Wood-Ridge, N. J. Wright Aero has been able to obtain a static thrust of 9800 lb from the engine.

## New Facilities

A NEW wind tunnel has been placed in operation at the Polytechnic Institute of Brooklyn capable of attaining Mach 5 in its 4-in. × 4-in. test section. This blow-down tunnel, designed by Dr. Paul A. Libby and Dr. Antonio Ferri, is supplied with 100 cu ft of air at 3000 psia from Navy-loaned torpedo air bottles. Other nozzles are available for operating the tunnel at Mach 2 and 3. Schlieren and shadowgraph apparatus may be used for photographic studies.

✦ ✦ ✦

A TRANSONIC wind tunnel at the Navy's David Taylor Model Basin, when completed late in 1953, will permit testing of models at speeds up to 900 mph. The tunnel, based on a design of a tunnel partly built by the Germans near Munich, will be of closed circuit type, 574 ft long. Construction will be of reinforced concrete, with a steel test section.

✦ ✦ ✦

THE world's largest and most powerful "human centrifuge," a machine to subject pilots to extreme gravitational conditions encountered in sonic-speed aircraft, has been put into operation at the Naval Aviation Medical Acceleration Laboratory. Built by the McKiernan-Terry Corporation, the centrifuge is capable of accelerating from a dead stop to 173 mph in less than seven seconds, and will speed up from zero to approximately 90 mph in one and one half seconds.

The giant "whirligig" is capable of exerting a force equal to 40 times the gravitational pull of the earth on a pilot seated in a gondola at the end of a 50-ft rotating arm. It will be used by the Navy to evaluate human tolerance to acceleration and to study the physiological systems which limit the tolerance. Since the human "guinea pig" is visible to researchers only when the centrifuge is motionless, high-speed television, x-ray, and motion picture cameras are mounted in the gondola.

## Personalities

W. L. ROGERS, who for the past year has been managing Aerojet's Washington office, has been appointed assistant general manager. The announcement is made by W. E. ZISCH, General Manager.

✦ ✦ ✦

RAYMOND W. YOUNG, president of Reaction Motors, Inc., of Rockaway, N. J., has announced the

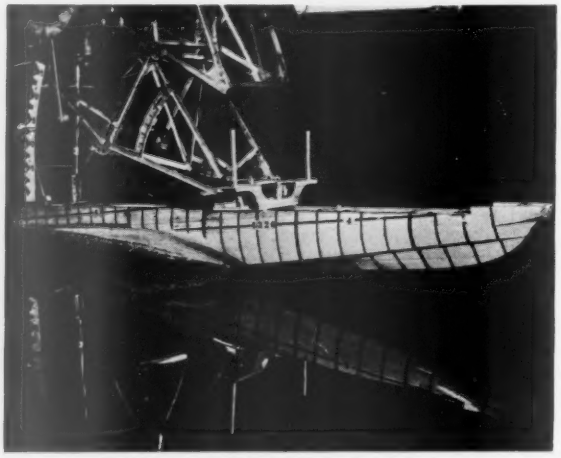

FIG. 5 MODEL OF M-270 IN TOWING TANK AT STEVENS INSTITUTE OF TECHNOLOGY

appointment of DR. LUIGI CROCCO, R. H. Goddard Professor at the Daniel and Florence Guggenheim Jet Propulsion Center, Princeton University, to the Advisory Board of the Company. In accepting the appointment to the Advisory Board of Reaction Motors, Dr. Crocco is joining two other outstanding scientists, DR. HUGH S. TAYLOR of Princeton University, and DR. WILLIAM R. SEARS of Cornell University.

✦ ✦ ✦

ROY E. MARQUARDT, president and chairman of the Board of Marquardt Aircraft Co., has announced the election of two new directors at the annual stockholders meeting held today at the Company's Van Nuys headquarters. Former board members were re-elected.

The new directors are DR. CLARK B. MILLIKAN of California Institute of Technology, and CLARENCE E. UNTERBERG of C. E. Unterberg & Co., a New York securities underwriting concern. Dr. Millikan, long associated with the aircraft industry, is chairman of the Guided Missiles Committee of the Research and Development Board, and is director of Southern California Cooperative Wind Tunnel and of the Guggenheim Aeronautical Laboratory at the California Institute of Technology. He is also a member of the Air Force Scientific Advisory Board Committee and chairman of the Subcommittee on Fluid Mechanics of the National Advisory Committee for Aeronautics. Mr. Unterberg founded the New York investment banking firm which bears his name.

In addition to Marquardt's development and production contracts with the U. S. Armed Services for subsonic and supersonic ramjet engines for many of their guided missiles projects, the Marquardt Aircraft Company is producing turbine-driven auxiliary power units, fuel and power controls for missile and other applications. The Company also has engineering and manufacturing subcontracts with such companies as Boeing, Douglas, Grumman, Westinghouse, and others.

## Isothermal Combustion Under Flow Conditions

(*Continued from page 251*)

However, the performance of the isothermal expansion cycle can exceed that of an adiabatic expansion cycle in the event that thermal limitations of structural materials preclude the adiabatic utilization of the total energy available to the working fluid.

### References

1 "Tasks We Face," by F. Zwicky, JOURNAL OF THE AMERICAN ROCKET SOCIETY, No. 84, March 1951, p. 3.

2 "A Comparison of Adiabatic and Isothermal Expansion Processes in Rocket Nozzles," by H. S. Seifert and D. Altman, J.P.L. C.I.T. Memo 9-15, 1950. (See also JOURNAL OF THE AMERICAN ROCKET SOCIETY, vol. 22, May-June, 1952, pp. 159–162.)

3 "The Mechanics and Thermodynamics of Steady One-Dimensional Gas Flow," by Ascher H. Shapiro and W. R. Hawthorne, *Journal of Applied Mechanics*, vol. 14, 1947, pp. A317–A336.

# American Rocket Society News

H. K. WILGUS, *Associate Editor*

## New Mexico-West Texas Section Elects New Officers

BECAUSE of increased interest in ARS activities among the personnel of the various organizations using the White Sands Proving Ground testing facilities, the New Mexico-West Texas Section is concentrating on an enlarged membership and has elected new officers to serve until December 13, 1952, or until 1953, the tenure of office to be decided later.

The election was completed on May 23, 1952, and the following officers were chosen: *President*, Edward T. Munnell; *Vice-President*, Robert B. Bolles; *Secretary-Treasurer*, Edward E. Francisco, Jr.

The Section also held a business meeting on July 31 to elect a board of directors and appoint several committees. The results of this meeting will be given in the next issue of the JOURNAL.

### A. C. Clarke Speaks at Open Meeting

On July 1, 1952, the New Mexico-West Texas Section held an open meeting at the Branigan Library, Las Cruces, N. M. Guests and members attended to hear Arthur C Clarke, chairman of the British Interplanetary Society and author of "The Exploration of Space," which was recently published by Harper & Bros. and chosen for the Book-of-the-Month Club July selection.

Mr. Clarke discussed various aspects of interplanetary flight, pointing out the various difficulties—engineering, medical, and economic—that must be overcome. He concluded that each of these problems was susceptible of eventual solution, and that extraterrestrial flight would some day be a reality.

The lecture was followed by a question-and-answer period in which a number of technical problems were discussed at considerable length.

## Alabama Section Hears Discussion on Rocket and Guided Missile Materials

THE ARS Alabama Section held its monthly meeting on July 8, 1952, in the auditorium of the Huntsville Electric System, Huntsville, Ala. Hans Heuter, vice-president of the Section, presided in the absence of the president, Martin B. Schilling.

Following a brief business meeting, a discussion of "Materials in the Development of Rockets and Guided Missiles" was presented by the guest speaker, W. H. Steurer, chief of the Material Test Lab Station, Guided Missile Development Group, Redstone Arsenal.

Dr. Steurer outlined the difference between rocket engineering and general engineering practices with regard to material requirements. He pointed out that the primary consideration in the former instance is development of materials to withstand wide extremes of temperatures for brief periods of time, whereas the latter case involves development of materials for application in nominal temperature ranges over long periods of time. Many properties of materials which heretofore have not been investigated, he said, are now being examined to determine new aspects of their high temperature behavior and their basic metallurgical background.

The speaker continued with an analysis of the properties required of metallic and nonmetallic materials during actual flight conditions, such as high temperatures and various atmospheric conditions, and the methods of testing materials to determine their acceptability. He compared properties of various materials to illustrate the criteria by which materials are selected for application in rockets and guided missiles with regard to fabrication and performance in flight. Some insight was given regarding the development of new materials, such as titanium and titanium alloys, and their acceptance in rocket engineering.

Dr. Steurer concluded by discussing the need for and methods of evaluating missile remnants after destruction (i.e., after firing) by metallurgical investigation to reconstruct events which occurred during flight. He illustrated his talk with movies and slides of test procedures.

## Arthur C. Clarke Guest Lecturer at Washington-Baltimore Section Meeting

ANOTHER successful lecture meeting of the ARS Washington-Baltimore Section was held on June 6, 1952, in the auditorium of the Baltimore Polytechnic Institute, Baltimore, Md. Approximately 250 members and guests were present to hear the British scientist and chairman of the British Interplanetary Society, Arthur C. Clarke, deliver a talk on his recently published book, "The Exploration of Space."

The meeting was called to order by Joel M. Jacobson of Aircraft Armaments, Inc., who substituted in the absence of the president, Harry J. Archer, Jr. Mr. Jacobson then introduced Andrew G. Haley, ARS general counsel, who spoke a few words about Mr. Clarke and his book before presenting the guest speaker to the audience.

Mr. Clarke was born at Minehead, Somerset, England, in 1917. Following his secondary education and a subsequent job as a government auditor, he entered the Royal Air Force in 1941. As flight lieutenant, he worked with a Blind Landing Unit and also lectured and wrote on radar, physics, and electronics. After World War II Mr. Clarke studied at King's College in London, where he obtained his B.Sc. in physics and mathematics. Since


ARTHUR C. CLARKE (SECOND FROM RIGHT), LECTURER, WITH ARS MEMBERS AT THE WASHINGTON-BALTIMORE SECTION MEETING, JUNE 6, 1952

(*Left to right:* William A. Webb, Baltimore vice-president; Andrew G. Haley, ARS general counsel; Mr. Clarke; and Miss Virginia R. Erwin, secretary of the Washington-Baltimore Section.)


DISCUSSION PANEL AT THE WASHINGTON-BALTIMORE SECTION MEETING, JUNE 6, 1952

(*Left to right:* Col. H. J. Halberstadt, Deputy Director of Aeronautics and Propulsion, ARDC; R. W. Bonner, Head of Propulsion, Glenn L. Martin Co.; G. L. Bryan, Jr., Professor of Aeronautical Engineering, The Johns Hopkins University; and John Creutz, consulting communication engineer.)

then he has been a full-time science writer and broadcaster and an energetic proponent of space flight, astronautics, and astronomy.

Following Mr. Clarke's speech, a panel type discussion of the lecture was conducted by the Baltimore vice-president, William A. Webb of Aircraft Armaments, Inc. Members of the panel included Col. H. J. Halberstadt, deputy director of aeronautics and propulsion for the Air Research and Development Command; R. W. Bonner, head of propulsion for the Glenn L. Martin Co.; G. L. Bryan, Jr., professor of aeronautical engineering at The Johns Hopkins University; and John Creutz, consulting communications engineer.

This meeting was the last of the spring meetings of the Washington-Baltimore Section. The next meeting is tentatively scheduled to be held in Washington in September, at which time an active membership drive will be undertaken.

# Technical Literature Digest

**H. S. SEIFERT, California Institute of Technology, *Associate Editor***

CONTRIBUTORS: D. Altman, D. I. Baker, R. B. Canright, F. C. Gunther, H. S. Seifert, F. H. Wright

## Book Reviews

ASTRONOMY OF STELLAR ENERGY AND DECAY, by Martin Johnson, London, Faber, 1950; Dover Publications, Inc., New York, 216 pp. $3.50.

Reviewed by A. G. WILSON
California Institute of Technology

Dr. Martin Johnson, already noted for his lucid scientific and philosophical expositions in his books, "Time, Knowledge, and the Nebulae" and "Science and the Meaning of Truth," engages in this latest book in the description of the physical problems germane to the stability and evolution of stars. The author has adopted a novel approach to an expository work. He has divided the book into two parts. The first half consists of a descriptive background at a popular level designed to familiarize the nontechnical reader with the significant aspects of the subject of stellar constitution; the second half amplifies the descriptive material of the first half by outlining, with mathematical aid, the methods used by the astrophysicist to arrive at his results. Such subjects as stellar models, stability criteria, and the size, masses, temperatures, and energy sources of stars are discussed.

The book serves as an excellent introduction to the subjects. But the attempt to compress the mathematical elaboration of the descriptive material of the first part into an equal number of pages in the second part necessarily results in a sketchiness which might prove frustrating to a beginning student. The book is further marred by a few careless statements, such as the remark on page 83 that "there are only one or two telescopes in the world of sufficient power to detect a Super-Nova."

FOUNDATIONS OF HIGH SPEED AERODYNAMICS. Facsimiles of Nineteen Original Papers, with a Bibiography, by G. F. Carrier, Dover Publications, Inc., New York, 1951, 286 pp. $1.75.

REVIEWED BY H. S. TSIEN
California Institute of Technology

Out of the immense volume of literature on the dynamics of compressible fluid from 1870 to 1950, Professor Carrier selected nineteen papers which he considered to be original and fundamental. The task was certainly not easy. Hence he should be excused for the somewhat arbitrary manner in making the selections. However, for a price of $1.75, students of compressible flow can be grateful to Professor Carrier that they can read the masterful works of W. Rankine, G. I. Taylor, Lord Rayleigh, J. Ackeret, H. Glauert, L. Prandtl, A. Busemann, and Th. von Kármán.

HANDBOOK OF SUPERSONIC AERODYNAMICS, VOLUME IV, NAVORD Report 1488, compiled and edited by C. N. Warfield, L. L. Cronvich, A. R. Eaton, Jr., G. M. Edelmann, and F. K. Hill, U. S. Govt. Printing Office, Washinton, D. C., 1952, 121 pp. $1.25

REVIEWED BY H. S. TSIEN
California Institute of Technology

The main body of this present volume of "Handbook of Supersonic Aerodynamics" consists of tabulated lift coefficients and moment coefficients for a two-dimensional, flat-plate airfoil in vertical and angular oscillations, computed under the supervision of E. C. Kennedy. The accuracy of these tables is very much higher than that of the previously published tables based upon the Curtiss-Wright Corporation Report No. P537V-28 (April 1948). The range of independent variables is: frequency parameter $\Omega$, 0.01 (0.01) 0.04 (0.02) 0.10 (0.05) 0.40 (0.10) 1.00 (0.20) 3.00 (0.50) 5.00 (2.50) 10.00 (5.00) 20.00; Mach number M, 1.1 (0.1) 2.0 (0.2) 4.0 (0.5) 5.0 (1.0) 12.0.

A brief review of the various flutter problems is included in the introduction.

OUT OF THE SKY, by H. H. Nininger, Univ. of Denver Press, 1952, viii + 336 pp., 52 plates and 21 text figures. $5.

Reviewed by JOHN D. BUDDHUE
Institute of Meteoritics
University of New Mexico

The author is the founder and director of the American Meteorite Museum which contains one of the finest private meteorite collections in this country, if not in the world. He is a recognized authority on meteoritics, especially as a field worker and by his efforts many meteorites have been brought to light that otherwise might have remained forever unknown and lost. He is also the author of two other books and more than 120 papers on meteorites.

The book contains 33 chapters devoted to such subjects as Early Man and Meteorites, Typical Falls, Meteors, Composition and Structure of the Various Kinds of Meteorites, Etching and Preservation, Size of Meteorites, Weathering of Meteorites, Shapes and Shaping, Meteorite Showers, Meteorite Craters, Meteoritic Clouds, Origin of Meteorites, Cosmic Heating, Planetoidal Encounters, Meteorites and the Moon, Tektites, and Great Meteorite Collections.

The book appears to have been directed primarily to the intelligent layman although it contains a great deal of interest to the student, the collector, the professional meteorist, and other persons who need a semitechnical knowledge of these objects. Some of its contents do not seem to have been published previously. Practically every phase of meteoritics is treated in more or less detail, although the reviewer would have preferred more analytical data in the chapters dealing with composition, especially the mineral composition. A more precise elucidation of the origin of the octahedral structure of most iron meteorites and how it is influenced by the nickel content would probably have been a useful addition. The chapter on weathering also lacks analytical data, but these omissions are doubtless intentional and due to the semipopular nature of the work.

Two chapters are devoted to the author's hypothesis that the Canyon Diablo meteorite crater was formed by the successive impacts of two meteorites, one following closely behind the other. Whether or not one is disposed to accept this hypothesis, the chapters contain a wealth of new, and relatively new, information about this crater.

Other meteorite craters are treated in considerably less detail, but cryptovolcanic structures, as possible meteorite craters, are not mentioned until a later chapter. Although he does not say so, the author seems to favor the hypothesis that the Carolina bays are of meteoritic origin.

One chapter describes the surface features of the moon and suggests that the craters are in fact meteorite scars. In another it is proposed that tektites are bits of

EDITOR'S NOTE: This collection of references is not intended to be comprehensive, but is rather a selection of the most significant and stimulating papers which have come to the attention of the contributors. The readers will understand that a considerable body of literature is unavailable because of security restrictions. We invite contributions to this department of references which have not come to our attention, as well as comment on how the department may better serve its function of providing leads to the jet propulsion applications of many diverse fields of knowledge.

fused lunar material blasted beyond its gravitational control by the impact of meteorites. The bulk of this chapter, however, is a résumé of the theories proposed by various workers to explain these mysterious objects. In the reviewer's opinion, it would have been well to include a fuller description of their surface markings and the ways in which the different kinds differ from one another, including representative analyses.

The book ends with a list of all the author's books and papers on meteoritics, followed by a 13-page index.

As a whole, the book is lucidly and interestingly written and fairly well documented. It contains a great deal of information and, while not all meteorists will agree with it in its entirety, it contains few real errors, typographical or otherwise. One might mention, however, that osbornite has been shown to be titanium nitride (not an oxysulfide of calcium and either titanium or zirconium), and a theory explaining the lamellar nature of meteorite rust, which the author generously credits to the reviewer, is actually due to D. M. Barringer, Sr. This book should be a valuable addition to the library of anyone interested in meteoritics or related fields of endeavor.

PUNCHED CARDS, edited by W. A. Casey and J. W. Perry, Reinhold Publishing Corp., New York, 1951, viii + 506 pp. $10.

Reviewed by HUGH DENSLOW
Jet Propulsion Laboratory
California Institute of Technology

The greater part of this book is directed to the application of punched-card systems as a means of organizing technical information. There are also sections on applications to industrial engineering and to scientific computations. The book comprises thirty sections, each an independent article by an authority on the subject. Short biographies of the authors precede the articles.

Putting first things first, the reader is inspired by case histories of applications of punched cards to specific problems in order to envision their application to his own problem requiring organization of facts for interpretation. Then, assuming no prior knowledge, the fundamentals necessary for formulation of a punched-card system are given. Basic theory, preferred practices in coding, and mechanical methods are discussed fully. An excellent bibliography is included. Of particular interest, an article by Ernst Hermann Erich Pietsch is included, entitled "Future Possibilities of Applying Mechanized Methods to Scientific and Technical Literature." A short history and a discussion of problems in organization of the "Gmelin Handbuch" are contained, and the peculiar problems of the organization of philosophical literature are discussed.

MODEL JETS AND ROCKETS FOR BOYS, by Raymond F. Yates, Harper and Bros., 1952, 108 pp. + viii, 45 illustrations. $2.50.

Reviewed by R. C. TERBECK
Jet Propulsion Laboratory
California Institute of Technology

This book is written to familiarize young people with the operation of rockets and jets and their history. The author has presented an authentic historical review of the subject and has outlined the progress in the field during the past years.

The fundamental principles are described in such a manner that the average youth can understand and utilize the information to design and build many types of rocket and jet motors.

The book describes in detail the construction and operation of model steam jets, a $CO_2$ cartridge jet, and simple vehicles to be driven by these motors. Many of the model jet and rocket motors such as the Dyna Jet, Jetex (solid propellant motor made in England), and Minijet are discussed together with installation and operation instructions for model installations.

The model rocket and jet enthusiast will find this a good reference book for answers to many of the operational problems that he encounters with his hobby.

## Books

Histoire de la Mécanique, by R. Dugan, Neuchâtel, Switzerland, Griffon, 1950, 649 pp. $17.50.

An Introduction to Acoustics, by R. H. Randall, Addison-Wesley Press, Inc., Cambridge, Mass., 1951, xii + 340 pp. $6.

Mechanics of Vibration by H. M. Hansen and P. F. Chenea, John Wiley & Sons, Inc., New York, 1952, 417 pp.

Internal Combustion Engines, 6th Edition, by L. C. Lichty, McGraw-Hill Book Co., Inc., New York, 1951, 598 pp. $7.

Creep of Metals, by L. A. Rotherham, Inst. of Phys., London, 1951, 80 pp. + 2 plates. 15 *s.*

Diffusion in Solids, Liquids, Gases, by W. Jost, Academic Press, Inc., New York, 1952, 558 pp. $11.

Rockets, Jets, Guided Missiles and Space Ships, by J. Coggins and F. Pratt, Random House, Inc., New York, 1951, 58 pp. $1.

Is Another World Watching?, by G. Heard, Harper and Bros., New York, 1951, 183 pp. $2.35.

## Jet Propulsion Engines

Some Fundamental Considerations on the Propulsion of Aircraft (in Dutch), by J. G. Slotboom, *Ingenieur*, vol. 63, Oct. 1951, pp. L.49–L.56.

## Rocket Propulsion Engines

Liquid Films Formed by Means of Rotating Disks, by B. E. Dixon, A. A. W. Russell, and J. E. L. Swallow, *Brit. J. Appl. Phys.*, vol. 3, Apr. 1952, pp. 115–119.

The Atomization of Liquid in a Flat Spray, by R. G. Dorman, *Brit. J. Appl. Phys.*, vol. 3, June 1952, pp. 189–192.

JATO and Auxiliary Rocket Power Plants, by H. Gartmann, *Weltraumfahrt*, no. 6, 1951, pp. 134–139.

Jet Assisted Take-Off, by W. J. Merboth, *Sailplane and Glider*, vol. 20, Feb. 1952, pp. 6–7.

Bazooka Rocket Motor Testing Now Fully Automatic, by H. E. Stein, *Iron Age*, vol. 169, Mar. 20, 1952, pp. 100–102.

Hot-Rod Jets, unsigned, *Aviation Week*, vol. 56, Mar. 24, 1952, p. 14.

Determination of Rocket Motor Heat Transfer Coefficients by the Transient Method, by S. Greenfield, *J. Aero. Sci.*, vol. 18, Aug. 1951, pp. 512–518.

## Heat Transfer and Fluid Flow

Concerning the Cooling of a Body in an Air Stream Through the Injection of Cold Air into the Boundary Layer, by K. S. Muller, translated from German by E. Knuth, Zentrale für Wissenschaftliches Berichtwesen Res. Report 2020, 29 pp.

Generalized Theory of Convective Heat Transfer in a Free-Molecule Flow, by A. K. Oppenheim, Univ. Calif. Report HE-150-93, Mar. 1952, 11 pp. + 9 pp. tables.

On the Convergence of Numerical Solutions of the Heat-Flow Equation, by F. B. Hildebrand, *J. Math. Phys.*, vol. 30, Apr. 1952, pp. 35–41.

Experimental Investigation of Heat Transfer Through Laminar and Turbulent Boundary Layers on a Cooled Flat Plate at a Mach Number of 2.4, by E. G. Slack, NACA TN 2686, Apr. 1952, 13 pp.

Liquid Metals Are Good Heat-Transfer Agents, by T. Trocki, *Gen. Elec. Rev.*, vol. 55, May 1952, pp. 22–25.

Heat and Momentum Transfer in Turbulent Flow Mercury, by S. E. Isakoff, Atomic Energy Comm. Report AECU-1199, 14 pp.

Experimental Verification of the Theory of Jet Formation by Charges with Lined Conical Cavities, by R. J. Eichelberger and E. M. Pugh, *J. Appl. Phys.*, vol. 23, May 1952, pp. 537–542.

Theory of Jet Formation by Charges with Lined Conical Cavities, by E. M. Pugh, R. J. Eichelberger, and N. Rostoker, *J. Appl. Phys.*, vol. 23, May 1952, pp. 532–536.

Heat Transfer in Nitrogen and Hydrogen Sweat-Cooled Tubes, by H. L. Wheeler, Jr., C.I.T. Jet Propulsion Lab. Progress Report 20-160, Jan. 4, 1952, 27 pp.

Internal-Film-Cooling Experiments with 2- and 4-Inch Smooth-Surface Tubes and Gas Temperatures to 2000 F, by G. R. Kinney, NACA RM E52B20, April. 1952, 27 pp.

Note on the Application of Near-Frozen Flow Criteria for One-Dimensional Nonviscous Expansion Through a Laval Nozzle, by S. S. Penner, *J. Chem. Phys.*, vol. 20, Feb. 1952, p. 341.

On the Uniqueness of Gas Flows, by J. L. Ericksen, *J. Math. Phys.*, vol. 30, Apr. 1952, pp. 63–68.

Investigation of Flow in Duct of Varyfng Cross Section with Application to Design of Ducts for Free-Flight Ground-Launched Model Tests, by C. H. E. Warren, R. E. Dudley, and P. J. Herbert, Aero. Res. Counc. Lond. Curr. Pap. 60, 1951, 37 pp., Brit. Inf. Serv., New York

Theoretical Aerodynamic Properties for an Inclined Flat Plate in Slip Flow, by S. F. Mack, Univ. Calif. Report HE-150-98, Mar. 1952, 14 pp. + 5 pp. tables.

Dynamics of Pulsative Flow Through Orifices, by R. C. Baird, *Instruments*, vol. 25, Apr. 1952, pp. 481–486.

Dynamical Instability in Flow Systems, by T. Baron, article from Proc. Midwest Conf. Fluid Dynamics, 1st conf., May 1950, J. W. Edwards, Ann Arbor, Mich., 1951, pp. 216–225, $10.

Diffusion and Flow of Gases and Vapours Through Micropores. IV. Flow of Capillary Condensate, by P. C. Carman, *Proc. Roy. Soc. Lond.* (*A*), vol. 211, Mar. 20, 1952, pp. 526–535.

The Flow of Gases Through Capillaries, by J. A. W. Huggill, *Proc. Roy. Soc. Lond.* (*A*), vol. 212, Apr. 8, 1952, pp. 123–136.

Evaporation from Drops. II, by W. E. Ranz and W. R. Marshall, Jr., *Chem. Engg. Prog.*, vol. 48, Apr. 1952, pp. 173–180.

Note on the Flow of Vapor Between Liquid Surfaces, by M. S. Plesset, *J. Chem. Phys.*, vol. 20, May 1952, pp. 790–793.

Some Aspects of Fluid Flow, Edward Arnold & Co., Lond., 1951, 50*s*. See especially: Problems in the Atomisation of Liquids, by H. L. Green, pp. 75–86, and Boundary Layers and Skin Friction in a Compressible Fluid Flowing at High Speeds, by A. D. Young, pp. 87–113.

The Emission of Radiation from Diatomic Gases. III. Numerical Emissivity Calculations from Carbon Monoxide for Low Optical Densities at 300°K and Atmospheric Pressure, by S. S. Penner, M. Ostrander, and H. S. Tsien, Guggenheim Jet Propulsion Center Tech. Report 1, 1951, 8 pp.

## Combustion

The Thermodynamics of Combustion Gases: General Considerations, by S. R. Brinkley, Jr., and B. Lewis, Dept. Interior Bur. Mines RI 4806, Apr. 1952, 61 pp.

Combustion Tunnel Laboratory, First Quarterly Report, 1952, by H. W. Emmons, Harvard Univ. Combustion Tunnel Proj. Qtrly. Report 1, Oct. 1951–Apr. 1, 1952.

Spectroscopic Studies of Low Pressure Combustion Flames, by S. S. Penner, M. Gilbert, and D. Weber, *J. Chem. Phys.*, vol. 20, Mar. 1952, pp. 1–2.

Flame Propagation Studies Using the Hydrogen-Bromine Reaction, by S. D. Cooley and R. C. Anderson, *Indus. Engg. Chem.*, vol. 44, June 1952, pp. 1402–1406.

Combustion in the Mixing Zone Between Two Parallel Streams, by F. H. Wright and J. L. Becker, C.I.T. Jet Propulsion Lab. Progress Report 3-25, June 9, 1952, 16 pp.

Evaluation of Flame Speed at Burner Flame Tip, by L. C. Lichty, *Ind. Engg. Chem.*, vol. 44, June 1952, pp. 1395–1398.

Burning Velocity Determinations, by P. J. Wheatley, *Trans. Faraday Soc.*, vol. 44, Apr. 1952, pp. 338–345.

Über den Einfluss starker Schallwellen auf Fortschreitende Gasflammen in Rohren, by L. Ehret, U. Neubert, and H. Hahnemann, *ZAP*, vol. 4, Apr. 1952, pp. 126–134.

Non-Isotropic Propagation of Combustion Waves, by G. H. Markstein, *J. Chem. Phys.*, vol. 20, June 1952, pp. 1051–1052.

High Temperature Propellant Reactions, by F. E. Osborne, *Aircr. Engg.*, vol. 24, May 1952, pp. 134–137.

The Combustion of Drops in a Fuel Spray, by G. Godsave, Nat. Gas Turbine Establishment, England, Memo. M-95, Oct. 1950, 10 pp.

Thermal Decomposition of Nitroethane and 1-Nitropropane, by T. L. Cottrell, T. E. Graham, and T. J. Reid, *Trans. Faraday Soc.*, vol. 47, 1951, pp. 1089–1092.

Gaseous Detonations. III. Dissociation Energies of Nitrogen and Carbon Monoxide, by G. B. Kistiakowsky, H. T. Knight, and M. E. Malin, *J. Chem. Phys.*, vol. 20, May 1952, pp. 876–883.

Reaction of Methyl Radicals with Nitric Oxide and the Rate of Combination of Methyl Radicals, by R. W. Durham and E. W. R. Steacie, *J. Chem. Phys.*, vol. 20, Apr. 1952, pp. 582–585.

The Heats of Combustion of the Methyl Substituted Hydrazines and Some Observations on the Burning of Volatile Liquids, by J. G. Aston, E. J. Rock, and S. Isserow, *J. Am. Chem. Soc.*, vol. 74, May 20, 1952, pp. 2484–2486.

Thermal Theory of Solid-Propellant Ignition by Hot Wires, by D. Altman and A. F. Grant, Jr., C.I.T. Jet Propulsion Lab. Ext. Pub. 140, May 23, 1952, 9 pp.

Steady State Burning of a Semi-Infinite Solid or Liquid, by W. P. Reid, NAVORD-R-1935, Dec. 7, 1951.

Gasification of Solid Fuels at Elevated Pressures, by W. Gumz, *Ind. Engg. Chem.*, vol. 44, May 1952, pp. 1071–1074.

Rates of Explosive Decomposition of Explosives, by H. Henkin and R. McGill, *Ind. Eng. Chem.*, vol. 44, June 1952, pp. 1391–1394.

Mode of Energy Release in Combustion of Carbon, by J. R. Arthur and J. A. Bleach, *Ind. Eng. Chem.*, vol. 44, May 1952, pp. 1028–1034.

Reactions of Artificial Graphite, by E. A. Gulbransen and K. F. Andrew, *Ind. Eng. Chem.*, vol. 44, May 1952, pp. 1034–1051.

Le domaine d'inflammation du méthane aux basses pressions, by M. Van Pee and G. Fally, *Bull. soc. chim. Belges*, vol. 61, Jan.-Feb. 1952, pp. 64–98.

The Stability of Butane Air Flames at Low Pressures, by K. Wohl and C. Peterson, United Aircr. Corp. Meteor Report 54, Feb. 1952.

The Oxidation of Hexane in the Cool Flame Region, by H. C. Bailey and R. G. W. Norrish, *Proc. Roy. Soc. Lond.* (*A*), vol. 212, May 7, 1952, pp. 311–330.

Polyhedral Flames with Hydrogen and Hydrocarbons, by H. Broida and W. Kane, *J. Chem. Phys.*, vol. 20, June 1952, p. 1042.

Induced Decomposition of Acetaldehyde by Radicals, by R. K. Brinton and D. H. Volman, *J. Chem. Phys.*, vol. 20, June 1952, pp. 1053–1054.

The Reaction of Methyl Radicals with Some Halogenated Methanes, by F. A. Raal and E. W. R. Steacie, *J. Chem. Phys.*, vol. 20, Apr. 1952, pp. 578–581.

The Azomethane Induced Oxidation of Propane, by M. D. Scheer and H. A. Taylor, *J. Chem. Phys.*, vol. 20, Apr. 1952, pp. 653–657.

## Fuels, Propellants, and Materials

Fluoroscope Tests Rocket Propellants, unsigned, *Tech. Data Digest*, vol. 17, May 1952, p. 13.

How One Base Meets Problems of Handling Rocket Fuels, unsigned, *Tech. Data Digest*, vol. 17, May 1952, pp. 3–5.

Interstate Commerce Commission Regulations for Transportation of Explosives and Other Dangerous Articles by Land and Water in Rail Freight Service and by Motor Vehicle (Highway) and Water Including Specifications for Shipping Containers, by H. A. Campbell, Interstate Commerce Commission 4, April 8, 1952, 340 pp.

The Borohydrides, by H. C. Brown, *Chem. Eng. News*, vol. 29, 1951, pp. 5231–5233.

Reaction Mechanism of the Raschig Synthesis of Hydrazine, by E. Wiberg and M. Schmidt, *Z. Naturforsch.*, vol. 6b, 1951, p. 336.

Powdered Metals; Old Art, New Science, by S. Baker, *Steel*, vol. 130, Apr. 28, 1952, pp. 56–57.

Titanium; the New Light Metal, unsigned, *Light Metals*, vol. 15, Apr. 1952, pp. 120–121.

Carbon and Graphite Materials and Parts, by P. O'Keefe, *Materials and Methods*, vol. 35, Apr. 1952, pp. 119–134.

New Refractories—Carbides, Borides, Nitrides, Silicides, by G. R. Finlay, *J. Electrochem. Soc.*, vol. 99, Mar. 1952, pp. 58c–61c.

Determination of Particle Size in the Sub-Micron Range, by Y. Schubert, *Powder Metal Bull.*, vol. 6, Apr. 1952, pp. 105–109.

Experimental Refractory Bodies of High-Melting Nitrides, Carbides, and Uranium Dioxide, by P. Chiotti, *J. Am. Ceram. Soc.*, vol. 35, May 1, 1952, pp. 123–130.

Stabilization of Zirconia with Calcia and Magnesia, by P. Duwez, *J. Am. Ceram. Soc.*, vol. 35, May 1, 1952, pp. 107–113.

Vapor Deposition of Metals on Ceramic Particles, by J. E. Cline and J. Wulff, *J.*

*Electrochem. Soc.*, vol. 98, Dec. 1951, pp. 385–387.

Ceramic Coating Saves Scarce Metals and Lengthens Life of High Temperature Parts, by H. Penton, *Western Metals*, vol. 10, Apr. 1952, pp. 37–39.

## Physical-Chemical Topics

Nucleation Phenomena, Symposium containing 17 papers, *Ind. Eng. Chem.*, vol. 44, June 1952, pp. 1270–1336.

New Thermodynamic Concepts Bring Theory and Practice into Agreement, by N. P. Bailey, *Chem. Eng.*, vol. 59, Mar. 1952, pp. 150–154, 336–338.

Thermodynamics of Irreversible Processes, by I. Prigogine, *Appl. Mechanics Reviews*, vol. 5, May 1952, pp. 193–195.

Experimental and Theoretical Activities in the Gas Properties Field, 1948 to date, by I. F. Weeks, Univ. Wisc. CM 703, Jan. 1952, 47 pp.

Equation of State of Gases at High Temperature, by H. M. Peek and Z. W. Salsburg, *J. Chem. Phys.*, vol. 20, Apr. 1952, p. 763.

Second Virial Coefficient of a 6–9 Gas at High Temperatures, by L. F. Epstein and C. J. Hibbert, *J. Chem. Phys.*, vol. 20, Apr. 1952, pp. 752–753.

The Second Coefficient of Viscosity of Liquids and Gases, by S. M. Karim and L. Rosenhead, *Rev. mod. Phys.*, vol. 24, Apr. 1952, pp. 108–116.

Measurement of the Vibrational Relaxation Effect in $CO_2$ by Means of Shock Tube Interferograms, by E. F. Smiley, E. H. Winkler, and Z. I. Slawsky, *J. Chem. Phys.*, vol. 20, May 1952, pp. 923–924.

Equilibrium of Solution in the System Nitromethane–Water, by R. M. Corelli, *Aerotecnica*, vol. 30, 1950, pp. 32–37.

Decomposition of Nitrogen Pentoxide in the Presence of Nitric Oxide. II. Details at Low Pressures, by H. S. Johnston and R. L. Perrine, *J. Am. Chem. Soc.*, vol. 73, 1951, pp. 4782–4786.

Four Mechanisms Involving Nitrogen Pentoxide, by H. S. Johnston, *J. Am. Chem. Soc.*, vol. 73, 1951, pp. 4542–4546.

The Thermal Decomposition of Potassium Perchlorate and Perchlorate-Halogenide Mixtures: a Study in the Pyrolysis of Solids, by A. Glasner and L. Weidenfeld, *J. Am. Chem. Soc.*, vol. 74, May 20, 1952, pp. 2467–2472.

Thermal Decomposition of Potassium Chlorate and Chlorate-Chloride Mixtures, by A. Glasner and L. Weidenfeld, *J. Am. Chem. Soc.*, vol. 74, May 20, 1952, pp. 2464–2467.

Photoelectric Observation of the Rate of Dissociation of Nitrogen Tetroxide by a Shock Wave, by T. Carrington and N. Davidson, *J. Chem. Phys.*, vol. 19, 1951, p. 1313.

Measurement of the Heat of Dissociation of Fluorine by the Effusion Method, by H. Wise, *J. Chem. Phys.*, vol. 20, May 1952, p. 927.

The Electron Affinity of Fluorine, by R. B. Bernstein and M. Metlay, *J. Chem. Phys.*, vol. 19, 1951, p. 1612.

Thermodynamic Properties of the Fluorine Atom and Molecule and of Hydrogen Fluoride to 5000°K, by L. G. Cole, M. Farber, and G. W. Elverum, Jr., *J. Chem. Phys.*, vol. 20, Apr. 1952, pp. 586–590.

Thermodynamic Properties of Chlorine Trifluoride, by M. D. Scheer, *J. Chem. Phys.*, vol. 20, May 1952, p. 924.

Bibliography on the Thermodynamic Properties of the Fluorine Compounds of Elements of Atomic Number 1 to 17, by W. H. Evans and others, Dept. Commerce, Nat. Bur. Stds., Jan. 21, 1952, 17 pp.

Thermal Properties of Fluorine Compounds: Heat Capacity, Entropy, Heat Content, and Free Energy Functions of Diatomic Fluorine in the Ideal Gaseous State, by L. Haar and C. W. Beckett, Dept. Commerce, Nat. Bur. Stds., Feb. 1, 1952, 16 pp.

Thermal Properties of Fluorine Compounds: Heat Capacity, Entropy, Heat Content, and Free Energy Functions of Carbon Difluoride, Carbon Tri-Fluoride, Carbon Tetrafluoride and Difluoro-Acetylene in the Ideal Gaseous State, by R. M. Potocki and D. E. Mann, Dept. Commerce, Nat. Bur. Stds., Feb. 15, 1952, 4 pp.

Recent Determinations of the Vapor Pressure of Graphite, by L. Brewer, *J. Chem. Phys.*, vol. 20, Apr. 1952, pp. 758–759.

## Instrumentation and Experimental Techniques

Electromagnetic Levitation of Solid and Molten Metals, by E. C. Okress and D. M. Wroughton, *J. Appl. Phys.*, vol. 23, May 1952, pp. 545–552.

A Linear Radio-Frequency Mass Spectrometer, by P. A. Redhead, *Canad. J. Phys.*, vol. 30, Jan. 1952, pp. 1–9.

Résumé of Thermocouple Checking Procedures, by H. C. Quigley, *Instruments*, vol. 25, May 1952, pp. 616–622.

Resistance-Thermometer Measurements in a Low-Pressure Flame, by M. Gilbert and J. H. Lobdell, C.I.T. Jet Propulsion Lab. Ext. Pub. 131, Feb. 11, 1952, 23 pp.

The Use of Doubly Refracting Solutions in the Investigation of Fluid Flow Phenomena, by B. Rosenberg, USN David Taylor Model Basin Report 617, Mar. 1952, 39 pp.

Determination of Air Velocity by Ion Transit-Time Measurements, by W. C. Cooley and H. G. Stever, *Rev. Sci. Instrum.*, vol. 23, Apr. 1952, pp. 151–154.

An Investigation of Electromagnetic Flowmeters, by H. G. Elrod and R. R. Fouse, *Trans. ASME*, vol. 74, May 1952, pp. 589–594.

Valve Control of Liquid Flow, by R. Milham and A. R. Catheron, *Instruments*, vol. 25, May 1952, pp. 596–598.

A Modified Budenberg Pressure Balance by J. F. Pearse, *J. Sci. Instrum.*, vol. 29, Jan. 1952, pp. 18–19.

A Miniature Electrical Pressure Gage Utilizing a Stretched Flat Diaphragm, by J. Patterson, NACA TN 2659, Apr. 1952, 47 pp.

Accelerometers for Determining Aircraft Flight Loads, by J. Taylor, *Engineering*, vol. 173, Apr. 11, 1952, pp. 473–475.

An Instrument to Measure and Compute the Mean and Standard Deviation of the Oscillations of a Recording Arm, by B. Hegley, *J. Sci. Instrum.*, vol. 29, Mar. 1952, pp. 76–81.

Noise, Explaining Its Nature and Origin, unsigned, *Wireless World*, vol. 58, May 1952, pp. 199–202.

On Sound Generated Aerodynamically. I. General Theory, by M. J. Lighthill, *Proc. Roy. Soc. Lond.* (*A*), vol. 211, Mar. 20, 1952, pp. 564–587.

The Noise Field of a Turbo-Jet Engine, by H. E. von Gierke, *J. Acoust. Soc. Amer.*, vol. 24, Mar. 1952, pp. 169–174.

A Survey of the Aircraft-Noise Problem with Special Reference to Its Physical Aspects, by H. H. Hubbard, NACA TN 2701, May 1952, 41 pp.

Design Characteristics for Noise Control of Jet Engine Cells, by H. C. Hardy, *J. Acoust. Soc. Amer.*, vol. 24, Mar. 1952, pp. 185–190.

The Design of Mobile Electronic Laboratories, by P. H. Parkin, *J. Sci. Instrum.*, vol. 29, Jan. 1952, pp. 8–11.

Tape Recording for Telemetry and Data Analysis, by K. B. Boothe, *Tele-Tech.*, vol. XI, May 1952, pp. 44–46 and 116.

Guided Missile Test Center Telemetering System, by J. B. Wynn, *Electronics*, vol. 25, May 1952, pp. 106–111.

A High-Speed Crystal Clutch, unsigned, *Engineer*, vol. 173, Apr. 25, 1952, p. 579.

Response Time of Magnetic Fluid Clutches, unsigned, *Engineer*, vol. 173, Apr. 25, 1952, p. 579.

Missile Timers, unsigned, *Aviation Week*, vol. 56, May 19, 1952, p. 73.

Calculating Speed of Snap-Action Mechanisms, by P. H. Winter, *Machine Design*, vol. 24, May 1952, pp. 162–164.

A 24-Way High-Speed Rotary Switch for Use in Static and Airborne Strain Gauge Measurements, by D. Peirson, Aero. Res. Counc. Lond. Rep. Mem. 2232, 1951, 9 pp., 1 diagram, 3*s*.

Modern Computing Machines, by G. T. Hunter, *J. Franklin Inst.*, vol. 253, June 1952, pp. 567–583.

## Terrestrial Flight, Ballistics, and Vehicle Design

Parachute Design, by T. F. Johns, Aero. Res. Counc. Lond. Rep. Mem. 2402, Dec. 1946 (published 1951), 23 pp., 11 figs.

Interferometric Analysis of Airflow About Projectiles in Free Flight, by F. D. Bennett, W. C. Carter, and V. E. Bergdolt, *J. Appl. Phys.*, vol. 23, Apr. 1952, pp. 453–469.

Dynamic Stability of a Missile in Rolling Flight, by R. E. Bolz, *J. Aero. Sci.*, vol. 19, June 1952, pp. 395–403.

Model Simulates Free Flight of Rotating Missiles, unsigned, *Tech. Data Digest*, vol. 17, May 1952, p. 9.

Notes on Dynamics for Aerodynamicists, by J. D. Schetzer, Douglas Aircr.

Co., Inc., Report SM-14077, Nov. 19, 1951, 203 pp.

Rocket Flight, by S. F. Singer, *Canad. Aviation*, vol. 25, May 1952, pp. 32–33.

On the Calculation of Groups of Trajectories of Remote Controlled Rockets (in German), by E. Roth-Desmeules, *ZAMP*, vol. 2, Nov. 1951, pp. 487–489.

Remarkable Points on a Trajectory. IV. Curvilinear Trajectories. Discontinuities, Extrema, Inflections (in French), by M. Garnier, *Mém. Artill. fr.*, vol. 25, 1951, pp. 693–741.

Ballistics of the Upper Atmosphere; Atmospheric Density Profile and Variations from the Study of Meteor Trajectories, by L. G. Jacchia, MIT Center of Analysis Report 2, 1948, 30 pp.

Flight in the Aeropause, by R. Hawthorne, *Aviation Age*, vol. 16, Dec. 1951, pp. 29–31.

Radio Direction-Finding and Navigational Aids, unsigned, *Nature*, vol. 169, May 24, 1952, p. 875.

Navigation in War, unsigned, *Flight*, vol. 61, Feb. 29, 1952, p. 246.

Deadly Sparrow Missile Revealed, unsigned, *Amer. Aviation*, vol. 15, Mar. 31, 1952, p. 61.

General Electric's Winged Messenger; Hermes Al, unsigned, *Aviation Week*, vol. 56, May 12, 1952, pp. 30 and 35–36.

The Armstrong-Siddeley "Snarler" Rocket Motor, unsigned, *J. Brit. Interplanetary Soc.*, vol. XI, Mar. 1952, pp. 73–75.

V-2 Rocket Tests, unsigned, *Mech. Eng.*, vol. 74, Apr. 1952, p. 329.

Red Rockets, by D. A. Anderton, *Aviation Week*, vol. 56, Jan. 14, 1952, pp. 37, 38, 41.

## Space Flight

How Far Are We From Space Flight?, by F. C. Durant, *Aviation Week*, vol. 56, May 26, 1952, pp. 25–35.

Interplanetary Communications and Navigation, by J. P. Elliott, *J. Space Flight*, vol. 4, May 1952, pp. 1–2.

Interplanetary Navigation, by S. Herrick, *J. Inst. Navigation*, vol. 3, Sept.–Dec. 1951, pp. 57–59.

Verständigungsmöglichkeiten mit Raumschiffen, by G. von Schrutka-Rechtenstamm, *Forschungsreihe der Nordwestdeutchen Gesellschaft für Weltraumforschung*, no. 2, Mar. 1951, Sonthofen, Germany.

Eine Methode interplanetarischer Ortsbestimmung, by C. Oesterwinter, *Forschungereihe der Nordwestdeutschen Gesellschaft für Weltraumforschung*, no. 2, Mar. 1951, Sonthofen, Germany.

Meteoric Collision Factor in Space Ship Design, by F. L. Whipple, *Aviation Age*, vol. 16, Dec. 1951, pp. 25–26.

The Cost of Interplanetary Cargo Transportation. II, by N. J. Bowman, *J. Space Flight*, vol. 4, Apr. 1952, pp. 1–9.

A Method of Landing a Space Ship Under Adverse Climatic Conditions, by M. Conley, *J. Space Flight*, vol. 4, May 1952, p. 6.

Artificial Satellites, by J. Humphries, *Aeronautics*, vol. 25, Apr. 1952, pp. 62, 65–66, and 69.

Generalized Interplanetary Orbits, by H. Preston-Thomas, *J. Brit. Interplanetary Soc.*, vol. XI, Mar. 1952, pp. 76–85.

Ecological Aspects of Planetary Atmospheres with Special Reference to Mars, by H. Strughold, *J. Aviation Medicine*, vol. 23, Apr. 1952, pp. 130–140.

Medical Research in Development of Manned Rocket Flight, by H. Haber, *Tech. Data Digest*, vol. 17, Feb. 1952, pp. 12–13.

Human Experiments in Subgravity and Prolonged Acceleration, by E. R. Ballinger, *Tech. Data Digest*, vol. 17, May 1952, pp. 10–12.

Man Without Gravity; the Physiological and Psychological Problems of Space-Flight, by L. N. Thompson, *Flight*, vol. 61, Mar. 14, 1952, pp. 298–300.

## Astrophysics and Aerophysics

The Origin of the Planets, by H. Brown, *Chem. Eng. News*, vol. 30, Apr. 21, 1952, pp. 1622–1626.

The Colloquium on Auroral Physics, by N. C. Gerson, *J. Franklin Inst.*, vol. 253, Apr. 1952, pp. 331–338.

The Role of Turbulence in the Evolution of the Universe, by G. Gamow, *Phys. Rev.*, vol. 86, Apr. 15, 1952, p. 251.

Structure of Comets and the Formation of Tails, by R. A. Littleton, *Nature*, vol. 169, Apr. 12, 1952, pp. 615–616.

On the Possibility of Obtaining Radar Echoes from the Sun and Planets, by F. J. Kerr, *Proc. Instn. Radio Engrs.*, vol. 40, June 1952, pp. 660–666.

Solar Radio Noise Bursts, unsigned, *Tech. News Bull.*, vol. 26, May 1952, pp. 65–67.

Radio Astronomy, by J. A. Ratcliffe, *Nature*, vol. 169, Mar. 1, 1952, pp. 348–350.

A New Radio Interferometer and Its Application to the Observation of Weak Radio Stars, by M. Ryle, *Proc. Roy. Soc. Lond.* (*A*), vol. 211, Mar. 6, 1952, pp. 351–375.

A Radio-Astronomical Investigation of Winds in the Upper Atmosphere, by A. Maxwell and C. G. Little, *Nature*, vol. 169, May 3, 1952, pp. 746–747.

Average Radio-Ray Refraction in the Lower Atmosphere, by M. Schulkin, *Proc. Instn. Radio Engrs.*, vol. 40, May 1952, pp. 554–561.

Atmospheric Density Profile and Gradients from Early Parts of Photographic Meteor Trails, by L. G. Jacchia, MIT Center of Analysis Report 4, 1949, 12 pp.

Photographic Meteor Phenomena and Theory; Meteor Photometry, Fundamental Equations and Constants, Durations and Flares, by L. G. Jacchia, MIT Center of Analysis Report 3, 1949, 36 pp.

Research in the Upper Atmosphere with Sounding Rockets and Earth Satellite Vehicles, by S. F. Singer, *J. Brit. Interplanetary Soc.*, vol. XI, Mar. 1952, pp. 61–73.

The World's High Altitude Laboratories, by S. A. Korff, *Physics Today*, vol. 5, May 1952, pp. 28–30.

On the Efficiency of the Engine Driving the Atmospheric Circulation, by O. R. Wulf, *J. Meteor.*, vol. 9, Apr. 1952, pp. 79–82.

## Other Classifications

Construction of an Intermediate Reactor for Submarines, unsigned, *Engineer*, vol. 173, Apr. 25, 1952, p. 579.

Errors in Rocket Development, 1, by H. Oberth, *Rocketscience*, vol. 6, Mar. 1952, pp. 2–7.

Problems of Astronautical Research, by E. Sänger, *J. Brit. Interplanetary Soc.*, vol. XI, Mar. 1952, pp. 57–60.

Let Punched Cards Solve That Problem, by R. Habermann, *Gen. Elec. Rev.*, vol. 55, May 1952, pp. 9–12.

A Discussion on Friction, a group of 30 notes and papers on friction organized under 3 headings; I. Friction of Metals, II. Friction of Non-Metals, III. Boundary and Extreme Pressure Lubrication, by F. P. Bowden, et al., *Proc. Roy. Soc. Lond.* (*A*), vol. 212, May 22, 1952, pp. 439–520.

Note sur l'autopropulsion avec source d'énergie séparée, by M. P. Blanc, *Mém. de l'artillerie française*, vol. 25, no. 95, 1951, pp. 103–116.

The Role of Physics in Aeronautical Development, by H. L. Dryden, *Physics Today*, vol. 5, May 1952, pp. 14–24.